STEM CELL SELF-RENEWAL AND NEURONAL DIFFERENTIATION IN THE *DROSOPHILA* CENTRAL NERVOUS SYSTEM

by

TRAVIS D. CARNEY

A DISSERTATION

Presented to the Department of Biology
and the Graduate School of the University of Oregon
in partial fulfillment of the requirements
for the degree of
Doctor of Philosophy

June 2013

DISSERTATION APPROVAL PAGE

Student: Travis D. Carney

Title: Stem Cell Self-renewal and Neuronal Differentiation in the *Drosophila* Central Nervous System

This dissertation has been accepted and approved in partial fulfillment of the requirements for the Doctor of Philosophy degree in the Department of Biology by:

Bruce A. Bowerman	Chairperson
Chris Q. Doe	Advisor
Judith S. Eisen	Core Member
Kenneth E. Prehoda	Institutional Representative

and

Kimberly Andrews Espy	Vice President for Research and Innovation; Dean of the Graduate School

Original approval signatures are on file with the University of Oregon Graduate School.

Degree awarded June 2013

DISSERTATION ABSTRACT

Travis D. Carney

Doctor of Philosophy

Department of Biology

June 2013

Title: Stem Cell Self-renewal and Neuronal Differentiation in the *Drosophila* Central Nervous System

The adoption and subsequent retention of distinct cellular fates upon cell division is a critical phenomenon in the development of multicellular organisms. A well-studied example of this process is stem cell divisions; stem cells must possess the capacity to self-renew in order to maintain a stem cell population, as well as to generate differentiated daughters for tissue growth and repair. *Drosophila* neuroblasts are the neural stem cells of the central nervous system and have emerged as an important model for stem cell divisions and the genetic control of daughter cell identities. Neuroblasts divide asymmetrically to generate daughters with distinct fates; one retains a neuroblast identity and the other, a ganglion mother cell, divides only once more to generate differentiated neurons or glia. Perturbing the asymmetry of neuroblast divisions can result in the failure to self-renew and the loss of the neural stem cell population; alternatively, ectopic self-renewal can occur, resulting in excessive neuroblast proliferation and tumorigenesis.

Several genetic lesions have been characterized which cause extensive ectopic self-renewal, resulting in brains composed of neuroblasts at the expense of differentiated cells. This contrasts with wild type brains, which are composed mostly of differentiated

cells and only a small pool of neuroblasts. We made use of these mutants by performing a series of microarray experiments comparing mutant brains (consisting mostly of neuroblasts) to wild type brains (which are mostly neurons). Using this approach, we generated lists of over 1000 putatively neuroblast-expressed genes and over 1000 neuronal genes; in addition, we were able to compare the transcriptional output of different mutants to infer the neuroblast subtype specificity of some of the transcripts. Finally, we verified the self-renewal function of a subset of the neuroblast genes using an RNAi-based screen, resulting in the identification of 84 putative self-renewal regulators. We went on to show that one of these genes, *midlife crisis* (mammals: *RNF113a*), is a well-conserved RNA splicing regulator which is required in postmitotic neurons for the maintenance of their differentiated state. Our data suggest that the mammalian ortholog performs the same function, implicating RNF113a as an important regulator of neuronal differentiation in humans.

This dissertation includes previously published, co-authored material.

CURRICULUM VITAE

NAME OF AUTHOR: Travis D. Carney

GRADUATE AND UNDERGRADUATE SCHOOLS ATTENDED:

University of Oregon, Eugene
Western Washington University, Bellingham
University of Idaho, Moscow

DEGREES AWARDED:

Doctor of Philosophy, Biology, 2013, University of Oregon
Bachelor of Science, Biology, 2005, Western Washington University

AREAS OF SPECIAL INTEREST:

Developmental Neurobiology

Molecular Biology

PROFESSIONAL EXPERIENCE:

Graduate Research Fellow, Chris Doe Laboratory, University of Oregon, June 2008 – June 2013

Graduate Teaching Fellow, Department of Biology, University of Oregon, August 2007 – June 2008

Post-Baccalaureate Research Assistant, Los Alamos National Laboratory, April 2006 – August 2007

National Science Foundation Research Experience for Undergraduates (REU) Intern, Western Washington University, June – December 2005

Production Manager/QA Laboratory Technician, Cook Composites and Polymers, February 1999 – September 2004

GRANTS, AWARDS, AND HONORS:

National Institutes of Health Cell & Developmental Biology Training Grant – University of Oregon, 2008-2011

PUBLICATIONS:

Carney, T.D., Struck, A.J., and Doe, C.Q. *midlife crisis* encodes a conserved zinc finger protein required to maintain neuronal differentiation in *Drosophila*. *In press - Development.*

Carney, T.D., Miller, M.R., Robinson, K.J., Bayraktar, O.A., Osterhout, J.A. and Doe, C.Q. (2012) Functional genomics identifies neural stem cell sub-type expression profiles and genes regulating neuroblast homeostasis. *Dev Biol* 361, 137-46.

Johnson, S.L., Kuske, C.R., **Carney, T.D.**, Housman, D.C., Gallegos-Graves, L.V., and Belnap, J. (2012) Increased temperature and altered summer precipitation have differential effects on biological soil crusts in a dryland ecosystem. *Global Change Biol* 18, 2583–2593.

Yeager, C.M., Kuske, C.R., **Carney, T.D.**, Johnson, S.L., Ticknor, L.O. and Belnap, J. (2012) Response of biological soil crust diazotrophs to season, altered summer precipitation, and year-round increased temperature in an arid grassland of the Colorado plateau, USA. *Front Microbiol* 3, 358.

ACKNOWLEDGMENTS

I am extremely grateful to my dissertation advisor, Professor Chris Q. Doe, for his kindness, patience, and encouragement – not to mention his effortless scientific insight! – throughout my graduate career. An inexperienced young graduate student such as myself may begin a meeting with Chris with trepidation – the data are not quantified, the experiments are taking longer than they were supposed to, the figures are not complete – but will consistently exit that meeting with excitement and renewed optimism for his or her project. I am also thankful to all the members of the Doe lab with whom I have had the good fortune to work; the Doe lab is a fantastic environment scientifically, but it is the Doe lab members themselves who have created a wonderful, welcoming atmosphere that usually makes us all happy to come in to work. Also, I would like to thank Janet Hanawalt in particular, whose kind disposition brightens every day. Any question you have, any favor you need, Janet is happy to help, and it makes all Doe labbers' lives incredibly easier, which ultimately makes the science better. I am indebted to many Doe lab members for thought-provoking discussions, invaluable feedback on papers, posters, and presentations, and for innumerable helpful pointers at the bench; in particular, Minoree Kohwi, Ellie Heckscher, Sen-Lin Lai, Khoa Tran, Omer Bayraktar, Mike Miller, and Leslie Gay have given me invaluable help during my graduate career. Thank you all. Thank you to my family for the lifelong support and encouragement, and to my wife for always making life outside the lab so enjoyable! And finally, I would like to thank the National Institutes of Health and the Howard Hughes Medical Institute for funding; without it, none of this research would have been possible.

I dedicate this dissertation to my parents, Carl and Christine, whose regular (perhaps misguided?) insistence in my brilliance has always been instrumental in convincing me that I can handle things like college, graduate school, and whatever comes next, and to my wife Carrie, without whose love, support, and constant longsuffering companionship, I am not sure my parents would have been right!

TABLE OF CONTENTS

LIST OF FIGURES

Figure Page

Chapter II

Chapter III

LIST OF TABLES

Table Page

Chapter II

Chapter III

CHAPTER I

INTRODUCTION

The importance of asymmetric daughter cell fates

A fundamental question in Developmental Biology is: How can a single fertilized egg generate all the various specialized cell types that comprise a complete multicellular organism? This question is extremely broad and encompasses much of Developmental Biology. From a more focused, cell-centric point of view, the question may be simply: How can a dividing cell generate daughter cells which differ from one another? In other words, how do distinct daughter cell identities arise? The genetic control of this central phenomenon in Developmental Biology is the broad focus of this dissertation.

Very frequently during development, cells must divide to yield dissimilar progeny, which themselves may undergo numerous divisions to generate different cell types and tissues. A well-studied example of such daughter cell asymmetry is evident in the early *C. elegans* embryo; even during the very first embryonic division, a physical and molecular asymmetry is apparent, resulting in dissimilar anterior (AB) and posterior (P1) cells. For example, the PDZ domain protein PAR-6 and the atypical protein kinase C (aPKC) homolog, PKC-3, are asymmetrically localized in the zygote and segregated into the AB cell, while the protein kinase PAR-1 and the RING domain protein PAR-2 are both segregated preferentially into the P1 cell (Nance 1995). These molecular asymmetries in turn result in distinct fates for these cells: the AB cell generates most of the hypodermis and nervous system of the resulting larva, and the P1 cell generates the entire germ line and many of the body wall muscles (Schnabel and Priess, 1997).

Perturbation of the initial cell fate asymmetries can have dire effects on the development of the organism.

The *Drosophila* neuroblast as a stem cell model

In animals, an important system in which daughter cell fates are critical is exemplified in stem cells. Many tissues house stem cells, which have the ability to generate the functional, differentiated cell types that comprise an organism. Thus stem cells hold the potential to generate mature cells for the repair of tissue injury or degeneration; it is due to this ability that stem cells are a promising potential therapeutic tool and the subject of intense research. Stem cells must have not only the capacity to generate differentiating progeny for tissue development or repair, but also the ability to generate new copies of themselves, or self-renew, in order to maintain a population of stem cells in the tissue. Thus an inherent problem for all stem cells is how to maintain a proliferative potential for self-renewal, but to simultaneously reign in this potential to prevent overproliferation and tumorigenesis. As a result, the choice that arises upon stem cell divisions – whether to self-renew or to differentiate – is an important example of an asymmetric cell fate decision.

In the *Drosophila* central nervous system (CNS), the neural stem cell (neuroblast) has become an important model for stem cell divisions (Doe, 2008; Homem and Knoblich; Knoblich, 2008). Neuroblasts are large (~10 μm) cells which delaminate from the embryonic neuroepithelium and thereafter self-renew at each division. Notably, unlike some types of stem cells, neuroblasts do not undergo periodic symmetric divisions to expand their numbers; as a result, a stereotyped number of neuroblasts is maintained in each CNS (Egger et al.; Reichert, 2011). In the larval central brain, the most abundant

neuroblast, termed type I, undergoes rigorously regulated asymmetric divisions to self-renew and to generate an intermediate progenitor, the ganglion mother cell (GMC), which itself divides once to form differentiated neurons or glia. Due to the characteristic division pattern and the highly stereotyped neuroblast number in larval central brains, these neuroblasts are an ideal system to study the effects of genetic perturbation of daughter cell fate decisions.

The molecular asymmetry of a dividing neuroblast

Numerous studies have aided in the elucidation of the mechanism responsible for generating the asymmetric fates of a dividing neuroblast [reviewed in: (Doe, 2008; Knoblich, 2008; Knoblich, 2010; Prehoda, 2009)]. The primary mechanism is the establishment of distinct apical and basal domains in a mitotic neuroblast. Numerous factors localize asymmetrically in cortical crescents in these domains such that upon cell division, the apical factors remain in the self-renewed neuroblast and the basal factors are segregated into the GMC. Moreover, the primary function of the apically-localized factors is to sequester the basal determinants to the differentiating daughter.

The basally-localized cell fate determinants include the Notch inhibitor Numb, the translational repressor Brain tumor (Brat), and the essential pro-differentiation transcription factor Prospero (Pros) (Betschinger et al., 2006; Broadus et al., 1998; Hirata et al., 1995; Knoblich et al., 1995; Lee et al., 2006b; Spana and Doe, 1995). *pros* is transcribed in the neuroblast but has no known function there, and the Pros protein remains cytoplasmic until mitosis when it is inherited exclusively by the GMC. In the GMC, Pros acts as a "binary switch," directly activating pro-differentiation genes and repressing neuroblast fate and cell cycle genes (Choksi et al., 2006; Li and Vaessin,

2000). Owing to its transcriptional regulatory activity, Pros is necessary and sufficient for differentiation. Misexpression of Prospero in neuroblasts can cause their premature cell cycle exit and differentiation (Cabernard and Doe, 2009). Conversely, loss of Prospero results in a failure of the GMC to begin a program of differentiation, the reversion to a neuroblast fate, and drastic overproliferation of neuroblast-like cells (Bello et al., 2006; Betschinger et al., 2006; Lee et al., 2006b). Brat and Numb also act as tumor suppressors, and loss of function of either factor can cause failure to differentiate and drastic neuroblast overproliferation.

As mentioned above, the primary function of the apically-restricted factors in mitotic neuroblasts appears to be to ensure the faithful segregation into the GMC of the basal cell fate determinants Brat and Pros [via the adapter protein Miranda (Mira)] and Numb [along with its adaptor, partner of Numb (Pon)] (Ikeshima-Kataoka et al., 1997; Kelsom and Lu, 2012; Lee et al., 2006b; Lu et al., 1998; Prehoda, 2009; Shen et al., 1997). This is accomplished by two complementary mechanisms. First, the Par complex (containing the PDZ domain-containing protein Bazooka, Par-6, and aPKC) is localized to the apical domain and actively prevents basal determinants from localizing apically (Prehoda, 2009). Secondly, the mitotic spindle aligns robustly with the polarity axis during mitosis [reviewed in: (Gillies and Cabernard; Lu and Johnston; Siller and Doe, 2009)]. In this way it is ensured that the polarized components are accurately separated into the neuroblast and GMC upon cytokinesis.

aPKC has emerged as a central player in the establishment of separate cortical domains. Both the apical localization and kinase activity of aPKC are required to prevent basal determinants from localizing apically, as aPKC phosphorylation of both Miranda

and Numb is sufficient to displace them from the cortex (Atwood and Prehoda, 2009; Rolls et al., 2003; Smith et al., 2007; Wirtz-Peitz et al., 2008). Forced localization of active aPKC to the entire cortex via the attachment of a lipid-associating CAAX domain results in completely cytoplasmic Mira and a concomitant failure of GMC differentiation, resulting in neuroblast overproliferation (Lee et al., 2006a). Moreover, the cytoskeleton associated protein Lethal giant larvae (Lgl) is a negative regulator of aPKC, and as such *lgl* loss of function affects the proper segregation of Pros, Numb, and Brat into the GMC, resulting in ectopic neuroblast formation (Betschinger et al., 2006; Lee et al., 2006a; Ohshiro et al., 2000). The Par complex proteins Baz and Par-6 are both required for aPKC localization (Prehoda 2009). More research is needed to determine how the Par proteins and aPKC are initially polarized in the neuroblast, and how aPKC localization and kinase activity are coordinated.

Central to the proper orientation of the mitotic spindle is Pins (Partner of Inscuteable) which links cortical polarity to the spindle. Pins links spindle microtubules to the apical cortex through two parallel pathways: through interaction with Mushroom body defect (Mud), which is thought to interact with the Dynein/Dynactin complex and generate pulling forces on spindle microtubules (Bowman et al., 2006; Izumi et al., 2006; Siller and Doe, 2008), and through interaction with Discs large (Dlg)/Kinesin heavy chain 73 (Khc73) (Johnston et al., 2009; Siegrist and Doe, 2005).

Type II neuroblasts

In addition to the type I neuroblasts described above, a small number of type II neuroblasts also exist in the *Drosophila* central brain. Unlike the simple division pattern exemplified by type I neuroblasts, they divide asymmetrically to produce small transit-

amplifying progenitors (intermediate neural progenitors, INPs). INPs themselves undergo molecularly asymmetric cell divisions to generate several GMCs which divide to generate neurons or glia (Bello et al., 2008; Boone and Doe, 2008; Bowman et al., 2008; Izergina et al., 2009; Viktorin et al., 2011). Due to the transit-amplifying INPs, type II neuroblasts are able to generate far more progeny than type I neuroblasts. Interestingly, the proliferation pattern of type II neuroblasts is similar to that of certain mammalian neural stem cells which also generate transit-amplifying progenitor cells. It is thought that this mode of proliferation is a mechanism for increasing neural cell number and diversity (Boyan and Reichert, 2011; Doe, 2008). Type II neuroblasts and INPs have joined the better-studied type I neuroblasts as important models of self-renewal and differentiation, and their similarity to the division pattern of mammalian neural stem cells has recently spurred a great deal of interest. Determining how these INPs are specified and maintained, and how they are able to generate increased neural diversity, may shed light on the function of mammalian neural stem cells.

Dedifferentiation: the failure to maintain a differentiated fate

As described above, much is known about the factors involved in the molecular asymmetry of neuroblast divisions and the cell fate determinants required for self-renewal of the neuroblast and the initial specification of GMC identity. However, much less is known about how these distinct fates are maintained. The neuroblast must retain its stem cell characteristics after each division: growing, retaining a proliferative potential, and remaining capable of molecularly asymmetric divisions in order to generate differentiating progeny. Conversely, the GMC has a very restricted proliferative potential, and due to pro-differentiation cell fate determinants begins a differentiation

program. The progeny of the GMC are postmitotic neurons or glia, which themselves must be able to maintain their differentiated identity: remain mitotically inactive, repress stem cell fate genes, and promote the expression of the appropriate program of terminal differentiation. The failure of either neuroblasts or neurons to rigorously maintain their identity could be developmentally catastrophic. Neuroblast cell cycle exit would prevent the formation of important neuronal progeny. Failure of neurons to maintain their fate could likewise have severe developmental consequences, as inability to create functional circuits would lead to a non-functional CNS. In light of these consequences, identifying the factors responsible for the long-term maintenance of both neuroblast and neuron fates is an important goal in developmental biology.

The cell fate determinants that are segregated into the GMC upon neuroblast mitosis (e.g., Pros, Brat, and Numb) are important in specifying the GMC fate and beginning a differentiation program. However, after the final GMC division, it is unknown how neurons retain their terminally differentiated, postmitotic identity. Intriguing clues have come from studies in the *Drosophila* retina, in which photoreceptors have been used as a tractable model to study cell fates. Two recent studies have revealed genotypes which cause differentiated photoreceptor cells to dedifferentiate. First, the combined loss of function of Retinoblastoma protein (Rbf) and Fat/Hippo pathway components causes the dedifferentiation of photoreceptor neurons (Nicolay et al., 2010). Interestingly, the authors found that this dedifferentiation was independent of the re-entry into cell cycle. Similarly, the Abelson tyrosine kinase (Abl) maintains photoreceptor cell differentiation in part by down-regulating Notch; loss of Abl causes a dedifferentiation phenotype, again without concomitant cell cycle entry (Xiong et al.,

2012). These studies give intriguing hints at the genetic control of the persistent maintenance of the differentiated state; however, it is currently unknown how differentiation is maintained in the neurons of the CNS. In Chapter III of this dissertation, I describe the characterization of a gene required to maintain neuronal differentiation in the *Drosophila* CNS (see Bridge below).

Bridge to subsequent chapters

In addition to the asymmetrically-localized factors which segregate preferentially into either the neuroblast or the GMC when a neuroblast divides, several factors have been identified which promote neuroblast self-renewal cell intrinsically. These include the transcription factors Worniu (Lai et al. 2012), Deadpan (San-Juán and Baonza 2011; Zhu et al. 2012), and Klumpfuss (Berger et al. 2012; Xiao et al. 2012). While these factors have been shown to promote self-renewal, their downstream transcriptional targets in neuroblasts are largely unknown. Similarly, although several fate determinants have been identified which are required for GMC fate, cell cycle exit, and entry into a path of neuronal differentiation, the genes required for the maintenance of the differentiated cell identity are largely unknown. The identification of these genes as well as cell-intrinsic neuroblast genes promises to yield insight into the mechanistic determination of neuroblast and neuronal fates and may give insight into the renewal of other stem cell types, including those of human tissues.

In Chapter II of this dissertation, I describe a series of microarray experiments in which co-authors and I attempted to get a clearer picture of the complements of genes expressed preferentially in neuroblasts and in differentiated cells. We made use of a series of genetic lesions which cause extensive neuroblast ectopic self-renewal at the

expense of neurons. We compared each of these mutants to wild type brain lobes, which are strongly enriched for neurons compared to the mutant brains. We hoped to address several questions with this study: 1) what are the neuroblast and neuronal fate genes required for both specification and maintenance of these cell types; 2) what are the genes responsible for the generation of different sub-types of neuroblast; 3) what genes may be expressed in only subsets of neurons? This work was performed in collaboration with the following co-authors: Michael R. Miller, Kristin J. Robinson, Omer A. Bayraktar, Jessica A. Osterhout, and Chris Q. Doe.

In Chapter III, I describe the detailed analysis of a gene which was identified in the studies described in Chapter II. This gene, which I have named *midlife crisis* (*mdlc*), is present in both neuroblasts and neurons and has cell type-specific roles in each. Most intriguingly, the protein Mdlc promotes the maintenance of the differentiated state in postmitotic neurons. Neurons lacking Mdlc initially correctly express the markers of terminally differentiated neurons, but later these markers are gradually lost and neural stem cell markers become derepressed. This observation is reminiscent of the beginning of a dedifferentiation phenotype and highlights the role of Mdlc in the long-term adoption of cell fate. This work was performed in collaboration with Adam J. Struck and Chris Q. Doe.

CHAPTER II

FUNCTIONAL GENOMICS IDENTIFIES NEURAL STEM CELL SUB-TYPE EXPRESSION PROFILES AND GENES REGULATING NEUROBLAST HOMEOSTASIS

This work was published in Volume 361 of the journal *Developmental Biology* in January, 2012. Chris Q. Doe and Michael R. Miller initially conceived of the expression analysis experiments; MRM and I performed the experiments. Kristin J. Robinson, Omer A. Bayraktar, and Jessica A. Osterhout assisted with expression pattern verification and confocal microscopy. CQD and I designed the RNAi screen; JAO assisted me with the screen. CQD and I wrote the manuscript. CQD was the principal investigator for this work.

INTRODUCTION

Drosophila neuroblasts are a powerful model system for understanding the molecular control of stem cell self-renewal versus differentiation. The majority of neuroblasts (type I neuroblasts) repeatedly divide asymmetrically with respect to size and fate to self-renew and produce a smaller daughter cell called a ganglion mother cell (GMC) that divides only once to produce two postmitotic neurons or glia (reviewed in: Chia et al., 2008; Doe, 2008; Knoblich, 2008). Neuroblast/GMC fate differences are due in part to the asymmetric partitioning of proteins into the GMC during neuroblast cell division. These factors include the transcription factor Prospero (Pros), the Notch inhibitor Numb, and the translational repressor Brain tumor (Brat) (Betschinger et al., 2006; Broadus et al., 1998; Hirata et al., 1995; Knoblich et al., 1995; Lee et al., 2006c; Spana and Doe, 1995). Proper segregation of Pros, Numb, and Brat into the GMC require the scaffolding protein Miranda (Mira) and the WD40-domain protein Lethal giant larvae (Lgl) (Betschinger et al., 2006; Lee et al., 2006c; Ohshiro et al., 2000; Peng et al., 2000).

In the GMC, Pros enters the nucleus and promotes cell cycle exit and differentiation by directly activating differentiation genes and repressing self-renewal and cell cycle regulatory genes (Choksi et al., 2006; Li and Vaessin, 2000). This process allows for a single neuroblast to generate a lineage of many differentiated neurons and glia and for a relatively small number of neuroblasts to generate the thousands of cells found in the central nervous system of the adult fly.

Recently, "type II" neuroblasts were identified in the larval brain which divide asymmetrically to produce small transit-amplifying progenitors (intermediate neural progenitors, INPs). INPs themselves undergo molecularly asymmetric cell divisions to generate 4-6 GMCs, each of which typically generates two postmitotic neurons or glia (Bello et al., 2008; Boone and Doe, 2008; Bowman et al., 2008; Izergina et al., 2009; Viktorin et al., 2011). Six type II neuroblasts inhabit the dorso-medial region of the lobe and are designated DM1-6, and two occupy more lateral positions (Bayraktar et al., 2010; Izergina et al., 2009). Type II neuroblasts behave in a manner similar to mammalian neural stem cells in that they generate transit-amplifying INPs. Transit-amplifying progenitors are important in the development of the nervous system in mammals as well as in flies because they permit the rapid amplification of neuronal progeny (Bello et al., 2008; Boone and Doe, 2008; Bowman et al., 2008; Merkle and Alvarez-Buylla, 2006; Morrison and Kimble, 2006). Thus, while there are ~95 type I neuroblasts per larval brain lobe and only eight type II neuroblasts, these few type II lineages produce a considerable fraction – approximately a quarter – of the neurons of the adult brain (Izergina et al., 2009). Type II neuroblasts and INPs have thus become a model for the study of transit-

amplifying neural progenitors, and determining how these cells are specified and maintained may shed light on the function of mammalian neural stem cells.

Type II neuroblasts are known to differ from type I neuroblasts in several ways. First, they generate INPs and thus make much larger lineages than type I neuroblasts (Bello et al., 2008; Boone and Doe, 2008; Bowman et al., 2008). Second, they are xxx major contributors of the intrinsic neurons of the adult central complex (intrinsic neurons have projections entirely within the central complex) (Bayraktar et al., 2010; Izergina et al., 2009). Third, they are more susceptible to tumor formation (Boone and Doe, 2008; Bowman et al., 2008; Ouyang et al., 2011; Weng et al., 2010). Numerous genotypes have been identified that cause the production of ectopic larval brain neuroblasts, and several of these specifically affect type II neuroblasts. For example, mutations in *brat* lead to "overgrowth" of just the type II neuroblasts, and mutations in *lgl* affect type II much more strongly than type I neuroblasts. On the other hand, loss of *Aurora-A* (*Aur*) or neuroblast misexpression of membrane-tethered atypical protein kinase C ($aPKC^{CAAX}$) leads to ectopic type I and type II neuroblasts (Bowman et al., 2008). It is likely that the lack of Pros in the new-born INP renders this daughter cell sensitive to the loss of a second growth inhibitor/differentiation factor, making it easier for this cell to revert to a type II neuroblast identity.

In spite of the marked differences between type I and type II neuroblasts in proliferative potential and susceptibility to tumor formation, only two molecular differences are known: type II neuroblasts lack the transcription factors Pros and Asense (Ase), while both are present in all type I neuroblasts (Bello et al., 2008; Boone and Doe, 2008; Bowman et al., 2008). It is currently unknown how many other genes are regulated

differentially between type I and type II neuroblasts, and which of them regulates each distinct aspect of type I and type II function. In order to discover such transcriptional differences, relatively pure populations of each neuroblast sub-type must be isolated from which to extract RNA. Complicating these efforts, the *Drosophila* central nervous system contains only a small number of neuroblasts which are dispersed throughout a complex population of thousands of neurons and glia, making it difficult to physically separate neuroblast sub-types from each other and from other cell types. Thus, comparing the transcriptional outputs of neuroblast sub-types is technically challenging due to the difficulty of isolating cell type-specific RNA.

In order to enrich for each type of neuroblast, here we make use of published and unpublished mutants in which type I and type II neuroblasts exhibit differential overproliferation phenotypes. We perform microarray-based whole-genome transcriptional profiling to compare each of these different mutant brains to wild-type; thus we are able to probe the transcriptional differences not only between each mutant and wild-type, but also between type I and type II neuroblasts. We identify only a small number of genes exhibiting transcriptional differences between type I and type II neuroblasts, providing a highly specific group of genes to screen for a function in establishing each type of neuroblast. We identify a large group of genes which are likely expressed in neuroblasts but not neurons, and we verify the neuroblast function of a subset of these genes using an RNAi-based targeted loss of function screen. Using this approach we identify 84 genes required to maintain neuroblast numbers in larval brains, all of which have conserved mammalian orthologs.

MATERIALS AND METHODS

Fly stocks

All fly stocks used in this study have been previously described except for *lgl⁻ lgd^{d7},* in which the *lgl* locus has been spontaneously lost (Jason Boone, unpublished data) from the *lgd^{d7}* chromosome (Jaekel and Klein, 2006). Other fly stocks used were: *lgl^{334}* (Rolls et al., 2003); *aurA^{8839}* (Lee et al., 2006a); *lgl^{334};pins^{62}* and *UAS-aPKC^{CAAX}* (Lee et al., 2006a); *brat^{11}* (Lee et al., 2006b); *wor-gal4* (Albertson et al., 2004); *R9D11-Gal4* and *R19H09-Gal4* (Bayraktar et al., 2010); *UAS-mCD8::GFP* and *UAS-Dicer2* (Bloomington Stock Center).

Microarray analysis

Mutant larvae were dissected at 144 hours after larval hatching (ALH); wild-type heterozygous larvae that were at the same developmental stage were dissected at 96 hours ALH as wild-type controls. The only exceptions were the *aPKC^{CAAX}* experiments, in which the experimental larvae were raised at 30°C and exhibited enlarged brains packed with ectopic neuroblasts, and genetically identical control larvae were raised at room temperature, where the ectopic neuroblast phenotype is much weaker. Total RNA was extracted from larval brain lobes using TRIzol extraction methods according to the manufacturer's instructions (Invitrogen, Carlsbad, CA, USA). First strand synthesis and amplification of Cy3- and Cy5-labeled RNA were accomplished using the Agilent Low Input Quick Amp Labeling Kit (Agilent, Santa Clara, CA, USA). Four experimental replicates were performed for each mutant genotype: two standard replicates (Cy5-labeled mutant RNA and Cy3-labeled wild-type RNA) and two dye-swapped replicates. Exceptions were the *aPKC^{CAAX}* experiments, in which one standard and two swapped

replicates were used for clustering, and the *lgl* experiments, in which three standard and one swapped replicates were used (Supplementary Figure 1; see Appendix A for all Chapter II supplementary materials). Hybridization was performed as previously described (Miller et al., 2009), except for each replicate, 825 ng of both mutant and wild-type RNA were mixed and hybridized to Agilent microarrays. The slides were scanned using an Axon GenePix 4000B, and GenePix software was used for feature extraction.

Cluster analysis

We selected genes for cluster analysis if, in at least one of the mutant genotypes, their average transcript levels over all biological replicate experiments deviated from the wild-type RNA sample by greater than two-fold. This criterion resulted in the selection of 2781 genes. To investigate the reproducibility of replicate experiments of the same mutant genotype and the overall transcriptional similarities between experiments, we first performed cluster analysis without averaging individual replicate experiments. This analysis allowed us to determine whether, for each experiment, the clustering analysis grouped replicates of the same genotype together (Supplementary Figure 1). To identify groups of genes with similar transcript patterns over the different mutant genotypes, we averaged replicates and performed cluster analysis on these averages in order to avoid artificial gene clustering relationships due to technical noise between experimental replicates. After performing cluster analysis, we found that a large group of genes with increased expression in mutant brains clustered with high correlation. Group A was defined by a tree branch that represented a large decrease in correlation, from >0.6 to ~0.38. We similarly found that a long branch in the genes with reduced expression in mutant brains caused a decrease in correlation that passed the 0.6 cutoff (from >0.7 to

~0.54); thus we considered all the genes clustering below this branch to comprise group C. The remainder of the genes exhibited variable expression patterns and did not cluster with high correlation, and was defined as group B.

RNAi screen

Knockdowns were performed on group A genes with annotated human orthologs and transgenic RNAi stocks available from the Vienna *Drosophila* RNAi Center (VDRC). We used these lines to knock down genes cell type-specifically by crossing RNAi line males to *wor-Gal4UAS-Dicer2* virgins. The progeny of these crosses were raised at 30°C and scored for lethality. Each knock-down was performed at least twice to judge the consistency of the phenotype. For those RNAi constructs that caused lethality, we performed crosses again and dissected brains from wandering third instar larvae. We took confocal stacks of these brains (see below) and determined the number of central brain neuroblasts per brain lobe using antibodies against the neuroblast-specific proteins Deadpan (Dpn) and Mira. Optic lobe neuroblasts were excluded from these counts based on their small size, tight clustering, and stereotyped lateral position in the brain lobe.

Fixation, antibody staining, and confocal microscopy

The following antibodies were used for immunohistochemical staining of larval brains: guinea pig anti-Dpn, 1:2000 (J. Skeath); rat anti-Dpn, 1:1-1:50 (Doe lab); rat anti-Elav, 1:50 (Developmental Studies Hybridoma Bank 7E8A10); rabbit anti-Ase, 1:2000 (Brand et al., 1993); rabbit anti-Optix, 1:500 (Kenyon et al., 2005); rabbit anti-Rx, 1:2000 (Davis et al., 2003); chicken anti-GFP, 1:1000 (Aves Laboratories, Tigard, OR, USA); mouse anti-Pros, 1:1000 (MR1A, Doe lab). Brains were dissected in Schneider's medium (Sigma Aldrich, St. Louis, MO, USA), fixed in PBST (phosphate-buffered saline + 0.1%

Triton-X100; Sigma Aldrich) with 4% formaldehyde for 20 minutes, rinsed for 30 minutes in PBST, blocked for 30 minutes using PBSBT (PBST + 1% bovine serum albumin) or PBST + 5% normal goat serum. Brains were incubated in primary antibody overnight at 4°C with rocking, and then rinsed in PBST + block for 1 hour. Brains were incubated with secondary antibodies (1:500; Molecular Probes, Eugene, OR, USA or Jackson Immunoresearch, West Grove, PA, USA) for 2 hours at room temperature with rocking, and then rinsed for 1 hour with PBST and stored in Vectashield (Vector Laboratories, Inc., Burlingame, CA, USA) until microscopy could be performed. Microscopy images were taken using a Bio-Rad Radiance or Zeiss700 confocal microscope.

RESULTS

Transcriptional profiling of larval brains containing ectopic type I or type II neuroblasts

We analyzed six different genotypes that generate ectopic neuroblasts in the third instar larval brain (Table 1). The *brat* and *lgl* single mutants produce primarily ectopic type II neuroblasts, whereas *aurA* mutation or misexpression of membrane-tethered aPKC is reported to generate ectopic type I and type II neuroblasts (Bowman et al., 2008). We also analyzed *lgl lgd* and *lgl pins* double mutants, both of which produce large numbers of ectopic neuroblasts of unknown type (Lee et al., 2006a; Lee et al., 2006b; Wang et al., 2006; Jason Boone, unpublished data). We stained these brains for the pan-neuroblast marker Dpn and neuronal marker Elav to determine the total number of ectopic neuroblasts and remaining number of neurons, showing that there is a graded

increase in the number of neuroblasts per brain from *lgl* (the fewest ectopic neuroblasts) to *lgl pins* (almost entirely neuroblasts; Figures 1A and 1B). As type I and type II neuroblasts can be distinguished by the presence of Ase only in type I neuroblasts (Figures 1C and 1D), we also stained the brains for Dpn and Ase to determine the proportion of ectopic type I/type II neuroblasts. We confirmed that the *brat* single mutant generates primarily ectopic type II Ase^- neuroblasts while *aur* and $aPKC^{CAAX}$ brains contain more type I Ase^+ neuroblasts, although there is also an increase in type II neuroblasts (Figure 1E). Moreover, we found that the *lgl lgd* double mutant is strongly enriched for type II neuroblasts, and *lgl pins* brains contain both neuroblast types with an enrichment of type I neuroblasts. We noted that in *lgl pins* brains, distinct regions of type I and type II neuroblast overproliferation are discernible based on the lack of Ase and Pros in ectopic cells derived from type II neuroblasts (Figure 1E and inset). We conclude that the six genotypes used here exhibit a range of type I/type II differential overproliferation phenotypes, with *brat, lgl,* and *lgl lgd* brains representing enriched pools of type II neuroblasts, and with *aur*, $aPKC^{CAAX}$, and *lgl pins* being more enriched for type I neuroblasts.

Next we used transcriptional profiling of the larval brain lobes from each of these six genotypes to identify (a) genes differentially regulated in type I vs. type II neuroblasts, that may function in establishing the striking differences between these two types of progenitors, and (b) genes expressed in all neuroblasts, that may function to regulate self-renewal or asymmetric cell division. For each experiment, we isolated RNA from mutant and wild-type brain lobes, amplified and fluorescently labeled each RNA

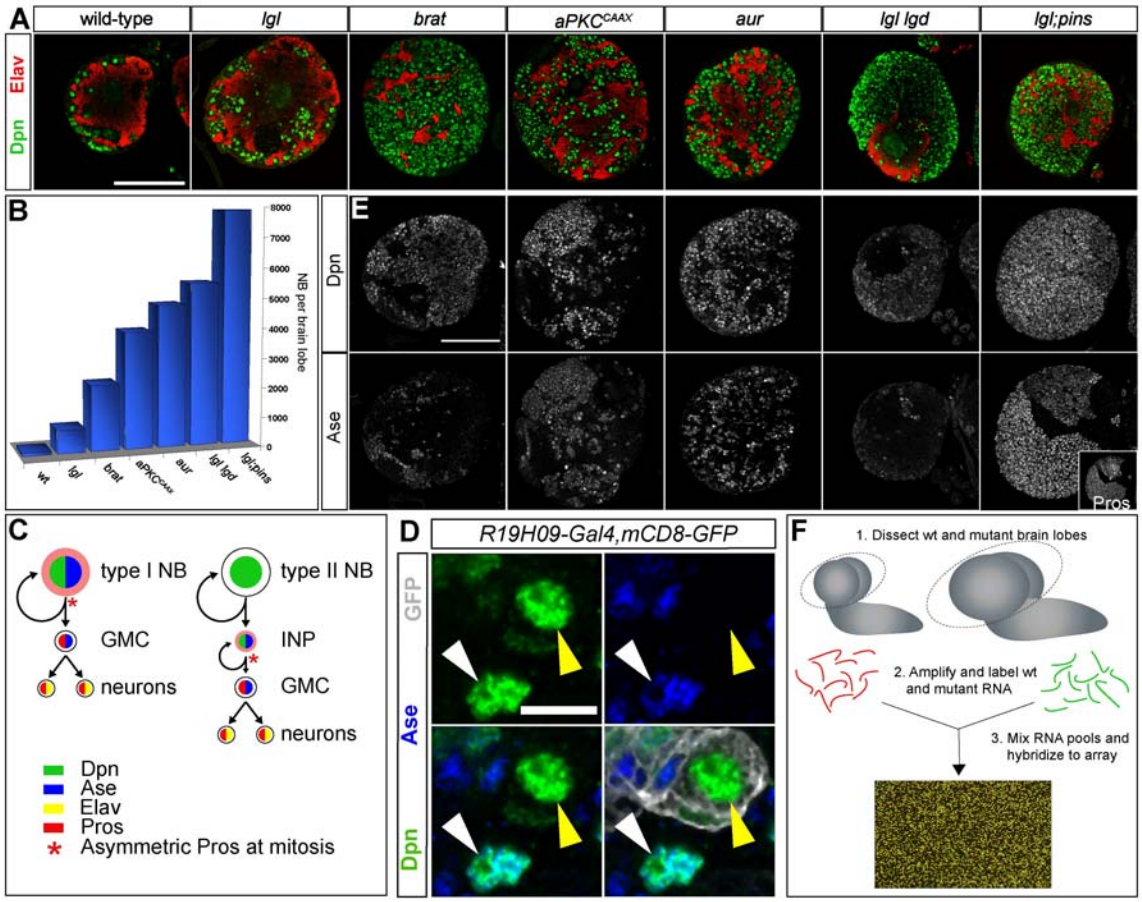

Figure 1: Using ectopic self-renewal mutants for expression profiling of neuroblasts
Six genotypes were used which are known to cause expansions in the number of neuroblasts in *Drosophila* larval central brains. (A) Single-slice confocal images of wild-type (120 hours ALH) and mutant (144 hours ALH) brain lobes stained for Dpn (neuroblast marker) and Elav (neuronal marker). (B) The variable level of ectopic neuroblast number per brain lobe of each mutant genotype (n=2 for each genotype). (C) Schematic of wild type type I and type II neuroblast divisions. Type I neuroblasts have nuclear Ase as well as diffuse cytoplasmic Pros, which is asymmetrically segregated into the GMC upon neuroblast division. Type II neuroblasts lack both Pros and Ase, both of which are expressed in INPs; Pros is then segregated asymmetrically into the GMC upon INP division. GMCs divide to generate Elav^{+} neurons. (D) High magnification image of a Dpn^{+} Ase^{+} type I neuroblast (white arrowhead) and a Dpn^{+} Ase^{-} type II neuroblast (yellow arrowhead) in the dorso-medial region of a wild-type brain. The type II neuroblast can be unambiguously identified based on the presence of GFP driven by *R19H09-Gal4* (Bayraktar et al., 2010). (E) Mutant brains (120 hours ALH) stained with anti-Dpn (to mark all neuroblasts) and anti-Ase (which only marks type I neuroblasts). Inset in the Ase panel of the *lgl pins* brain shows that the Pros staining pattern in the same brain matches very closely to the Ase pattern. (F) Schematic of the methodology used here. Scale bars: 10 μm in (D); 100 μm in (A and E).

Table 1. Mutants affecting brain neuroblast numbers used in this study

Genotype	Synonym	type I / type II neuroblast phenotype	References
lgl^{334}	*lgl*	ectopic type II	(Bowman et al., 2008)
brat^{11}	*brat*	ectopic type II	(Bowman et al., 2008)
wor-gal4 UAS-aPKC^{CAAX}	*aPKC*^{CAAX}	ectopic type I (some II)	(Bowman et al., 2008)
aurA^{8839}	*aur*	ectopic type I (some II)	(Bowman et al., 2008)
lgl^{-} *lgd*^{d7}	*lgl lgd*	ectopic type II	this work
lgl^{334}*;pins*^{62}	*lgl pins*	ectopic type I (some II)	this work

sample, and hybridized them directly against each other to microarrays representing the entire complement of protein-coding *Drosophila* genes with at least two-fold redundancy (Figure 1F). We used cluster analysis to group genes according to transcriptional pattern similarities in the different experiments. Genes exhibiting no change between wild-type and mutant were not included in the cluster analysis (see Methods). Biological replicates and dye-swap experiments cluster much more closely to one another than to replicates for any other mutant (Supplementary Figure 1); this demonstrates that our data are highly reproducible and that each mutant exhibits a distinct transcriptional profile.

We sorted genes into three groups based on their transcript pattern in the six genotypes (Figure 2A). Group A contains 1045 genes with elevated expression in the mutant genotypes (Figure 2B); these genes are likely to be expressed in neuroblasts and are good candidates for regulating neuroblast function (see below). Group B contains 467 genes that have variable expression between mutants. Group C contains 1269 genes with decreased transcript levels in each mutant (Figure 2A and 2B); thus the genes in this large group are good candidates for genes expressed in neurons or glia but not in neuroblasts. Interestingly, we did not see clustering of the genotypes that generate ectopic type II neuroblasts (*lgl, lgl lgd*, and *brat*) – note that the dendrogram at the top of Figure 2A

shows that each of these genotypes has a more closely related genotype that generates ectopic type I neuroblasts – suggesting type I and type II neuroblasts are much more similar transcriptionally than different.

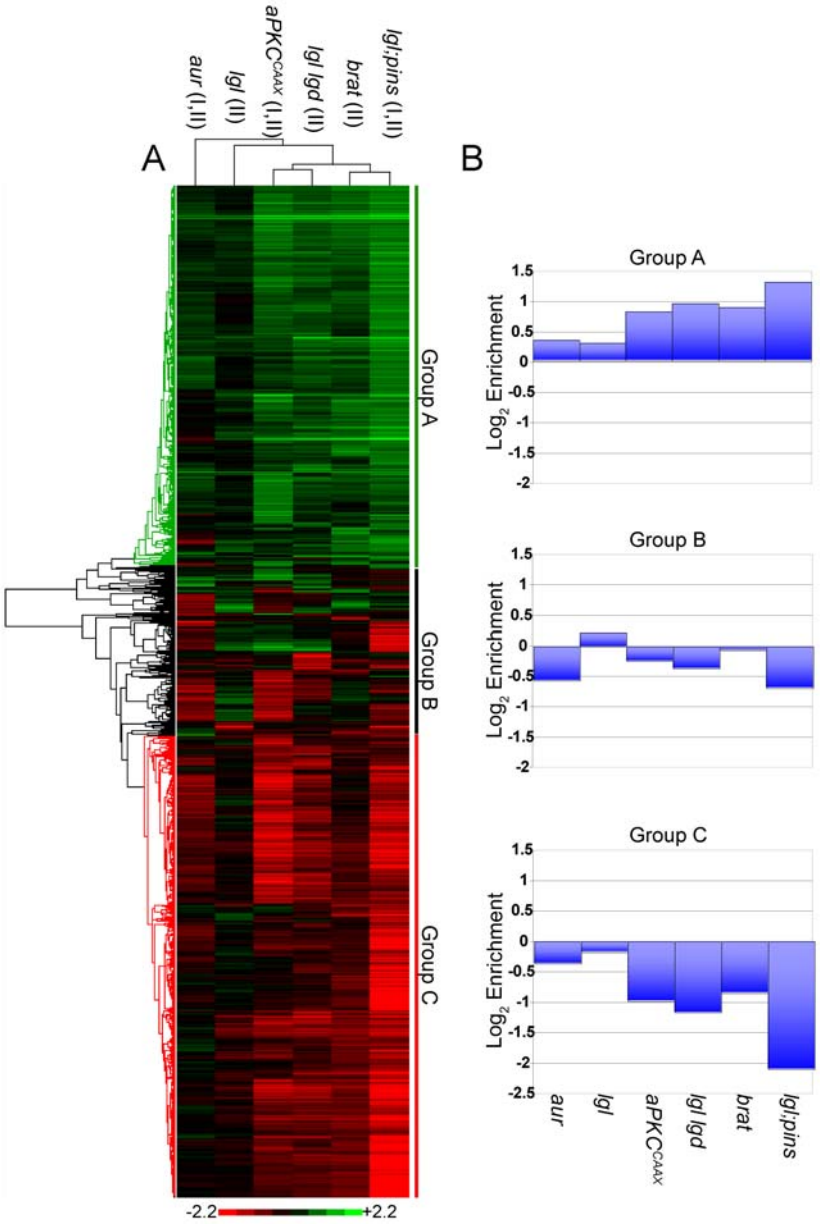

Figure 2: Results of cluster analysis
(A) Cluster analysis-categorized genes with expression changes in mutant compared to wild-type brains, divided into three groups (A, B, and C).The dendrogram at the top is labeled according to the mutant genotype; Roman numerals indicate the neuroblast subtype(s) enriched in each mutant (I = type I; II = type II). (B) Log_2 expression changes (mutant/wild-type) averaged over all genes in each group.

Identification of genes transcribed preferentially in type I or type II neuroblasts

To identify genes expressed differentially between type I and type II neuroblasts, we looked for genes clustered with *pros* and *ase*, the only two genes known to be differentially expressed in type II neuroblasts. We found that *pros* and *ase* reside together in a small sub-cluster of only 11 genes within group B (Figure 3A). This sub-cluster as a whole exhibits reduced expression in *brat*, *lgl,* and *lgl lgd* mutants and enrichment in *aur,* $aPKC^{CAAX}$, and *lgl pins;* remarkably, no other sub-cluster exhibits such a pattern. This suggests that the other nine genes in the cluster may also be specifically expressed in type I neuroblasts, like *pros* and *ase,* and that these are potentially the only genes that exhibit this unique pattern.

To test whether other genes in the small *pros/ase* cluster are also expressed in type I neuroblasts but not type II neuroblasts, we obtained an antibody to a candidate from this cluster, Retinal homeobox (Rx), a homeodomain-containing transcription factor (Davis et al., 2003; Eggert et al., 1998). We found that Rx is completely absent from type II neuroblasts, similar to Pros and Ase; Rx is detected in several type I neuroblasts as well as in a subset of differentiated type II progeny (Figure 3B and 3C). Consistent with this expression pattern, we found that *brat* mutants, which overproduce type II neuroblasts, show a loss of Rx staining (Figure 3D). In contrast, *lgl pins* mutants, which have ectopic type I neuroblasts, show territories of strong Rx expression which is confined to $Pros^{+}$ (likely type I-originating) cells (Figure 3E). The fact that only a small patch of *lgl pins* mutant brain tissue is Rx^{+} is probably because Rx is normally expressed in a subset of type I neuroblasts. We conclude that Rx, like Pros and Ase, is expressed in

type I but not type II neuroblasts. Thus, most or all of the 11 genes in the *pros/ase* sub-cluster may be expressed in type I but not type II neuroblasts.

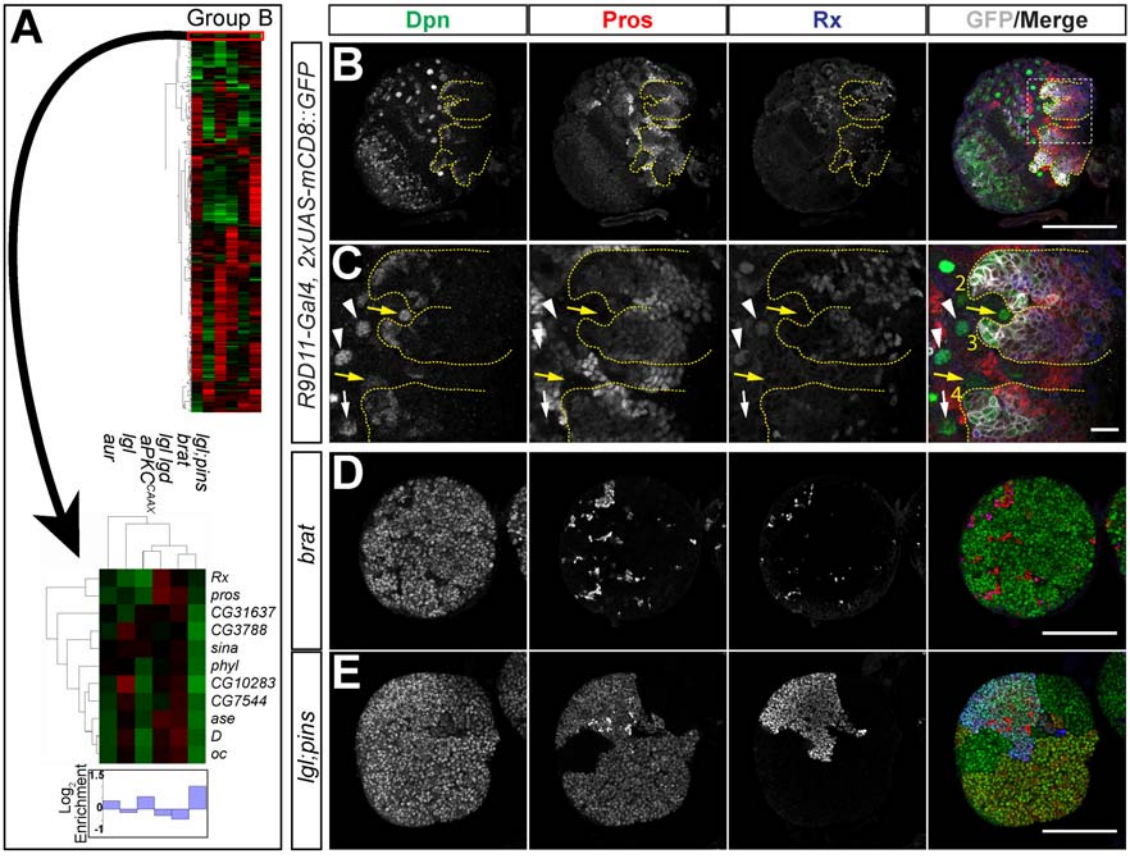

Figure 3: Differential expression of genes excluded from type II neuroblasts
(A) Position within group B of sub-cluster containing *pros* and *ase* as well as nine other genes with unknown expression patterns. Log_2 enrichment over wild-type is shown, averaged over all genes in the sub-cluster. (B) Confocal image of a wild-type brain lobe at 120 hours ALH. Multiple type I neuroblasts, four type II lineages, and three type II neuroblasts are visible. (C) Enlargement of the region boxed in (B). All neuroblasts are Dpn^+; a subset of type I neuroblasts are Rx^+, while type II neuroblasts are Rx^-. INPs are also Rx^-. Rx is expressed in a subset of neuronal progeny in both type I and type II lineages. (D) *brat* mutant brain lobe (120 hours ALH) contains many Dpn^+ neuroblasts, but these cells do not express Rx. Rx is expressed in a few of the $Pros^+$ cells, all of which in this focal plane are neurons and do not express Dpn. (E) *lgl pins* brain lobe (120 hours ALH) in which Rx is expressed in a subset of ectopic Dpn^+ neuroblasts. Rx expression is limited to cells expressing Pros, which in *lgl pins* also express Ase (Figure 1E, inset) and are likely derived from expansion of type I neuroblasts. The $Pros^-$ regions (type II-derived) are entirely Rx^-. White arrow: Rx^- type I neuroblast; white arrowheads: Rx^+ type I neuroblasts; yellow arrows: Rx^- type II neuroblasts; mCD8::GFP driven by *R9D11-Gal4* marks a subset of type II lineages, but not the type II neuroblasts themselves (Bayraktar et al., 2010). Shown outlined here with yellow dashed lines are several dorso-medial type II lineages [DM 2, 3, 4, 5, and 6 in (B); DM 2, 3, and 4 in (C)]. Scale bars: 100 µm in (B), (D), and (E); 10 µm in (C).

We next wanted to find genes expressed in type II neuroblasts but not type I neuroblasts, as there are currently no known markers specifically expressed in type II neuroblasts. We reasoned that transcripts expressed in type II neuroblasts should be enriched in genotypes that overproduce type II neuroblasts: *brat, lgl* and *lgl lgd*. We found one small cluster enriched in two of the three mutants (*brat* and *lgl lgd*) (Figure 4A). This cluster contains just 10 genes, seven encoding transcription factors. To verify the expression pattern of this gene cluster, we examined the expression of one gene product, Optix. Optix is a conserved homeodomain-containing transcription factor required for eye development (Kenyon et al., 2005; Seimiya and Gehring, 2000; Toy et al., 1998). Consistent with our microarray data, we found that most of the Optix expression in the brain is indeed restricted to type II lineages; four of the six dorso-medial type II neuroblasts (DM1, 2, 3, and 6) express Optix, as do most of the INPs, GMCs, and neurons in these lineages (Figures 4B and 4C). In addition, recent work has shown that another gene in this cluster, *pointedP1*, is also preferentially expressed in type II neuroblasts (Sijun Zhu and Y.N. Jan, personal communication). The other two dorso-medial type II lineages (DM4 and 5) exhibit some expression of Optix in a subset of neuronal progeny, but it is absent from the neuroblasts and INPs in these lineages (Figures 4B and 4C and not shown). In addition, a single dorsal type I neuroblast expresses Optix (Figure 4C). Inspection of mutant brains further confirmed the type II-biased expression of Optix, in that *brat* mutant brains exhibit a marked increase in $Optix^{+}$ neuroblasts (Figure 4D), and in *lgl pins*, the increase in Optix is almost exclusively in a $Pros^{-}$ (type II-originating) region of the brain (Figure 4E). Our results indicate that our clustering relationships can be used to predict type I/type II expression bias with good

accuracy. We conclude that Optix is primarily expressed in type II but not type I neuroblasts, and that Optix and the other nine xxx genes in this cluster are excellent candidates for regulators of type II neuroblast identity.

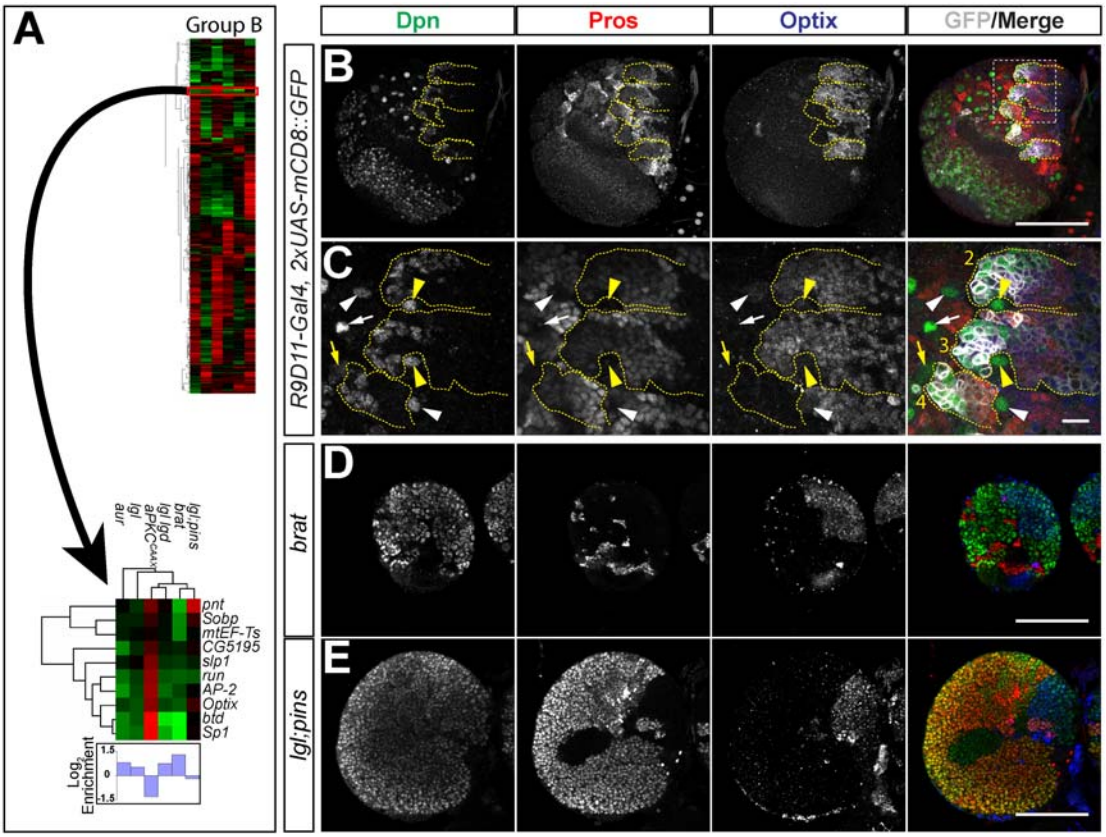

Figure 4: Identification of a cluster with type II-biased expression
(A) Position in group B of a sub-cluster in which genes are expressed higher in *brat* and *lgl lgd* than in other genotypes. Enrichment shown is averaged over all genes in the sub-cluster. (B) Wild-type brain lobe (120 hours ALH). Visible are multiple type I neuroblasts as well as several type II neuroblasts and their lineages. Most type I neuroblasts are Optix$^-$, while four of the six dorso-medial type II neuroblasts are Optix$^+$ (DM1,2,3,6); Optix is absent from type II neuroblasts DM 4&5 and their INPs, but present in a subset of their progeny. (C) Enlargement of the box in (B) shows both Optix$^+$ and Optix$^-$ type I and type II neuroblasts. Shown are type II lineages DM 2, 3, and 4. Optix is nearly absent from the entire DM4 lineage. (D) *brat* brain (120 hours ALH) shows that Optix is expressed in a dorso-medial region in which nearly all cells are Dpn$^+$ ectopic neuroblasts. (E) *lgl pins* brain (120 hours ALH) exhibits Optix expression primarily in Dpn$^+$ Pros$^-$ regions (type II-derived ectopic neuroblasts). White arrows: Optix$^-$ type I neuroblasts; white arrowheads: Optix$^+$ type I neuroblasts; yellow arrow: Optix$^-$ type II neuroblast; yellow arrowheads: Optix$^+$ type II neuroblasts. GFP driven by *R9D11-Gal4* marks dorso-medial type II lineages, but not the type II neuroblasts themselves. Shown outlined here with yellow dashed lines are several dorso-medial type II lineages [DM 2, 3, 4, 5, and 6 in (B); DM 2, 3, and 4 in (C)]. Scale bars: 100 µm in (B), (D), and (E); 10 µm in (C).

Identification of genes predicted to be expressed in neuroblasts but not neurons

To determine whether the ectopic neuroblasts in the mutant brains express wild-type neuroblast genes, we tested whether genes known to be expressed primarily or exclusively in neuroblasts are found in group A; indeed all such positive control genes (with the exception of the type II-negative *pros* and *ase* genes) are represented in group A, including *worniu* (*wor*)*, deadpan,* and *CyclinE* (Table 2). Conversely, neuronal and glial genes are excluded from group A and found in group C [e.g. *elav, glial cells missing* (*gcm*)*,* and *reversed polarity* (*repo*)] (Table 2). In addition, there is a good correlation between the number of neuroblasts in each mutant brain and the level of enrichment shown for group A genes (Figures 1B and 2B).Thus, the genes in group A are likely to be expressed in both type I and type II neuroblasts, but not in neurons or glia. Conversely, genes in group C are likely to be expressed in differentiated neurons or glia, but not in neuroblasts. We conclude that ectopic neuroblasts are similar transcriptionally to wild-type neuroblasts, and thus the mutant genotypes represent an enriched source of neuroblast-expressed mRNA.

We next determined the gene ontology (GO) terms that represent the neuroblast-enriched group A genes and the neuron/glia-enriched group C genes. We found that group A genes are strongly enriched for several GO terms, including cell cycle and ribosome biosynthesis – processes expected in neuroblasts that must repeatedly divide and grow (Figures 5A and 5B). For example, a small sub-cluster in group A exhibits a very significant enrichment for genes involved in DNA replication ($p<10^{-15}$); this process is not significantly represented in any other cluster ($p>.01$ for all other group A genes combined; Figure 5A). Conversely, we found group C to be significantly enriched for the

Table 2. Representation of cell type-specific genes within microarray groups A, B, and C.

Gene	Cell type (in larval brain)	Array group	References
wor	neuroblast	A	(Ashraf et al., 2004)
dpn	neuroblast	A	(Bier et al., 1992)
cycE	neuroblast	A	(Caldwell and Datta, 1998)
grh	neuroblast	A	(Uv et al., 1997)
dmyc	neuroblast	A	(Betschinger et al., 2006)
E(spl)mγ	neuroblast	A	(Almeida and Bray, 2005)
insc	neuroblast	A	(Parmentier et al., 2000)
mira	neuroblast	A	(Peng et al., 2000)
pros	type I neuroblast, GMC, neurons	B	(Bello et al., 2008; Boone and Doe, 2008; Bowman et al., 2008)
ase	type I neuroblast, GMC	B	(Bowman et al., 2008)
elav	neurons	C	(Robinow and White, 1988)
gcm	glia	C	(Hosoya et al., 1995)
repo	glia	C	(Xiong et al., 1994)

GO terms morphogenesis, signal transduction, and differentiation – all expected for postmitotic neurons and glia (Figure 5B). In addition, neuropeptide signaling and cell morphogenesis are both significantly enriched ($p<10^{-20}$ and $p<10^{-21}$, respectively) in distinct sub-clusters (Figure 5C). We conclude that group A is enriched for genes that are expressed in neuroblasts but not differentiated neurons and glia, and group C is primarily composed of genes expressed in postmitotic neurons and glia.

Functional analysis of genes predicted to be expressed in neuroblasts but not neurons

To determine if group A genes are required for neuroblast survival, proliferation, or self-renewal, we performed RNAi knock-down experiments. We selected genes for which transgenic RNAi stocks were available from the Vienna *Drosophila* RNAi Center, and we further restricted our analysis to those genes with human orthologs in order to enhance the relevance of our study to issues of human stem cell function (Figure 6). This

resulted in our analyzing 691 RNAi lines representing 595 genes. We reasoned that loss of function of genes with critical functions in neuroblasts would cause defective central nervous system development and eventual lethality, as seen in other genotypes which

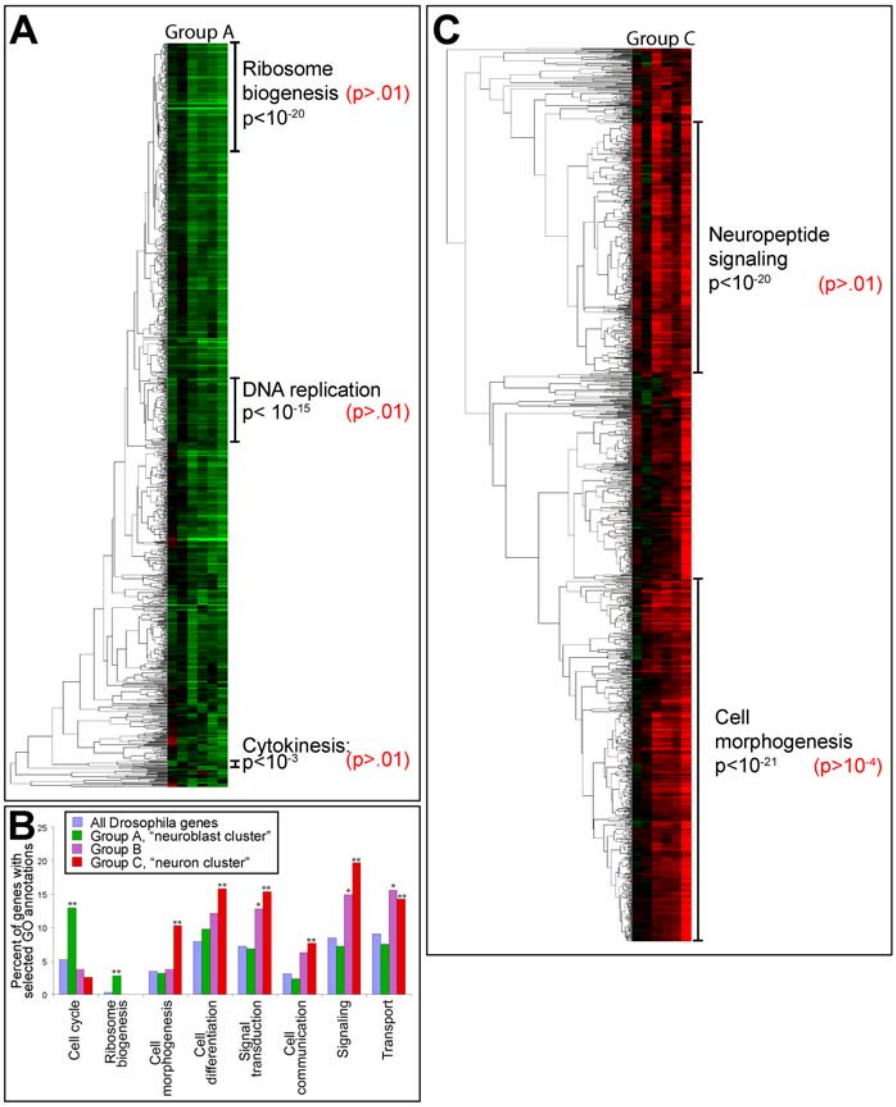

Figure 5: Gene Ontology terms enriched in each group
(A) Group A, the "neuroblast cluster" with three sub-clusters marked in which the indicated GO annotations are significantly enriched compared to all *Drosophila* genes. Each value in red indicates the enrichment of the GO term in all group A genes *excluding* the adjacent sub-cluster. (B) Chart depicting the percent of all *Drosophila* genes characterized by select GO annotations as well as percent of genes in each group with those annotations. Asterisks indicate significant enrichment of GO term compared with all *Drosophila* genes (*: p<.05; **: p<.001). (C) Group C, the "neuron cluster" with sub-clusters labeled indicating significantly enriched GO terms; each value in red indicates the enrichment of the GO term in all group C genes *except* the adjacent sub-cluster.

affect neuroblast function. Thus we screened for lethality in the progeny of males from each RNAi line crossed to *wor-Gal4 UAS-Dicer2* flies at 30°C [*wor-Gal4* drives expression in neuroblasts (Albertson et al., 2004), while *Dicer2* improves RNAi efficacy (Dietzl et al., 2007)]. Of the 691 RNAi lines tested, 195 (28%) cause lethality or semi-lethality (Figure 6A). We found that of the genes for which we tested multiple RNAi lines, 84% exhibit the same lethality phenotype for both lines. Few RNAi lines cause embryonic lethality at 30°C, and in these cases larval stages were obtained by setting up crosses at 18°C and shifting larvae to 30°C after embryogenesis. The lack of a lethal phenotype in 72% of the lines may be due to either inefficient RNAi knock-down of gene expression or the non-essential function of the gene in larval neuroblasts. Hence we restricted our subsequent analysis to the 28% of lines with a lethal or semi-lethal phenotype.

We tested each of the lethal or semi-lethal genes for a change in neuroblast number, reasoning that genes expressed in neuroblasts but not neurons may play a role in neuroblast survival, quiescence, identity, asymmetric division, or self-renewal. We performed the same RNAi experiments as above and determined the number of Dpn^+ $Mira^+$ central brain neuroblasts (optic lobe neuroblasts were not assayed). We found that nearly one half of lethal genes (86) cause a significant change in central brain neuroblast numbers (Figures 6B and 6C; Supplementary Table 1). A majority of these changes are decreases in neuroblast number, as expected based on the predicted expression of these genes in neuroblasts. Two genes known to regulate neuroblast numbers were detected in the screen, *mira* and *aurora borealis*, thereby validating this approach. Importantly, all of these genes have clear mammalian orthologs. We conclude that our RNAi-based

screening method has yielded a list of 84 new candidates for regulating neuroblast self-renewal (Supplementary Table 1).

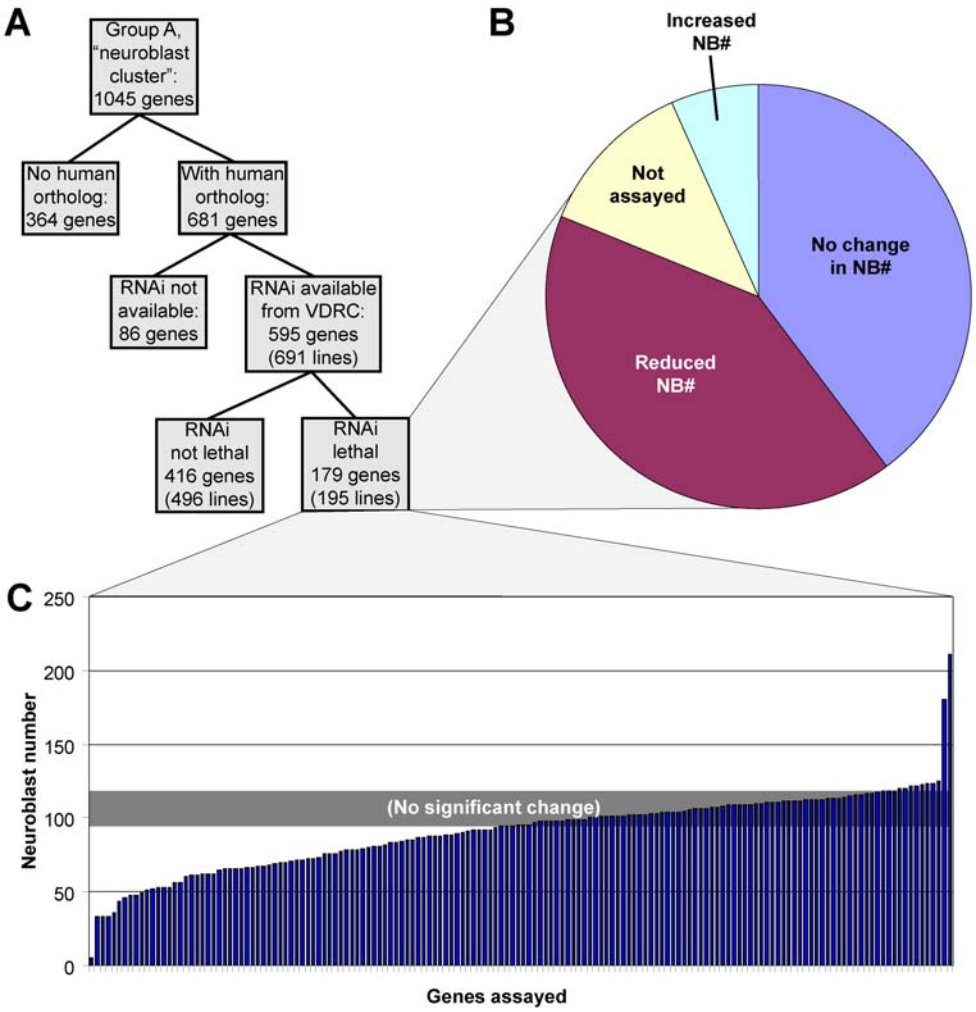

Figure 6: RNAi screen identifies neuroblast homeostasis genes
(A) Flowchart describing the selection of 691 RNAi lines used in this screen. (B) Neuroblast number gain and loss phenotypes of the 179 genes for which RNAi knock-down caused lethality. (C) Neuroblast numbers per brain lobe of the genes which were assayed for neuroblast number phenotype.

DISCUSSION

It has previously been shown that co-clustering of genes in expression profiling data is likely to reflect physical or genetic interactions (Ge et al., 2001; Jansen et al.,

2002) and participation in the same pathways (van Noort et al., 2003). Our results are consistent with these conclusions. For example, we identified a small group of 11 genes containing the only two genes known to be expressed in type I but not type II neuroblasts, and showed that a third gene has a similar pattern of expression – thus all genes in this cluster are likely to be expressed in type I but not type II neuroblasts. Furthermore, the strong enrichment of GO terms in small sub-clusters within both group A and group C (Figure 5) indicates that genes within these clusters are likely to share similar functions or processes.

Differences between type I/type II neuroblasts are caused by a small number of genes

At the outset of this study, we expected to find a large group of genes that were differentially expressed in type II versus type I neuroblasts, because these neuroblasts have such strikingly different cell lineages. However, we were only able to identify a few gene clusters that were differentially regulated in such a type I/type II consistent manner – the 11 genes in the *pros/ase* cluster depleted in type II neuroblasts and the 10 genes enriched in type II neuroblasts (Figures 3A and 4A). This suggests that the small number of genes that we identified may play a disproportionately large role in generating differences between type I and type II neuroblasts. Might *pros* and *ase* be the only genes regulating type I/type II differences? Both Ase and Pros can promote cell cycle exit (Choksi et al., 2006; Dominguez and Campuzano, 1993; Li and Vaessin, 2000; Southall and Brand, 2009; Wallace et al., 2000), which may result in the Ase^{+} $Pros^{+}$ type I progeny taking a GMC identity and undergoing just one terminal division and the Ase^{-} $Pros^{-}$ type II progeny taking an INP identity and continuing to proliferate. Indeed, the

misexpression of either Ase or low levels of Pros in type II neuroblasts is sufficient to cause the loss of INPs and/or their premature cell cycle exit, thereby decreasing lineage size toward the size of type I neuroblasts (Bayraktar et al., 2010; Bowman et al., 2008). However, it is unclear what is required to fully transform these cells into type I neuroblasts; addressing this question will require additional molecular markers (some provided by our work here) and tracing the axon projections of the progeny of these "transformed" neuroblasts (e.g. do they now fail to make intrinsic neurons of the adult central complex?). The fact that mutants in *ase* and *pros* do not transform type I neuroblasts into type II neuroblasts (Bowman et al., 2008; Weng et al., 2010) indicates that other genes, perhaps some in the *pros/ase* cluster described here, are also important for specification of type I neuroblast identity.

Group A: candidate neuroblast-specific genes and neuroblast homeostasis regulators

We found that the neuroblasts in each mutant have remarkably similar expression profiles, as shown by the extensive list of similarly expressed genes in group A and by the list of genes with depleted expression in mutant brains, represented by group C. We believe that these categories provide lists of genes that are representative of those expressed in neuroblasts and neurons, respectively, based on all known neuroblast-specific genes showing up in group A and all known neuron- or glial-specific genes being excluded from group A.

Our RNAi-based screen helped to substantiate this claim, in that a substantial percentage of group A genes caused lethality when subjected to neuroblast-specific knock-down. We do not believe that off-target effects lent a significant amount of error to

these lethality data for two reasons: (1) a similar percentage of lethal and non-lethal RNAi lines (about 30%) had more than one non-specific target, which indicates that the observed lethality was due to specific target knock-down; and (2) a majority of genes (about 85%) caused the same lethality phenotype when targeted with multiple independent RNAi lines. Interestingly, we found that many RNAi lines caused lethality with no concomitant change in neuroblast numbers (Figure 6). We believe this to be due to neuroblast defects which disrupt normal brain development without causing neuroblast loss, per se. For instance, neuroblast failure to make the proper number or type of progeny might be expected to cause such a phenotype. It will be interesting to investigate the specific effects these essential genes have on neuroblast function. We note that all of the putative regulators of neuroblast homeostasis identified here have mammalian orthologs; these genes are excellent candidates for regulating self-renewal of mammalian neural stem cells.

Group B: expression in subsets of neuroblasts or neurons?

Group B genes apparently are not expressed in all neuroblasts like the group A genes, nor in all neurons or glia like group C genes. However, group B genes are more likely to be expressed in subsets of neurons, not neuroblasts, because group B genes as a whole have an over-representation of GO terms more similar to group C than to group A (Figure 5B). Why then are group B genes excluded from group C, the neuron cluster? One possible explanation is that different neuroblast lineages are affected in each mutant, and thus different subsets of neurons are missing in each mutant. If different neuroblast lineages express different genes (which seems likely), then each mutant would be missing a unique subset of neural differentiation genes, leading to the cluster being excluded from

group C. This model raises the intriguing possibility that group B sub-clusters may represent lineage-specific genes.

It is also possible that the mutant genotypes themselves may cause unique transcriptional differences, leading to a cluster of genes in group B. For example, several small sub-clusters in group B are expressed differently only in *aPKC*^{CAAX} brains (Supplementary Figure 2). These transcriptional differences are not correlated with the number of type I or type II neuroblasts. Instead, these genes appear to be differentially expressed in response to elevated aPKC. *Drosophila* aPKC has been best studied as a component of the apical complex in mitotic neuroblasts, and its capacity for causing ectopic self-renewal has been shown to be reliant on both its catalytic activity and its membrane localization (Atwood and Prehoda, 2009; Lee et al., 2006b). However, aPKC has been ascribed a role in neuroblast proliferation as well as in polarity (Chabu and Doe, 2008; Rolls et al., 2003), and a vertebrate homolog, PKC-ζ, was shown to possess a nuclear role in both proliferation of neural progenitors and neuronal cell fate specification (Sabherwal et al., 2009). These observations are consistent with a role of aPKC in causing transcriptional differences.

CONCLUSIONS

Our findings highlight the importance of expression profiling of multiple genotypes. This method allowed us to get a more reliable picture of the group A genes expressed in neuroblasts, because genes with lineage-specific or genetic background-specific changes in expression appeared to be focused into group B, where they do not interfere with the clustering of groups A and C. In addition, we identified two small sub-

clusters of genes in group B that are excellent candidates for being preferentially expressed in type I or type II neuroblasts, for which there have been few examples to date. Finally, we conclude that group A genes are likely to be expressed in neuroblasts, and our functional studies have identified 84 genes that are conserved in mammals and required for regulating neuroblast numbers in *Drosophila*. Future phenotypic analysis in *Drosophila* will determine whether these genes regulate neuroblast survival, quiescence, asymmetric cell division, and/or self-renewal. Future studies on the expression and function of orthologous genes in mouse neural progenitors and human stem cells (IP or neural) will reveal whether they have conserved roles from flies to mammals.

BRIDGE TO CHAPTER III

Chapter II described the high-throughput identification of putative neuroblast and neuronal genes, as well as the RNAi-based verification of the neuroblast function of a subset of genes. Using this approach, we identified numerous genes responsible for the maintenance of wild type neuroblast number in the central brain. Next we wanted to focus on a single candidate gene and investigate its specific role in the important cell fate decision of self-renewal versus differentiation. In Chapter III, I describe the analysis of one gene from the RNAi screen described in Chapter II: a previously uncharacterized gene, *CG4973*, which we have renamed *midlife crisis.* Surprisingly, we found that *midlife crisis* is not involved in neuroblast self-renewal, per se, but in the maintenance of neuronal differentiation, establishing it as a uniquely important cell identity gene in the central nervous system.

CHAPTER III

MIDLIFE CRISIS ENCODES A CONSERVED ZINC FINGER PROTEIN REQUIRED TO MAINTAIN NEURONAL DIFFERENTIATION IN *DROSOPHILA*

This work is in press at the journal *Development* as of June, 2013. Chris Q. Doe and I conceived of all experiments. Adam J. Struck and I performed the RNA-seq experiments; I performed all other experiments. CQD and I wrote the manuscript. CQD was the principal investigator for this work.

INTRODUCTION

A defining characteristic of stem cells is the ability to produce daughters that retain stem cell fate (self-renew) as well as daughters that begin the process of differentiation. The robust adoption of these distinct fates is critical both for the retention of stem cell pool size and for the production of differentiated progeny. In the *Drosophila* CNS, neuroblasts divide in a manner asymmetric by both progeny size and fate. The majority of neuroblasts – termed "type I" neuroblasts – divide to generate a self-renewed neuroblast and a smaller ganglion mother cell (GMC), which divides only once more to produce neurons or glia. Additionally, there are eight bilateral "type II" neuroblasts in the brain that repeatedly divide to self-renew and generate smaller intermediate neural progenitors (INPs); INPs each undergo a series of molecularly asymmetric divisions (similar to type I neuroblast divisions) to self-renew and generate a series of 4-6 GMCs (Bayraktar et al., 2010; Bello et al., 2008; Boone and Doe, 2008; Bowman et al., 2008; Izergina et al., 2009). Type I and II neuroblasts have emerged as an important model for studying stem cell self-renewal and differentiation.

Type I neuroblast asymmetric division results in the segregation of cell fate determinants into the GMC. The coiled-coil protein Miranda (Mira) is a scaffolding protein localized to the basal cortex of the neuroblast during mitosis and partitioned into the daughter GMC (Ikeshima-Kataoka et al., 1997; Matsuzaki et al., 1998; Shen et al., 1997; Shen et al., 1998). Mira cargo proteins include the translational repressor Brain tumor (Brat), the homeodomain transcription factor Prospero (Pros), the RNA-binding protein Staufen and its cargo, *pros* mRNA (Broadus et al., 1998; Ikeshima-Kataoka et al., 1997; Lee et al., 2006b; Matsuzaki et al., 1998; Shen et al., 1997; Shen et al., 1998). A separate protein complex containing Partner of Numb (Pon) and Numb are also segregated into the GMC. These fate determinants inhibit neuroblast self-renewal, direct cell cycle exit, promote neuronal differentiation, and prevent tumor formation (Doe, 2008; Knoblich, 2010). Type II neuroblast lineages contain INPs which are particularly susceptible to dedifferentiation. Loss of function of *earmuff* (*erm*), *barricade* (*barc*), *brat*, or misexpression of activated Notch all lead to failure in neuronal differentiation and an expansion of type II neuroblast or INP fates (Bowman et al., 2008; Neumuller et al., 2011; Weng et al., 2010).

One of the most critical differentiation factors is the Pros transcription factor. In type I neuroblasts, Pros protein and mRNA are asymmetrically segregated into the GMC. In the GMC, *pros* mRNA is translated and Pros protein is imported into the nucleus (Broadus et al., 1998; Knoblich et al., 1995; Spana and Doe, 1995), where Pros represses cell cycle genes and promotes differentiation (Choksi et al., 2006; Li and Vaessin, 2000). Therefore, it is critical that GMCs inherit Pros from the neuroblast; in a Pros loss of function, GMCs fail to exit the cell cycle, derepress neuroblast fate genes, and can form

tumorous overgrowths (Bello et al., 2006; Betschinger et al., 2006; Choksi et al., 2006; Lee et al., 2006). In the embryo, Pros protein can be detected in the GMC and transiently in newly-born embryonic neurons (Srinivasan et al., 1998). In the larval CNS, on the other hand, Pros is detected in nearly all postmitotic neurons. In contrast to its tumor suppressor function in the GMC, the function of Pros in postmitotic larval neurons is unknown.

Here we report the identification of *midlife crisis* (*mdlc*; Flybase: *CG4973*) as a gene required to maintain neuronal differentiation in larval neuroblast lineages. *mdlc* encodes a conserved protein containing both a RING domain (common in E3 ubiquitin ligase proteins) and a CCCH-type zinc finger (often found in RNA-binding proteins involved in splicing). The yeast and human orthologs of Mdlc have been reported as components of the spliceosome (Bessonov et al., 2008; Goldfeder and Oliveira, 2008). Clonal analysis of larval neuroblast lineages demonstrates that loss of *mdlc* function results in the loss of neuronal Pros expression followed by loss of the neuronal marker Elav and ectopic expression of the neuroblast transcription factors Asense (Ase) and Deadpan (Dpn). This results in single neuroblast clones containing multiple Dpn^{+} Ase^{+}, $Elav^{-}$ $Pros^{-}$ cells, more like neuroblasts than neurons in terms of molecular marker expression, indicating that Mdlc promotes the maintenance of neuron fate gene expression in larval neurons and inhibits neuronal dedifferentiation. Mdlc also functions in neuroblasts to promote their characteristic rapid (~2 hour) cell cycle. Surprisingly, these roles for Mdlc do not require the RING domain, while the CCCH-type zinc finger is essential for all known Mdlc CNS functions.

MATERIALS AND METHODS

Fly stocks

Fly stocks used were *UAS-Dicer2* (*Dcr2*)*, inscuteable-Gal4, tubulin-Gal4, UAS-mCD8:GFP, elav-Gal4; UAS-Dcr2* and w^{1118}*; Df(3R)ED6027* from the Bloomington *Drosophila* Stock Center (BDSC); w^{1118}*; P[GD11492]v42015* and w^{1118}*; P[KK101588]VIE-260B* from the Vienna *Drosophila* RNAi Center (VDRC); $mdlc^{c04701}$ from the Exelixis collection at Harvard Medical School; *worniu-Gal4* (Albertson et al., 2004); *UAS-Dcr2; worniu-Gal4 asense-Gal80; UAS-mCD8:GFP* (Neumuller et al., 2011). MARCM clones were generated using *hs-flp70; tub-Gal4 UAS-mCD8:GFP; FRT82B tub-Gal80*; this was crossed to *FRT82B* to generate control clones and *FRT82B* $mdlc^{c04701}$ to generate mutant clones.

Immunostaining and confocal microscopy

Antibodies used were rat anti-Dpn (1:50; Doe lab), guinea pig anti-Mira (1:1000 or 1:2000; Doe lab), chicken anti-GFP (1:2000; Aves Labs, Inc., Tigard, OR USA), rabbit anti-Ase (1:2000; (Brand et al., 1993), mouse anti-Pros (1:1000; Developmental Studies Hybridoma Bank [DSHB] MR1A), rat anti-Elav (1:50; DSHB 7E8A10), mouse anti-Repo (1:4; DSHB), and guinea pig anti-Mdlc (1:100; this study). Secondary antibodies were used at 1:500 and were from Molecular Probes (Eugene, OR USA) or from Jackson Immunoresearch (West Grove, PA USA). Antibody staining was performed as described (Carney et al., 2012) with the following change: block used was 2.5% normal goat serum + 2.5% normal donkey serum. Microscope images were captured using either a Zeiss700 or a Zeiss710 confocal microscope.

EdU incorporation

EdU (Life Technologies, Carlsbad, CA USA) was delivered to larvae by incorporating it into their food to a final concentration of 100 μg/mL. Detection was performed according to the manufacturer's instructions.

RNAi and MARCM

RNAi experiments were performed at 30°C, and larvae were removed immediately prior to dissection of brains for immunostaining. MARCM clones were induced at 24±4 hours after larval hatching (ALH) by heat shock at 37°C for 20 minutes. Larvae were then raised at 23°C until late third instar, when brains were dissected for immunostaining.

Molecular cloning and antibody generation

UAS-mdlc and *UAS-RNF113a* constructs were generated by PCR-mediated mutagenesis (where applicable) and cloned into a *pUAST-attB* vector (Bischof et al., 2007) using XhoI (5′) and XbaI (3′) overhangs. Forward primers included a kozak sequence (CAAC) immediately upstream of the start codon, as well as sequence coding for an N-terminal hemagglutinin (HA) epitope tag (amino acid sequence YPYDVPDYA). All transgenes were site-specifically inserted via PhiC31 integrase-mediated transgenesis at the VK37 site on chromosome 2L (GenetiVision Corporation, Houston, TX USA).

For the generation of the anti-Mdlc antibody, sequence coding for the N-terminal 165 residues of Mdlc was PCR amplified and cloned into a pET-15b vector using NdeI (5′) and XhoI (3′) overhangs. The vector has been modified to encode an N-terminal penta-Histidine epitope tag and has a TEV (Tobacco Etch Virus), rather than thrombin, cleavage site between the His tag and peptide-of-interest sequence. Protein was expressed

in BL21 *E. coli* cells and purified by adsorption to Ni-NTA agarose (Qiagen Inc., Valencia, CA USA), followed by elution via cleavage with TEV protease. Antibody was raised in guinea pig (Alpha Diagnostics, San Antonio, TX USA) and affinity purified using the ImmunoLink Plus Immobilization Kit (Thermo Scientific, Rockford, IL USA) according to the manufacturer's instructions.

To verify the presence of the transposon insertions c04701 and c04654, we performed PCR on genomic DNA extracted from single flies from both lines. We used the following primers: 5′ TACCATCACTAGCCGGGAAG 3′, which recognizes the *mdlc* 5′ UTR upstream of the transposon insertion site, and 5′ CCTCGATATACAGACCGATAAAACACATG 3′, which recognizes a site near the 3′ end of the Piggybac 'PB' transposon (Thibault et al., 2004), allowing us to determine not only the presence of the transposon insertions, but also to verify the annotated minus orientation.

RNA-seq

Genotypes used were *elav-Gal4; UAS-Dcr2/+* and *elav-Gal4; UAS-Dcr2/UAS-mdlc RNAi*. We performed two biological replicates for both treatments. Larvae were raised at 25^{o}C for 48 hours and then transferred to a 30^{o}C environment for the remainder of their development. Total RNA was isolated from wandering third instar larval brains using previously described methods (Miller et al., 2009). Mature mRNA transcripts were enriched using the Poly(A)Purist Kit (Ambion, Inc., Foster City, CA USA). The mRNA was fragmented to generate 250-400 base long fragments using the NEBNext Magnesium RNA Fragmentation Module (New England Biolabs, Ipswich, MA USA). The fragmented mRNA was then prepared for Illumina sequencing using the ScriptSeq v2

RNA-seq Library Preparation Kit (Epicentre Biotechnologies, Madison, WI USA). In brief, the mRNA was reverse transcribed into cDNA and then Illumina adapters were attached to each end. Unique barcodes were attached to each sample and then were multiplexed into a single lane on an Illumina sequencing flow cell for sequencing on an Illumina HiSeq 2000 machine. This resulted in 16.5-29.3 million single-end 100 base-pair reads from each barcoded library. The reads were aligned against the *Drosophila melanogaster* release 5.69 genome sequence (Ensembl) using GSNAP (Wu and Nacu, 2010) (http://research-pub.gene.com/gmap/) allowing for up to 7 mismatches and set to look for novel splice junctions.

Detecting differentially expressed genes

The number of reads mapping to the exons of each gene was quantified using the HTseq-count python script in "union" mode (http://www-huber.embl.de/users/anders/HTSeq/doc/index.html). The BAM alignment files for each sample and a downloaded Ensembl GTF file were used as inputs. Differentially expressed genes were called using the DEseq package (Anders and Huber, 2010) following the developer's recommended workflow in R (http://www.R-project.org). We required an adjusted p-value of less than 0.01 to regard a gene as differentially expressed.

Detection of differential intron retention (DIR) using MISO

The software package MISO (Katz et al., 2010) was used to detect differentially regulated introns across samples. An "exon-centric" MISO analysis was performed according to the developer's recommended workflow using single-end reads (http://genes.mit.edu/burgelab/miso/docs/). The BAM alignment files produced by GSNAP and a custom set of *pros* annotations as well as the alternative events file

provided by MISO were used as inputs. To identify highly reliable *mdlc*-associated DIR events, we required the following stringent criteria be met: 1) the absolute value of the difference ($\Delta\Psi$) > 0.2; 2) the sum of inclusion and exclusion reads is greater than 10 (≥1 inclusion read and ≥1 exclusion read); 3) the Bayes factor > 1000; 4) these criteria must be met for all comparisons between wild type and *mdlc* RNAi samples; and 5) the event did not appear differentially regulated between wild type biological replicates. Alternative events were visualized using the included sashimi_plot software from the MISO package (http://genes.mit.edu/burgelab/miso/docs/sashimi.html).

RESULTS

mdlc RNAi results in ectopic Dpn$^+$ neuroblast-like cells

We initially observed ectopic Dpn$^+$ cells in the *mdlc* RNAi central brain lobes in an RNAi screen (Carney et al., 2012). The screen used the neuroblast-specific *worniu-Gal4* [*wor-Gal4* (Albertson et al., 2004)] driving expression of *UAS-Dcr2* to increase RNAi efficacy (Dietzl et al., 2007) and single *UAS-RNAi* transgenes targeting transcripts enriched in neuroblasts. Wild type type I neuroblast lineages contain a single large Dpn$^+$ neuroblast (Fig. 1A), whereas knockdown of *mdlc* results in small ectopic Dpn$^+$ cells at a distance from the large parental neuroblast (Fig. 1B). This indicates that the ectopic Dpn$^+$ cells are not the result of symmetric neuroblast divisions, which always results in adjacent Dpn$^+$ neuroblasts (Cabernard and Doe, 2009). To determine if the ectopic Dpn$^+$ cells might be dedifferentiating neurons, we stained for Pros, which marks GMCs and young neurons in wild type lineages (Fig. 1A). Indeed, we observed loss of Pros in *mdlc*

knockdown brains (Fig. 1B). We conclude that *mdlc* RNAi leads to ectopic Dpn and loss of Pros in type I neuroblast progeny.

We next determined the *mdlc* knockdown phenotype in type II neuroblasts, which generate small Dpn^+ intermediate neural progenitors (INPs); each INP undergoes asymmetric cell division to generate small Dpn^- $Pros^+$ GMCs and neurons (Bayraktar et al., 2010; Bello et al., 2008; Boone and Doe, 2008; Bowman et al., 2008; Izergina et al., 2009). We performed *mdlc* RNAi knockdown using *UAS-Dcr2; wor-Gal4 ase-Gal80; UAS-mCD8:GFP,* which results in Gal4-induced gene expression specifically in type II neuroblasts (Neumuller et al., 2011). In wild type, each type II neuroblast lineage contains a single large Dpn^+ Ase^- neuroblast and several adjacent smaller Dpn^+ Ase^+ INPs (Fig. 1C). In contrast, *mdlc* knockdown resulted in many ectopic small Dpn^+ Ase^+ cells, as well as many Dpn^+ Ase^- cells (Fig. 1D). Thus, the ectopic Dpn^+ cells could have either neuroblast or INP identity. We also observed a strong loss of Pros in the *mdlc* knockdown type II lineage (compare Fig. 1C,D), similar to the loss of Pros phenotype following *mdlc* knockdown in type I lineages (Fig. 1A,B). In addition, we observed loss of some type II neuroblasts, fewer cells per lineage, and enlarged cell size (data not shown); these phenotypes will be explored below. We conclude that *mdlc* knockdown causes ectopic Dpn^+ neuroblast-like (or INP-like) cells and loss of $Pros^+$ cells in both type I and type II neuroblast lineages.

***mdlc* RNAi results in failure to maintain Pros in postmitotic neurons**

The loss of Pros expression in *mdlc* RNAi knockdown appeared more penetrant than the ectopic Dpn^+ cells, suggesting that it might be the earliest detectable phenotype,

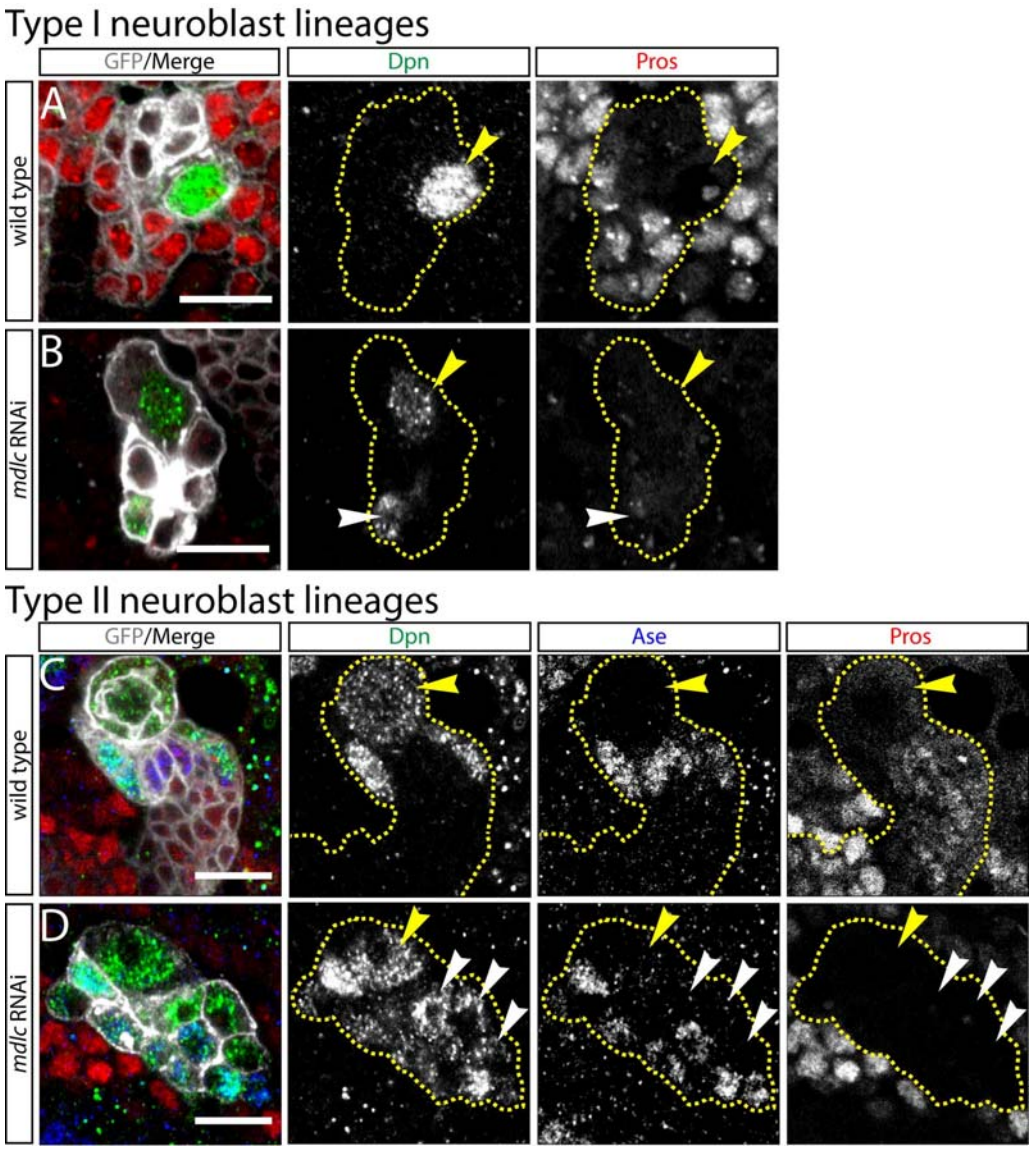

Figure 1. Knockdown of *mdlc* causes ectopic Dpn and loss of Pros in larval neuroblast lineages.

(A,B) Type I central brain neuroblast lineages. Yellow dashed lines indicate lineage boundaries; yellow arrowheads mark type I neuroblasts. (A) Wild type lineages show a single large Dpn^+ neuroblast and multiple smaller $Pros^+$ neurons (genotype: *wor-Gal4 UAS-Dcr2; UAS-mCD8:GFP*). (B) *mdlc* RNAi causes small ectopic Dpn^+ cells (white arrowhead) as well as a strong loss of Pros in many neurons (genotype: *wor-Gal4 UAS-Dcr2 / UAS-mdlc RNAi; UAS-mCD8:GFP*).

(C,D) Type II central brain neuroblast lineages. Yellow dashed lines indicate lineage boundaries; yellow arrowheads mark type II neuroblasts. (C) Wild type lineage showing Dpn^+ type II neuroblast (yellow arrowhead) and Dpn^+ mature INPs; Ase is absent from the type II neuroblast but present in mature INPs and GMCs (genotype: *UAS-Dcr2; wor-Gal4 ase-Gal80; UAS-mCD8:GFP*). (D) *mdlc* RNAi lineage showing ectopic Dpn^+ cells; some are Ase^+ indicating an INP fate, while others are Ase^- indicating reversion to a type II neuroblast-like fate (genotype *UAS-Dcr2; wor-Gal4 ase-Gal80 / UAS-mdlc RNAi; UAS-mCD8:GFP*). Pros staining is strongly reduced. Yellow arrowhead marks the presumptive type II neuroblast; white arrowheads indicate ectopic Dpn^+ Ase^- cells. Scale bars: 10 μm.

and may directly result in the ectopic Dpn expression. In this section, we address whether *mdlc* knockdown leads to a failure to properly establish Pros expression in new-born GMCs or failure to maintain Pros in mature postmitotic neurons. In subsequent sections, we will address the timing of the Pros vs. Dpn phenotypes and whether loss of Pros is sufficient to derepress Dpn in neurons.

To determine if *mdlc* knockdown results in failure to establish or to maintain Pros expression, we used EdU labeling to identify new-born GMCs or mature postmitotic neurons derived from type I neuroblasts. To unambiguously identify new-born GMCs, we fed 48h ALH larvae EdU for 4 hours and immediately fixed and stained brains; using this approach, only the neuroblast and new-born GMCs are EdU^{+}. We found that both wild type and *mdlc* knockdown brains have Pros present in all new-born GMCs (Fig. 2A,B; quantified in C). Similar results were observed for type II neuroblast lineages (Fig. 2G,H). Of course, this could be due to a lag in *mdlc* RNAi knockdown of Mdlc protein, but RNAi knockdown begins over 36h prior to assaying GMC gene expression and we detected no Mdlc protein over background levels (Supplementary Figure 1; See Appendix B for all Chapter III Supplementary materials). We conclude that Mdlc is not required to establish Pros expression in new-born GMCs.

To unambiguously identify mature postmitotic neurons, we fed 48h ALH larvae EdU for 4 hours and then "chased" for 36h with EdU-negative food; this approach ensures that only postmitotic neurons are EdU^{+} (neuroblasts dilute out all EdU labeling, and new-born GMCs are born during the EdU-negative chase period). We found that some wild type neurons lose Pros protein, as expected due to downregulation of Pros in the most mature neurons in the lineage (Fig. 2D) but significantly more *mdlc* knockdown

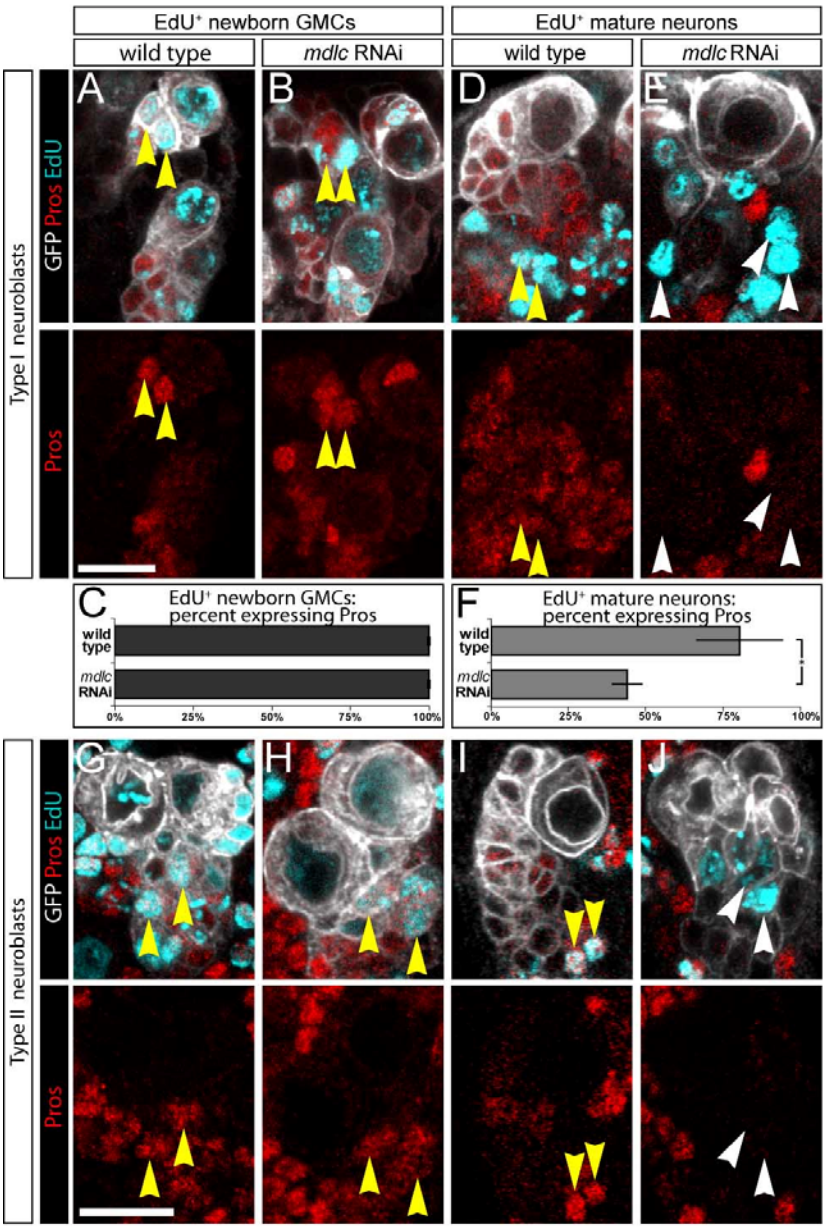

Figure 2. *mdlc* RNAi results in repression of Pros in postmitotic neurons.
(A-F) Type I neuroblasts. (A-C) New-born GMCs marked by a 4h pulse of EdU and immediately stained; both wild type GMCs (A) and *mdlc* RNAi GMCs (B) are $Pros^{+}$; quantified in (C). (D-F) Mature neurons marked by a 4h pulse of EdU followed by a 36h EdU-free chase; wild type neurons are $Pros^{+}$ (D) whereas *mdlc* RNAi neurons (E) fail to maintain Pros; quantified in (F). Yellow arrowheads mark EdU^{+} $Pros^{+}$ cells; white arrowheads mark EdU^{+} $Pros^{-}$ cells. Scale bar, 10 μm.
(G-J) Type II neuroblasts. (G,H) New-born GMCs marked by a 4h pulse of EdU and immediately stained; both wild type GMCs (G) and *mdlc* RNAi GMCs (H) are $Pros^{+}$. (I,J) Mature neurons marked by a 4h pulse of EdU followed by a 36h EdU-free chase; wild type neurons are $Pros^{+}$ (I) whereas *mdlc* RNAi neurons (J) fail to maintain Pros. Yellow arrowheads mark EdU^{+} $Pros^{+}$ cells; white arrowheads mark EdU^{+} $Pros^{-}$ cells. Scale bar, 10 μm.

neurons do not have detectable Pros protein (Fig. 2E; quantified in F). Similar results were observed for type II neuroblast lineages (Fig. 2I,J). We conclude that *mdlc* RNAi results in failure to maintain Pros levels in "middle-aged" neurons, leading to our choice of gene name (*midlife crisis*).

mdlc mutants fail to maintain Pros and Elav in postmitotic neurons

To confirm that the *mdlc* RNAi phenotype is due to loss of function of the *mdlc* gene (and not an off-target RNAi effect) we analyzed a genetic lesion in the *mdlc* gene. *mdlc* is on chromosome 3R and resides within an intron of *CG4390* on the opposite strand (Fig. 3A). Two mutant alleles are annotated at the *mdlc* locus (c04701 and c04654); both are Piggybac transposons from the Exelixis collection (Thibault et al., 2004). Both are annotated to be inserted at the same locus in the 5′ UTR, 10 bp upstream of the *mdlc* translation start site (Fig. 3A). We used PCR analysis to confirm the presence of c04701, which is homozygous lethal (see Methods); however, PCR analysis indicated that the c04654 line, which is viable, does not contain an insertion at the *mdlc* locus. Thus, we renamed the insertion c04701 as $mdlc^{c04701}$ and used it for subsequent genetic analysis of *mdlc* function.

We analyzed $mdlc^{c04701}$ mutant phenotypes using the MARCM method (Lee and Luo, 2001). Wild type type I neuroblast clones possess a single neuroblast that is Dpn^{+}, Ase^{+}, and Cyclin E $(CycE)^{+}$, and all neurons in the clone are $Pros^{+}$ with the exception of the oldest neurons at the most distal tip of the clone (Fig. 3B and data not shown). In contrast, $mdlc^{c04701}$ mutant clones frequently have cells in the middle of the clone that have lost Pros expression (Fig. 3C), which is very rarely observed in wild type neuroblast

clones. This phenotype is less penetrant but remarkably similar to the *mdlc* RNAi phenotype (Figs 1, 2). We conclude that both *mdlc* RNAi and *mdlc* mutants lead to the failure to maintain Pros levels in "middle-aged" neurons.

We next wanted to determine the timing of Pros loss and Dpn derepression, as well as to examine a second neuroblast marker, Ase, and a second neuronal differentiation marker, Elav, within *mdlc* mutant clones. First, we co-stained for Pros, Dpn, and Ase. GMCs lying adjacent to the parental neuroblast typically co-express Pros and Ase and sometimes have weak Dpn due to perdurance from the neuroblast; therefore they were not considered to be ectopically expressing cells and were excluded from our counts. We observed some clones where the $Pros^{-}$ cells do not show detectable Dpn or Ase (Fig. 3C); some have derepressed Ase but are Dpn^{-} (Fig. 3D); and some are both Dpn^{+} and Ase^{+} (Fig. 3E; quantified in Fig. 3H,I). Similar results were observed for the

Figure 3. (*Next page*) *mdlc* mutants fail to maintain Pros and Elav in postmitotic neurons.
(A) Genomic context of *mdlc,* which resides in the intron of *CG4390* on the opposite strand. The Piggybac transposon *c04701* is inserted in the 5′ UTR of *mdlc*.
(B) Wild type MARCM clone showing $Pros^{+}$ neurons lacking expression of Dpn and Ase.
(C-E) *mdlc* mutant MARCM clones, chosen to indicate the progression of neuronal phenotypes shown in (J). (C) Middle-aged neurons (lying midway between the neuroblast and the oldest, most distal neurons) lack Pros expression (yellow arrowheads) but have not upregulated Dpn or Ase. (D) Middle-aged neurons lack Pros expression (yellow arrowheads) and Ase is derepressed in one of them (white arrow). (E) Middle-aged neurons lack Pros expression (arrow and arrowheads); Ase is derepressed in several of these cells (e.g., arrow), and two Ase^{+} cells have also derepressed Dpn (arrowheads).
(F-G) *mdlc* mutant neurons lose Elav. (F) Wild type neurons in which Pros and Elav are present but Ase is absent.
(G) *mdlc* mutant MARCM clone showing the loss of both Pros and Elav from a small number of neurons (arrow and arrowhead); Ase is derepressed in one of these cells (white arrow). Scale bar: 10 μm.
(H) Quantification of neuronal phenotypes in $mdlc^{-}$ clones (n=54 clones). Numbers are given as percentage of the total number of cells in the clone. (*: $p<.05$; **: $p<.01$.)
(I) Comprehensive quantification of absolute numbers of non-wild type neuronal phenotypes in *mdlc* mutant clones, showing the overlap of $Pros^{-}$, Ase^{+}, and Dpn^{+} neurons (n=54 clones). This analysis demonstrates that the majority of Dpn^{+} cells comprise a subset of Ase^{+} neurons [81 of 94 Dpn^{+} neurons (86%) are also Ase^{+}], and that the Ase^{+} cells are a subset of $Pros^{-}$ neurons [164 of 174 Ase^{+} neurons (94%) are $Pros^{-}$].
(J) Model illustrating the progression of *mdlc* mutant clone phenotypes. New-born neurons are $Pros^{+}$ $Elav^{+}$, Dpn^{-} Ase^{-}. Middle-aged neurons first lose Pros expression, then they lose Elav expression and derepress Ase, and finally they derepress Dpn.

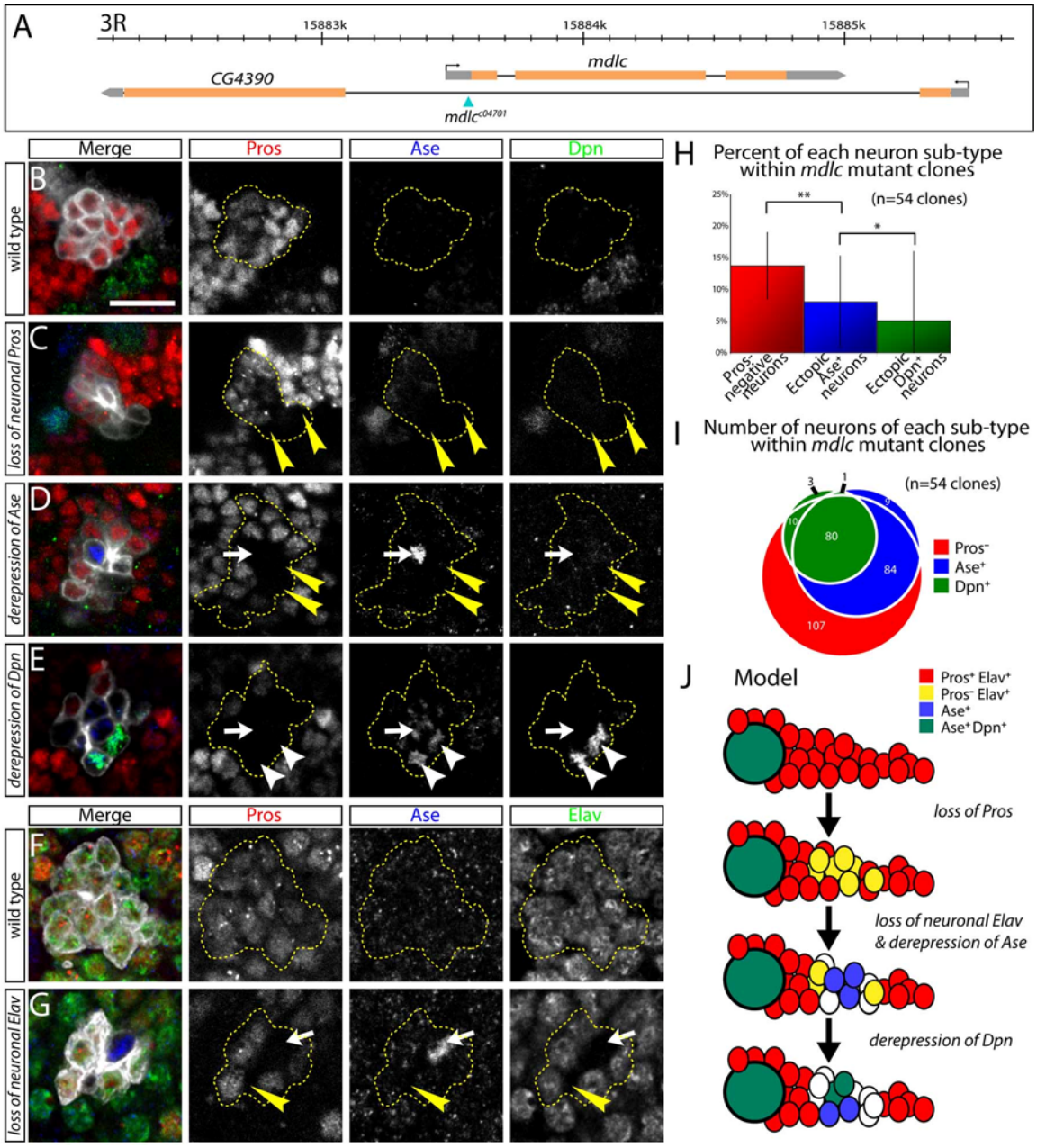

well-characterized neuronal differentiation marker Elav (mouse: Hu): it is present in all wild type neurons, but absent from most (but not all) of the Pros$^-$ neurons in *mdlc* mutants (Fig. 3F,G). We conclude that that loss of the neuronal differentiation factor Pros precedes the loss of the neuronal marker Elav and the ectopic expression of the neuroblast markers Dpn and Ase in *mdlc* mutant neurons (Fig. 3J).

mdlc mutant neuroblasts have a longer cell cycle and reduced clone size

In addition to the neuronal dedifferentiation phenotype shown by *mdlc* RNAi and mutant clones, we noticed that *mdlc* mutant neuroblast lineages have fewer cells than comparable wild type lineages. We quantified this phenotype by counting total cells in both mutant and wild type clones generated in 96 hours (slightly longer or shorter intervals were normalized to 96h). We found that wild type clone size averages 89 ± 35 cells, which is significantly larger than the *mdlc* mutant clone size (43 ± 19 cells; $p<10^{-5}$; Fig. 4A). Decrease in clone size was not due to apoptosis, as there was no increase in the apoptotic marker Caspase-3 in *mdlc* mutant clones (Fig. 4B). Instead, we found that the cell cycle is extended: wild type neuroblast clones generate 14 ± 4 EdU^+ cells over 8 hours of EdU labeling, but *mdlc* mutants only generate 4 ± 6 EdU^+ cells during the same span ($p<10^{-5}$; Fig. 4C). The variability stems from the fact that some mutant neuroblasts generate near wild type numbers of progeny while others fail entirely to undergo S-phase during the EdU incorporation period (not shown). We conclude that Mdlc promotes larval neuroblast cell cycle progression.

Mdlc is a conserved zinc finger-containing protein with broad expression

mdlc encodes a well-conserved protein that is 70% similar (58% identical) to the human ortholog, RNF113a. Both proteins have two conserved zinc finger domains: a CCCH zinc finger, commonly found in RNA-binding proteins involved in splicing, and a RING domain, frequently found in E3 ubiquitin ligases (Fig. 5A). In order to analyze the expression patterns and sub-cellular localization of Mdlc, we generated an antibody against the N-terminal 165 amino acids. Immunofluorescent staining with this antibody

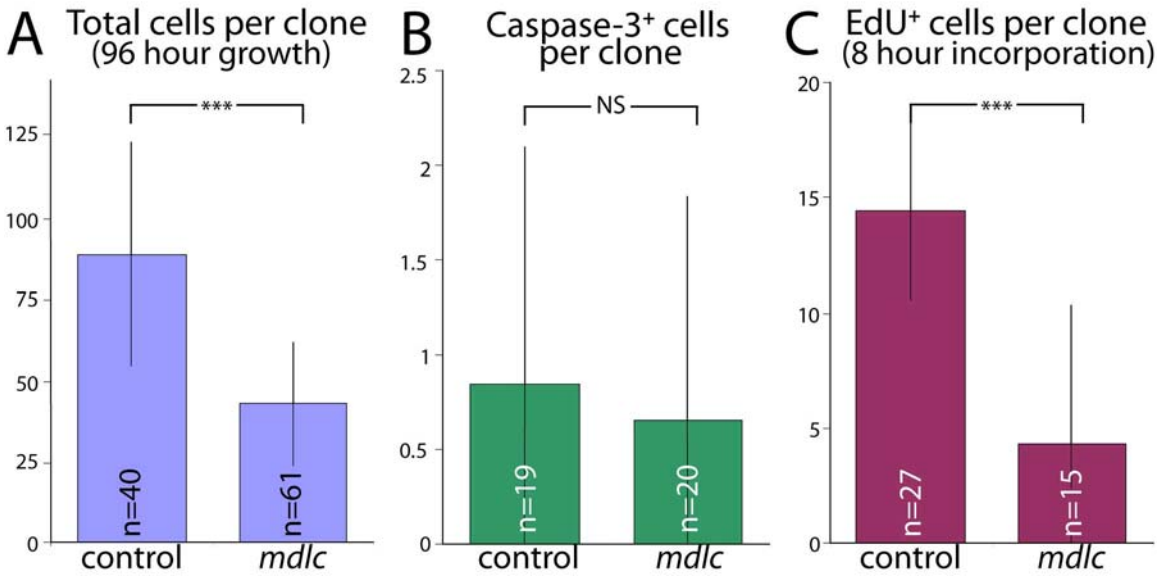

Figure 4. *mdlc* mutant neuroblasts have an extended cell cycle.
(A) Comparison of wild type and *mdlc*$^{-}$ clone sizes; time between clone induction and dissection was 96 hours. (B) Number of Caspase-3^{+} cells per clone in wild type and *mdlc*$^{-}$ clones. (C) Comparison of wild type and *mdlc*$^{-}$ EdU incorporation rates. EdU incorporation period was eight hours prior to dissection. (***: $p<10^{-5}$; NS: not significantly different.)

revealed that Mdlc is a nuclear protein that is detected throughout the larval CNS (Fig. 5B). Performing *mdlc* knockdown using *inscuteable-Gal4* (*insc-Gal4*) to drive *UAS-mdlc RNAi* causes a marked decrease in Mdlc immunostaining in the larval central brain (but not in glia or optic lobe; Fig. 5C), validating the efficacy of *mdlc* RNAi and the specificity of the Mdlc antibody. Furthermore, mosaic clones of homozygous *mdlc*^{c04701} cells show strongly reduced Mdlc levels compared to the surrounding wild type cells, indicating that *mdlc*^{c04701} is a strong loss of function allele (Fig. 5D). Upon close examination of larval brains, we found that Mdlc is expressed ubiquitously, including expression in NBs, neurons, and glia, as judged by staining with antibodies against Mira, Elav, and Reversed polarity (Repo), respectively (Fig. 5E,E′). We also found that Mdlc is broadly expressed in larval imaginal discs (Fig. 5F), in the embryo (Fig. 5G), and in the adult ovary (Fig. 5H).

Mdlc zinc finger deletions reveal different requirements for CCCH and RING domains

We have shown that Mdlc has context-dependent functions: it is required for neuroblast cell cycle progression as well as required in middle-aged neurons to prevent dedifferentiation. Here we asked whether the CCCH and RING zinc finger domains (proposed to regulate RNA splicing and ubiquitination, respectively) have specific roles in either of these two phenotypes. We generated fly lines expressing different Mdlc domains under *UAS* control: full-length Mdlc ($Mdlc^{FL}$); Mdlc lacking the CCCH zinc finger ($Mdlc^{\Delta CCCH}$); Mdlc lacking the RING domain ($Mdlc^{\Delta RING}$); Mdlc with the RING domain isoleucine 266 mutated to alanine ($Mdlc^{I266A}$), which is reported to interfere with E2/E3 interactions in RING domain-containing E3 ubiquitin ligases (Mulder et al., 2007); and Mdlc lacking both zinc fingers ($Mdlc^{\Delta CCCH+RING}$). In addition, we generated a transgene expressing the full-length human ortholog of Mdlc (RNF113a). Each construct included a hemagglutinin (HA) epitope tag at the N-terminus of the protein (Fig. 6A).

Figure 5. (*Next page*) Mdlc is a zinc finger protein with broad expression in the CNS and other tissues.
(A) Mdlc protein and the human ortholog RNF113a have a conserved CCCH zinc finger and a C-terminal RING domain. Numbers represent amino acids.
(B-D) Anti-Mdlc shows ubiquitous nuclear localization of Mdlc that is lost upon *mdlc* loss of function. (B) Wild type. Mdlc is expressed in larval brain neuroblasts (yellow arrowhead) and glia (yellow arrow). (C) *mdlc* RNAi in central brain neuroblasts and their immediate progeny reduces Mdlc protein staining in the central brain, particularly in neuroblasts (yellow arrowhead), identified by the presence of Dpn (not shown). Mdlc expression is still visible in glia (yellow arrow) and in the optic lobe (OL), where the RNAi transgene was not expressed. (D) Homozygous mutant $mdlc^{c04701}$ clones (yellow dashed lines) show a strong reduction in Mdlc protein.
(E-E′) In the wild type larval brain, Mdlc protein is detected in neuroblasts (wide arrowheads), neurons (narrow arrowheads), and glia (arrows), which can be identified based on staining with antibodies against Mira, Elav, and Repo, respectively.
(F-H) Mdlc is ubiquitously expressed in all tissues examined. (F) Representative imaginal disc showing ubiquitous Mdlc; all imaginal discs show similar staining. (G) Embryo showing ubiquitous Mdlc, including in neuroblasts (yellow arrowheads), identified by Mira expression (not shown). (H) Mdlc is detected throughout the adult ovariole. Scale bars: 100 μm in B, C, D, F, G, and H; 10 μm in E.

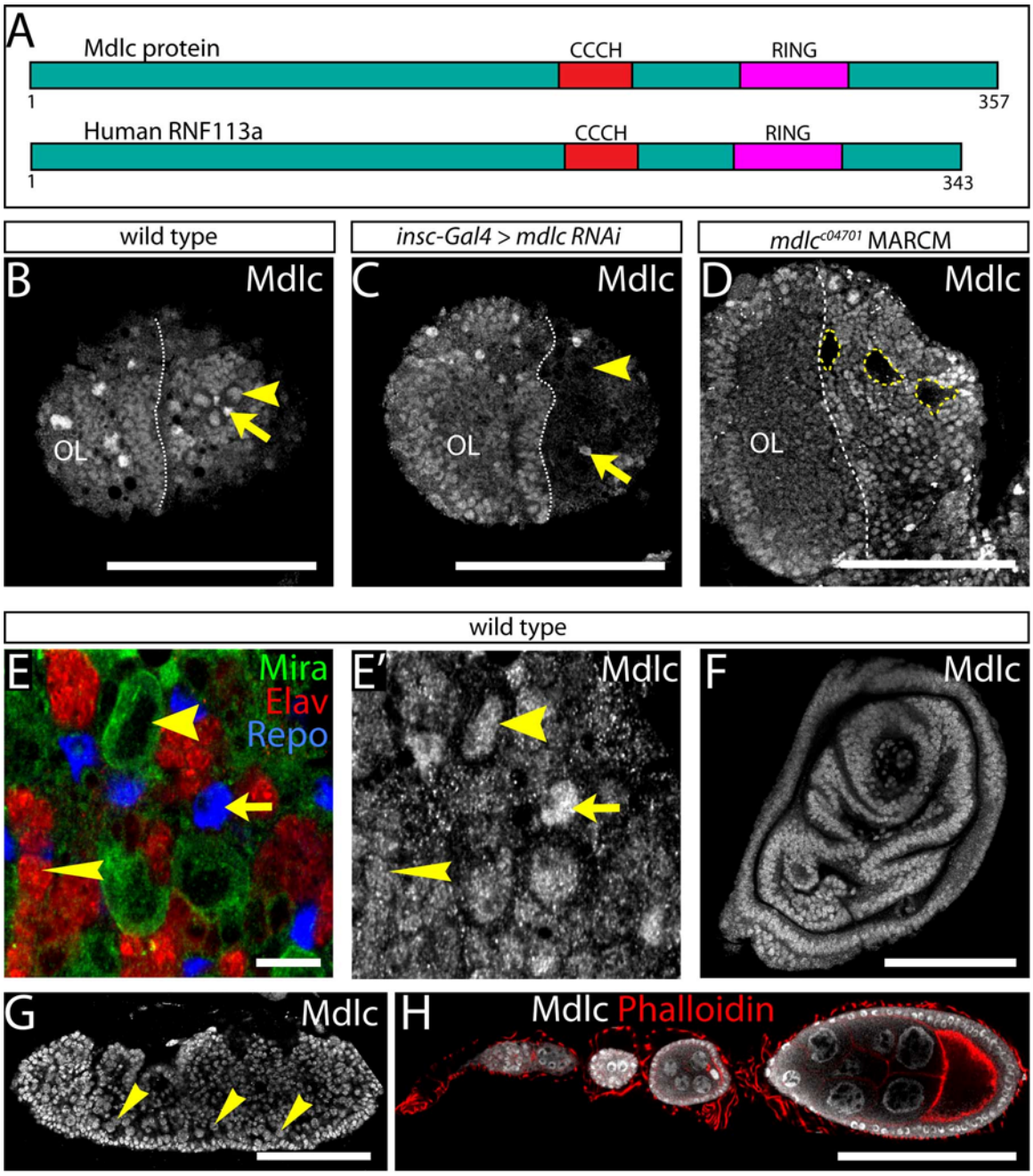

We assayed the ability of each construct to rescue mutant phenotypes by monitoring both the most penetrant neuronal phenotype (loss of Pros) and the most severe phenotype (ectopic Dpn expression), as well as neuroblast lineage size and amount of EdU incorporation. We found that misexpression of Mdlc^{FL}, or the full-length human ortholog RNF113a, in *mdlc* mutant clones is able to significantly rescue clone size (Fig.

6B) and completely rescue the loss of Pros/ectopic Dpn^{+} phenotypes (Fig. 6C). In addition, ubiquitous expression of either protein using *tubulin-Gal4* is able to rescue $mdlc^{c04701}$/*Df(3R)ED6027* hemizygotes to viability (Table 1). These results indicate that the epitope-tagged full-length version of Mdlc is functional and that Mdlc and its human ortholog have conserved cellular functions.

Next we tested the ability of Mdlc proteins lacking RING domain function ($Mdlc^{\Delta RING}$ or $Mdlc^{I266A}$) to rescue *mdlc* mutant phenotypes. We found that expression of $Mdlc^{\Delta RING}$ or $Mdlc^{I266A}$ fully rescues $mdlc^{c04701}$/*Df(3R)ED6027* hemizygotes to viability (Table 1), as well as fully rescues *mdlc* mutant neuroblast lineage size and cell cycle phenotypes and prevents dedifferentiation phenotypes of neurons (Fig. 6B,C and data not shown). We conclude that the RING domain, and its presumptive function in ubiquitination, is not required for any known aspect of the Mdlc neural function; the role of the conserved Mdlc RING domain remains to be elucidated.

Lastly, we tested the requirement of the CCCH domain to rescue *mdlc* mutant phenotypes; this domain has been implicated in regulating splicing in yeast and human cells (Bessonov et al., 2008; Coltri and Oliveira, 2012; Goldfeder and Oliveira, 2008). We found that both $Mdlc^{\Delta CCCH}$ and $Mdlc^{\Delta CCCH+RING}$ proteins fail to rescue $mdlc^{c04701}$/*Df(3R)ED6027* hemizygotes to viability (Table 1). In addition, both proteins fail to rescue both the *mdlc* mutant lineage size and neuronal dedifferentiation (Fig. 6B,C); in fact, expression of $Mdlc^{\Delta CCCH}$ (but not $Mdlc^{\Delta CCCH+RING}$) in *mdlc* mutant clones results in even smaller clones than the *mdlc* mutant alone (Fig. 6B). Furthermore, misexpression of $Mdlc^{\Delta CCCH}$, but none of the other proteins, using the neuroblast driver *insc-Gal4*, causes pupal lethality (Table 1). As the misexpression of $Mdlc^{\Delta CCCH}$ in wild

Table 1: Summary of rescue and misexpression phenotypes

	Mdlc^{FL}	**RNF113a**	**Mdlc$^{\Delta CCCH}$**	**Mdlc^{I266A}**	**Mdlc$^{\Delta RING}$**	**Mdlc$^{\Delta CCCH+RING}$**
Rescues viability in *mdlc* mutants?	Y	Y	N	Y	Y	N
Rescues clone size in *mdlc* clones?	partial*	Y	N**	Y	Y	N
Rescues Pros/Ase/Dpn phenotypes in *mdlc* clones?	Y	Y	N	Y	Y	N
Driving with *insc-Gal4* causes lethality in wt background?	N	N	Y	N	N	N
Clonal misexpression yields wt clone size in wt background?	Y	Y	Y	Y	Y	Y
Clonal misexpression causes Pros/Ase/Dpn phenotypes in wt background?	N	N	N	N	N	N

* Mdlc^{FL} misexpression significantly increases clone size over *mdlc^{c04701}*, but not to wt clone size.
** Smaller clones than *mdlc^{c04701}* alone.

type brains results in lethality, and misexpression in *mdlc* mutant clones causes a more severe clone size phenotype than the *mdlc* mutant alone, we suspected that this truncated protein may have a dominant negative function. To investigate this, we expressed each of the Mdlc proteins in wild type MARCM clones and monitored both clone size and Pros/Dpn levels in neurons. We found that none of the constructs assayed caused cell cycle or neuronal dedifferentiation phenotypes (Table 1), suggesting that the presence of wild type Mdlc is sufficient to suppress any dominant negative effects in neuroblast lineages; it remains unclear why pan-neuroblast expression of Mdlc$^{\Delta CCCH}$ causes lethality. We conclude that the Mdlc CCCH zinc finger domain is critical for all known neural functions of Mdlc.

RNA-seq of *mdlc* RNAi brains reveals *prospero* splicing defects

The *Saccharomyces cerevisiae* ortholog of Mdlc, Cwc24p, is known to have a role in RNA splicing (Coltri and Oliveira, 2012; Goldfeder and Oliveira, 2008), and the human ortholog, RNF113a, associates with the pre-activation spliceosome in HeLa cells (Bessonov et al., 2008). We hypothesized that the most penetrant phenotype in *mdlc* loss

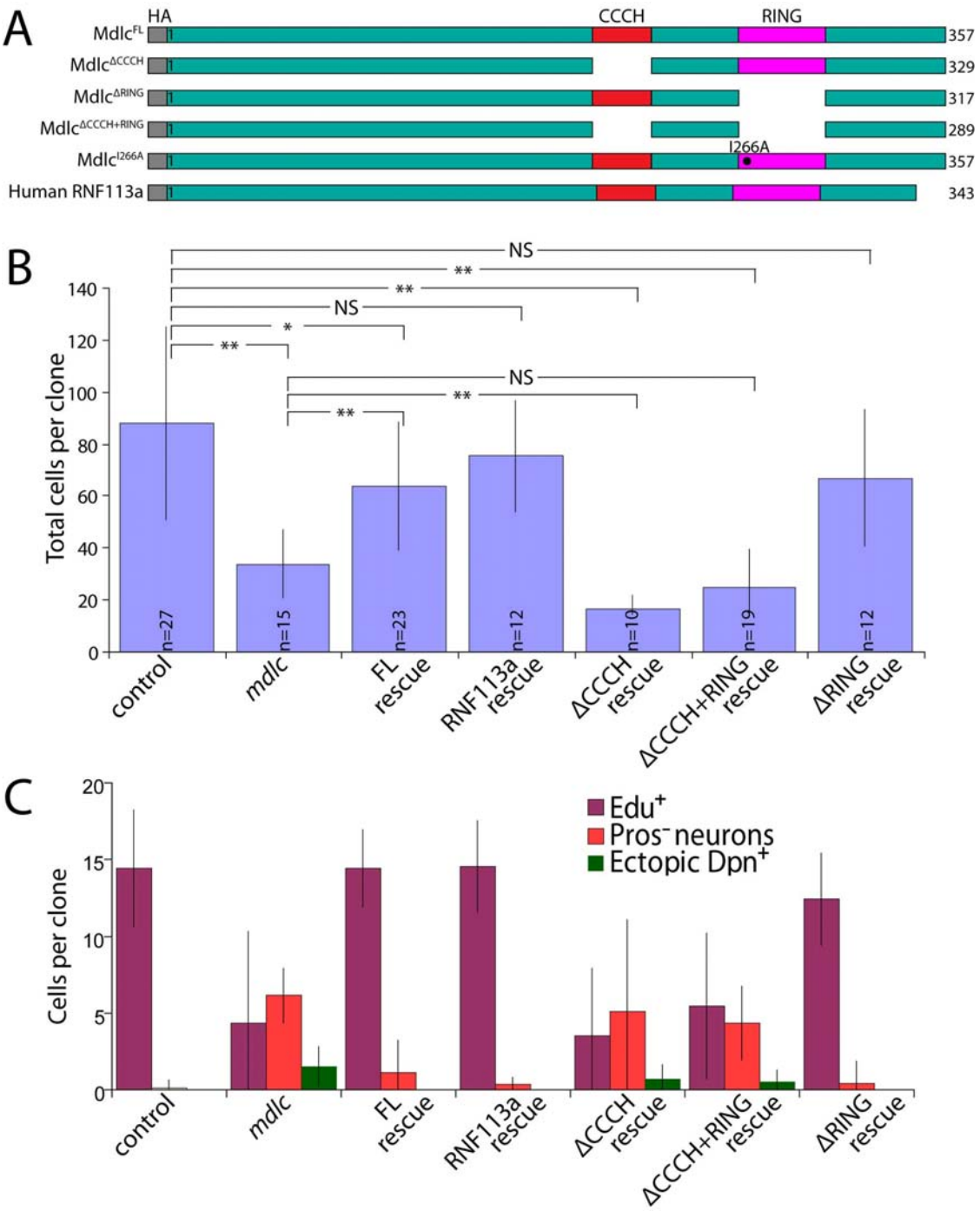

Figure 6. The CCCH zinc finger of Mdlc is critical for CNS function, while the RING finger is dispensable.

(A) Schematic of protein truncations used in misexpression and rescue experiments. (B) Quantification of clone size in rescue experiments. Time between clone induction and brain dissection was 96 hours. Control and *mdlc*$^{-}$ clone sizes are given as references. (*: p<.01; **: p<10^{-3}; NS: not statistically different.) (C) Quantification of EdU cells per clone (eight-hour EdU incorporation), Pros^{-} neurons per clone, and ectopic Dpn^{+} cells per clone in rescue experiments. Expression of Mdlc^{FL}, RNF113a, or Mdlc$^{\Delta RING}$ rescues all of these phenotypes while expression of Mdlc$^{\Delta CCCH}$ or Mdlc$^{\Delta CCCH+RING}$ fails to rescue.

of function, the loss of neuronal Pros, may be due to splicing defects. We performed transcriptional and differential splicing analyses to compare wild type to *mdlc* loss of function brains. We used *elav-Gal4* to drive a *mdlc* RNAi construct in all neuroblasts and neurons of the larval brain, which strongly decreased *mdlc* transcript and protein levels (data not shown). We extracted mRNA from wild type and *mdlc* RNAi brains and performed whole-transcriptome RNA-seq (see Methods). Detailed transcriptome analysis will be presented elsewhere; here we focus on the effect of *mdlc* loss of function on the *pros* transcript.

We observed a striking reduction in *pros* transcript levels in *mdlc* RNAi brains (3.45-fold reduction, $p<10^{-26}$), consistent with the loss of Pros protein observed by immunostaining (Figs 1-3). Next we assayed differential intron retention (DIR) events within the *pros* transcript. *pros* has multiple alternatively spliced isoforms with a maximum of seven introns, three of which are within the 5′ UTR in the longest isoforms (Fig. 7A). Two introns within the *pros* coding domain were found to be differentially spliced (asterisks in Fig. 7A,B). Interestingly, intron 4 is retained more frequently in wild type than in *mdlc* RNAi (44.5% in wild type versus 23.0% in *mdlc* RNAi), whereas intron 5 is retained more in the *mdlc* RNAi (32.0% in wild type versus 77.8% in *mdlc* RNAi) (Fig. 7B). The observation that the loss of Mdlc causes differential effects on introns 4 and 5 indicates that Mdlc is involved in splice-specific regulation, rather than a general function in promoting splicing efficiency.

The intron that is retained more in *mdlc* RNAi brains is one of a small group of *Drosophila* twintrons (Scamborova et al., 2004). The *pros* twintron is composed of two nested pairs of splice sites whose usage is mutually exclusive, and the choice of which

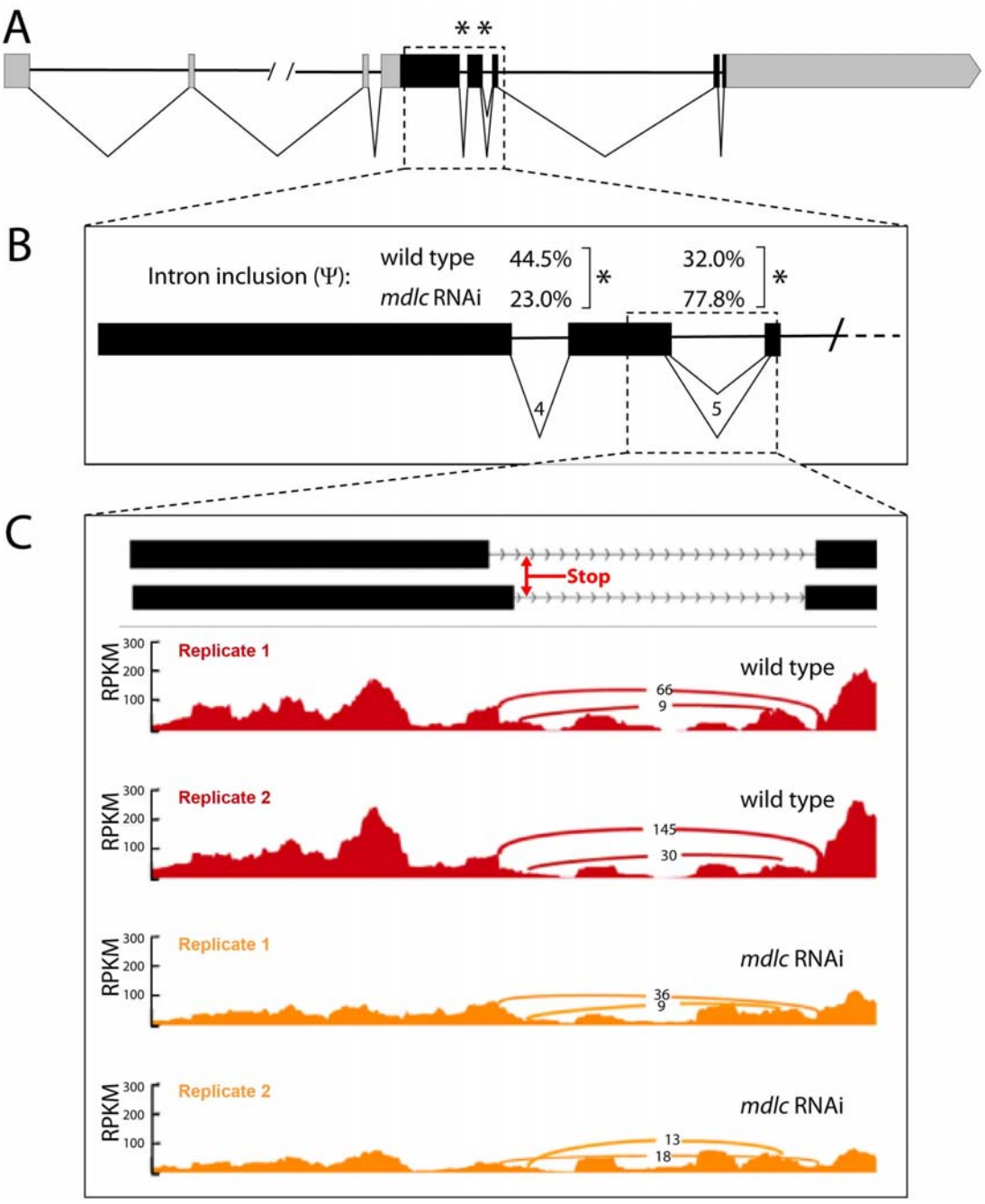

Figure 7. *mdlc* RNAi results in reduced levels and aberrant splicing of *pros* mRNA.
(A) The *pros* locus. Black boxes indicate exonic regions, grey boxes indicate UTRs, and horizontal lines indicate introns. Percent spliced in (psi, Ψ) estimates were generated by the MISO software package. Asterisks indicate introns that met our stringent criteria (see Methods) for calling introns that are retained at differential levels between the wild-type and *mdlc* RNAi samples.
(B) Higher resolution view of the region boxed in (A) showing *pros* introns 4 and 5, which exhibit differential intron retention between wild type and *mdlc* RNAi.
(C) Read density, RPKM (reads per kilobase per million), across the *prospero* twintron and its flanking exons. Arches represent the number of reads mapping to each exon-exon junction. Retention of the twintron results in the introduction of a premature stop codon, as indicated.

splice sites to use is developmentally regulated (Scamborova et al., 2004). Failure to splice the twintron results in a premature stop codon (Fig. 7C), which is likely to result in the nonsense-mediated decay of the *pros* transcript. We utilized the sashimi_plot utility within MISO (Katz et al., 2010) to visualize the read density across the twintron in both wild type and both *mdlc* RNAi samples (Fig. 7C). We found that reads per kilobase per million mapped reads (RPKM) across the twintron decreased more in wild type than in *mdlc* RNAi, illustrating the more frequent retention of the twintron in the absence of Mdlc than in wild type (Fig. 7C). We conclude that Mdlc is a regulator of mRNA splicing in *Drosophila*. Furthermore, the *pros* splicing defects in *mdlc* loss of function reduce the number of *pros* transcripts, which could contribute to the loss of Pros observed in middle-aged neurons.

DISCUSSION

Function of Mdlc and Pros in larval postmitotic neurons

We have identified Mdlc as a ubiquitous nuclear protein that is required to maintain neuronal differentiation. Mdlc maintains the expression of Pros in larval postmitotic neurons and inhibits expression of neuroblast genes, thus maintaining neuronal differentiation. Interestingly, Mdlc is not required for Pros expression in the oldest neurons, located most distal from the neuroblast in *mdlc* mutant clones (not shown); there may have been enough Mdlc protein or RNA present at the time of mutant clone induction to allow the first neurons born after clone induction to successfully pass through middle-age without dedifferentiation. This suggests that after a certain age, neurons do not require Mdlc to maintain neuronal differentiation. Alternatively, neurons

born at early larval stages may not have the same requirement for Mdlc as neurons born at later larval stages.

Interestingly, *mdlc* mutant clones never show EdU incorporation in ectopic Dpn^+ cells, raising the question of whether they are true neuroblasts or have a mixed neuroblast/neuronal fate. We note that loss of Mdlc results in cell cycle delay in parental neuroblasts, so it may not be unexpected that the ectopic Dpn^+ cells do not proliferate. Nevertheless, our data show that Mdlc is not required to suppress cell cycle entry in post-mitotic neurons. Similarly, our data show that Pros is not required to suppress cell cycle entry in post-mitotic neurons, as *pros* RNAi specifically within post-mitotic neurons removes all detectable Pros protein but does not trigger entry into the cell cycle (data not shown). This is comparable to wild type embryonic neurons, which rapidly lose Pros but never re-enter the cell cycle, and contrasts with the role of Pros in GMCs, where it is required to repress neuroblast genes and promote cell cycle exit (Choksi et al., 2006). The maturation step taken by neurons to make them incapable of re-entering the cell cycle in the absence of Pros is not well understood.

Pros is known to bind the *dpn*, *ase*, and *cycE* loci (Choksi et al., 2006; Southall and Brand, 2009), and is known to keep the expression of these genes low in embryos (Li and Vaessin, 2000). Does Pros directly maintain repression of the *dpn*, *ase*, and *cycE* neuroblast genes in larval neurons? This appears unlikely, because we found that driving *UAS-pros RNAi* with either *atonal-Gal4* or *acj6-Gal4* specifically eliminates Pros protein in multiple clusters of post-mitotic neurons, yet does not lead to the derepression of Dpn (Supplementary Figure 2). Our *pros* RNAi knockdowns could have been too late to hit "middle aged" neurons; alternatively, Mdlc may independently regulate Pros and

Dpn/Ase. It is likely that, in addition to other Mdlc targets, Pros has some role in neuronal repression of neuroblast genes, because we nearly always observe derepression of Dpn/Ase in neurons which have already lost Pros (Fig. 3I).

The role of Mdlc in splicing regulation

We have found that the CCCH zinc finger domain, implicated in RNA-binding in other proteins, is essential for Mdlc function in the nervous system and for organismal viability. The *S. cerevisiae* and human orthologs are reported to have roles in splicing (Bessonov et al., 2008; Chan et al., 2003; Coltri and Oliveira, 2012; Goldfeder and Oliveira, 2008; Ohi et al., 2002). In yeast, Cwc24p is reported to be a splicing efficiency factor primarily affecting primary transcripts with atypical branchpoints. For example, splicing of the transcripts snR17A and B, which encode the U3 snoRNAs, was strongly affected, resulting in defects in the processing of pre-rRNA (Coltri and Oliveira, 2012; Goldfeder and Oliveira, 2008). Our observation that loss of Mdlc causes specific splicing defects (both increased and decreased intron retention) in the *pros* transcript, together with our finding that RNF113a can rescue the *mdlc* loss of function phenotypes, suggests that the fly and human proteins may have a more complex role in regulating splicing than that of the yeast general splicing factor Cwc24p.

What might be the CNS splicing targets of Mdlc, in addition to *pros*? Alternative splicing is known to be widely used in neural development, function, and plasticity, as well as for cell fate decisions. In mammals, alternatively spliced transcripts resulting in protein isoforms that influence stemness or differentiation are known, including within the nervous system (Lipscombe, 2005; Nelles and Yeo, 2010). Work from our lab has recently identified splice isoforms that are differentially regulated by the neuroblast

transcription factor Wor (Lai et al., 2012). The analysis of genome-wide changes in splicing in *mdlc* RNAi brains is in progress but beyond the scope of this paper.

Relevance of alternative splicing of the *pros* twintron

The *pros* twintron undergoes alternative splicing, resulting in at least two protein isoforms that differ by the presence or absence of 29 amino acids at the N-terminus of the homeodomain (Chu-Lagraff et al., 1991), and this splice is developmentally regulated (Scamborova et al., 2004), but whether each protein isoform has distinct functions is unknown. The two nested pairs of splice sites in the *pros* twintron are utilized mutually exclusively by two separate spliceosomes, U2 and U12. The U2 spliceosome is the complex that is predominantly used in *Drosophila*, and it is responsible for splicing the shorter *pros* intron, resulting in the long Pros protein, Pros-L, which is the more abundant isoform during early embryogenesis. The U12 spliceosome utilizes the external splice sites, resulting in the shorter protein isoform, Pros-S, which is more abundant during larval stages (Scamborova et al., 2004). The observation that we see a less penetrant neuronal Pros phenotype at early larval stages, together with the above result that indicates that the U12 spliceosome is primarily responsible for twintron splicing at late larval stages, raised the possibility that Mdlc preferentially affects U12 splicing. To address this possibility, we examined the DIR pattern for the other 12 introns in *Drosophila* that are known to utilize the U12 spliceosome. We found that of these introns, the *pros* intron was the sole example of differential retention (data not shown). This indicates that Mdlc does not affect either spliceosome preferentially.

A role for Mdlc as a ubiquitin ligase?

The RING-type zinc finger proteins comprise one of the largest protein families, with over 600 members (Deshaies and Joazeiro, 2009). Many of these proteins have been shown to function as E3 ubiquitin ligases, and the presence of a RING domain is often sufficient for such an annotation. The Mdlc human ortholog, RNF113a, is no exception and is thought to function as an E3 ligase; consistent with this assumption, RNF113a was found to physically interact with one of the human E2 proteins, UBE2U (Li et al., 2008; van Wijk et al., 2009). Moreover, the Mdlc RING domain is very well conserved from yeast to humans, suggesting its functional importance. We were therefore surprised to find that the RING domain was completely dispensable not only for CNS function but also for organismal viability, since the ubiquitous misexpression of a version of Mdlc lacking the RING domain was able to substitute for full-length protein. Therefore we believe that the RING domain plays a more subtle role than that of the CCCH domain.

CHAPTER IV

CONCLUSIONS

This dissertation has focused on the broad question of how daughter cells adopt and maintain distinct identities. I have used the *Drosophila* neuroblast asymmetric division as a model to study this important question in developmental biology. The progeny of a neuroblast division – a self-renewed neuroblast and a differentiating GMC – provide a great system to assay the effects of genetic disruption of cell fate: failure to self-renew or too much self-renewal can lead to alterations in the wild type number of neuroblasts in the brain.

In Chapter II, I described experiments in which co-authors and I used high-throughput methods to identify novel regulators of neuroblast self-renewal and differentiation. We used microarrays to compare the transcriptional output of neuroblasts to that of neurons, providing us with valuable lists of cell type-enriched genes, among which likely exist regulators of cell fate. In order to verify the cell type specificity of these genes as well as their role in cell fate, we functionally assayed a subgroup of genes: those enriched in neuroblasts. This secondary screen identified over 80 genes required for maintaining proper neuroblast number, all of which have human orthologs and are thus great candidates for regulators of neural stem cell self-renewal in mammals as well as in *Drosophila*.

In addition to the important question of how neuroblasts self-renew, we wished to address the genetic basis of the difference between type I and type II neuroblasts. Importantly, the mutants used in our microarray experiments, each of which we

compared to wild type, differ in the neuroblast subtype (type I or II) that overproliferates (see Chapter II, Fig. 1; Appendix A, Supplementary Fig. 1). Clustering analysis allowed us to identify genes that are more strongly upregulated in type II than type I neuroblasts (and vice versa), yielding valuable insight into how these different types of stem cells are genetically controlled. Many of the genes we identified (for example, the genes listed in Chapter II, Figs 3, 4) have not been functionally characterized in neuroblasts; this is an important goal for future study, particularly in determining whether any of these genes is involved in the generation of lineage size or neural diversity inherent in type II neuroblast lineages.

The identification of putative self-renewal and neuroblast subtype-specific genes described in Chapter II was an important step toward understanding neuroblast function and the generation of distinct cell fates, but detailed genetic, phenotypic, and functional analyses on these genes is crucial not only to verify their importance but also to elucidate their precise functions in neuroblasts, GMCs, and neurons. With that in mind, in Chapter III of this dissertation I described the detailed phenotypic and functional characterization of one of the genes identified in the RNAi-based functional screen described in Chapter II. We have chosen to name this gene *midlife crisis* (*mdlc*) due to the dedifferentiation phenotype seen in mutant middle-aged neurons. Importantly, our analysis of *mdlc* and verification of its importance in maintaining neuronal fates validates the screening processes described above and highlights the potential value of further in-depth analysis of these genes.

The dedifferentiation phenotype seen in *mdlc* loss of function is intriguing, and is directly relevant to the question of how differentiated states are maintained. We have

shown that Mdlc is a splicing regulator, and its targets are likely regulators of this maintenance. The transcript encoding Pros is mis-spliced in *mdlc* loss of function, and given the well-documented function of Pros as an important pro-differentiation transcription factor, this implicates Pros as a likely regulator of neuronal identity maintenance. Surprisingly, we have shown that the strong RNAi-induced loss of Pros alone is insufficient to cause dedifferentiation in postmitotic neurons; however, it is likely that Pros acts in parallel to other Mdlc targets to maintain neuronal identity.

What are these other targets? While the detailed analysis of our RNA-seq data are ongoing, a tantalizing candidate has emerged and awaits functional analysis: the transcription factor Jim (data not shown). *pros* and *jim* were the two most downregulated transcripts that were mis-spliced in the *mdlc* loss of function. Both of these genes encode transcription factors, which suggests that they affect differentiation via transcriptional control. However, an enticing possibility exists as to how Jim may affect the maintenance of cell identity. In a recent study, Schneiderman and colleagues performed an elegant inducible misexpression screen to find novel regulators of heterochromatic gene silencing (Schneiderman et al., 2010). This screen made use of the *brown dominant* (bw^D) allele, which contains repetitive satellite DNA that causes the heterochromatic silencing of a wild type bw^+ allele on the homologous chromosome; this silencing is visible in the reduction of pigmentation in the adult eye. The authors discovered that misexpression of Jim enhanced this silencing, resulting in the near complete loss of eye pigmentation. Furthermore, misexpressing Jim late in development using the *GMR-Gal4* driver, but not early using *eyeless-Gal4*, enhanced silencing. This indicates that Jim-induced silencing must be maintained in the postmitotic cells of the eye. These results are consistent with a

model in which Jim is required in postmitotic neurons to maintain silencing of target genes such as *dpn* and *ase*, the genes that are derepressed in *mdlc* mutant neurons. Further research is needed to address this exciting possibility.

APPENDIX A

SUPPLEMENTARY MATERIALS FOR CHAPTER II

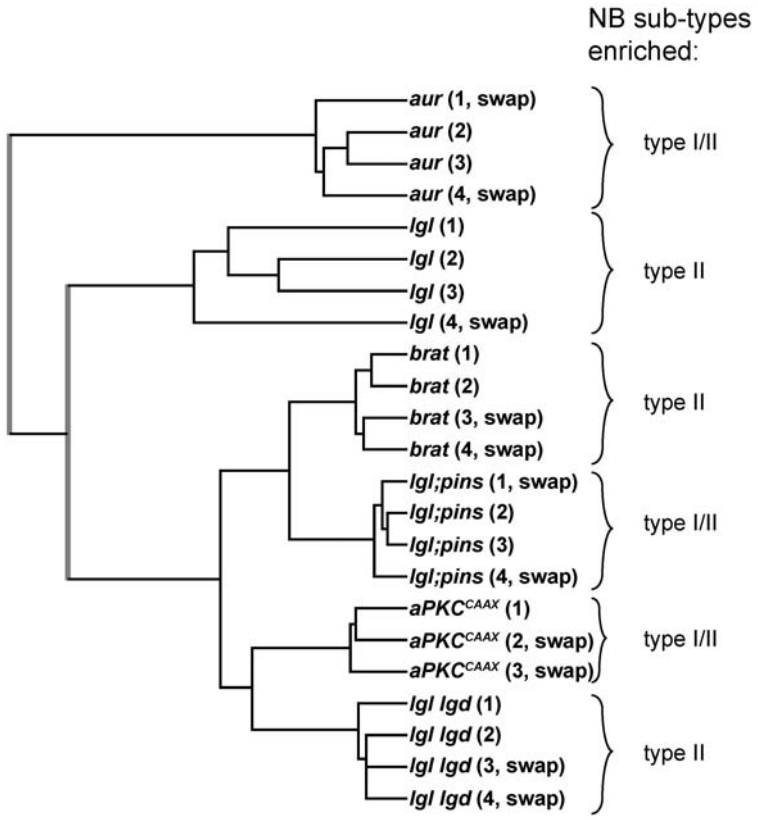

Supplementary Figure 1. Biological replicates cluster closely with one another
The biological replicates for each set of experiments clustered much more closely to each other than with those from any other experiment. Indicated to the right of each genotype are the neuroblast sub-types (type I/type II) which are enriched in that genotype.

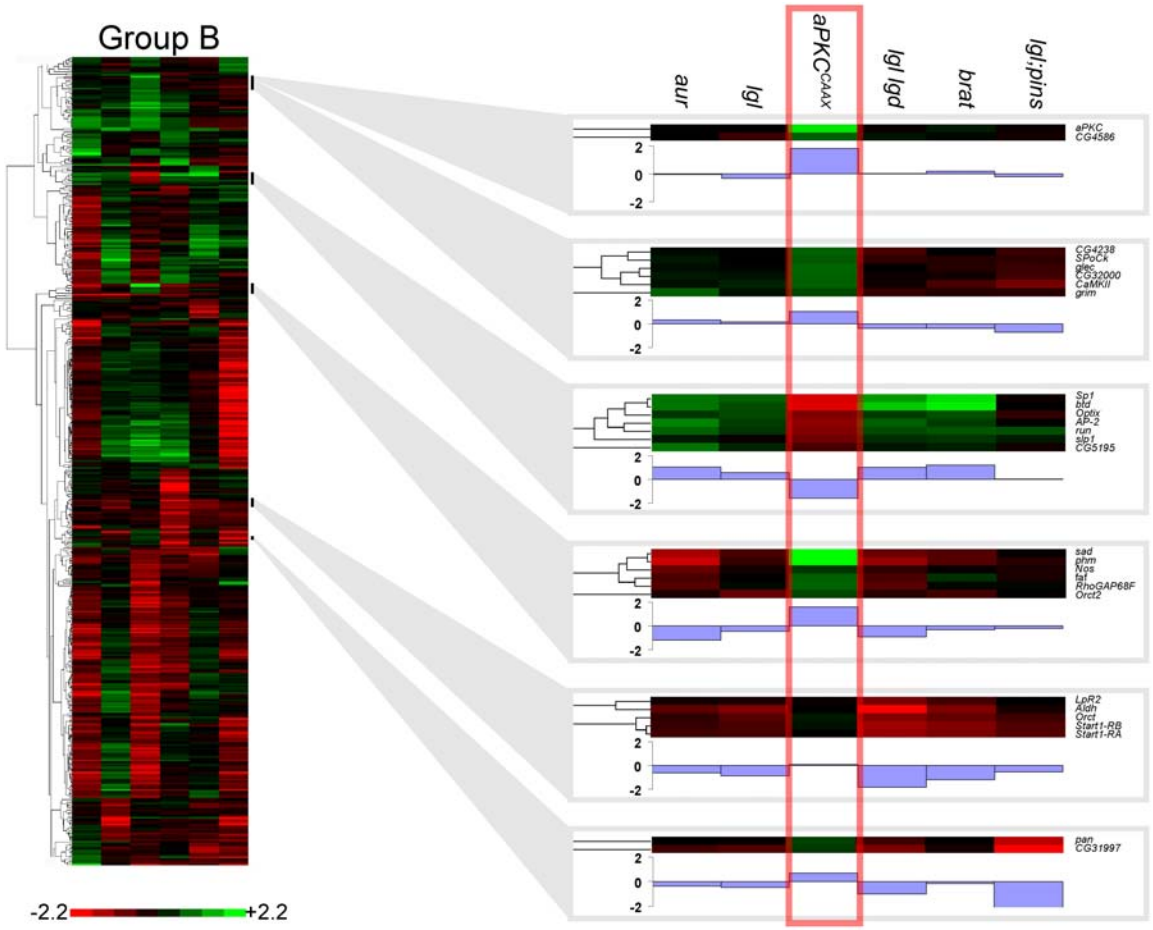

Supplementary Figure 2. Sub-clusters in group B exhibit *aPKC^{CAAX}*-dependent differential expression

Several group B sub-clusters in which expression is differentially enriched or depleted in *aPKC^{CAAX}* brains.

Supplementary Table 1. Group A genes tested for a role in regulating neuroblast self-renewal.

worniu-Gal4 UAS-Dicer2 UAS-RNAi assayed for Dpn^{+} neuroblast numbers in third instar larval brains. I, increased neuroblasts; R, reduced neuroblasts; NC, no change in neuroblasts; NA, not assayed. GO annotations describing each gene's function or process are included.

Gene	Synonym	Neuroblast phenotype	GO annotation
CG33123	CG33123	I	amino acid-tRNA ligase; oxidative stress response
CG12249	miranda	I	asymm. mRNA localization; GMC fate determination
CG6897	aurora borealis	I	asymmetric protein localization; PNS development
CG4973	CG4973	I	binds nucleic acid, Zn, & protein
CG10628	CG10628	I	GTP binding
CG4337	mtSSB	I	mitochondrial single stranded DNA-binding protein
CG4806	CG4806	I	mRNA binding
CG9755	pumilio	I	mRNA binding; cell fate determination
CG4817	Ssrp	I	nucleic acid binding; regulates chromatin packaging
CG1666	Hlc	I	RNA helicase activity
CG3782	mRpL28	I	structural ribosomal component; mRNA processing
CG4897	RpL7	I	structural ribosomal component; translation
CG9198	shattered	R	anaphase-promoting complex
CG4554	CG4554	R	binding
CG3725	Ca-P60A	R	Ca-transporting ATPase activity
CG6191	CG6191	R	CDK regulator
CG4364	CG4364	R	cell proliferation; nucleolar
CG1135	Rcd5	R	centriole replication
CG5354	pineapple eye	R	compound eye development
CG14999	RfC4	R	DNA helicase; DNA replication & repair; mitosis
CG18013	Psf2	R	DNA helicase; DNA replication; txn elongation
CG7538	Mcm2	R	DNA helicase; replication
CG5602	DNA ligase I	R	DNA repair; DNA ligase
CG8648	Fen1	R	DNA repair; endonuclease activity
CG6768	DNApol-ε	R	DNA replication
CG8171	double parked	R	DNA replication
CG8975	RnrS	R	DNA replication; caspase activation
CG4039	DmMCM6	R	DNA replication; DNA helicase
CG6349	DNApol-α180	R	DNA-directed DNA polymerase activity
CG5553	DNApol-α60	R	DNA-directed DNA polymerase; DNA primase activity
CG9938	Ndc80	R	kinetochore component; chromosome segregation
CG4274	fizzy	R	kinetochore; centrosome; spindle
CG8902	Nuf2	R	kinetochore; mitotic spindle organization
CG1569	Rough Deal	R	kinetochore; spindle assembly checkpoint
CG14437	Dclk1	R	mitochondrial; protein metabolic processes
CG10726	barren	R	mitosis; chromosome condensation; condensin complex
CG10480	Bj1	R	mitosis; CNS development
CG3460	dNmd3	R	mRNA binding; ribosomal large subunit export
CG33505	U3-55K	R	mRNA binding; rRNA processing
CG8395	Rrp42	R	mRNA processing; exoribonuclease activity
CG5000	mini spindles	R	MT organization;bicoid mRNA localization
CG1994	p110	R	N-acetyltransferase activity

Supplementary Table 1. (*continued*).

Gene	Synonym	Neuroblast phenotype	GO annotation
CG9300	CG9300	R	nuclear transport
CG11180	CG11180	R	nucleic acid binding
CG13849	Nop56	R	nucleolus; SNP complex
CG11859	CG11859	R	protein kinase activity
CG7719	greatwall	R	protein kinase involved in: cell cycle; mitosis
CG12306	Polo	R	protein kinase involved in: cell cycle; mitosis; cytokinesis
CG4933	CG4933	R	proteolysis activity
CG8070	Mys45A	R	ribosome biogenesis
CG9680	Dbp73D	R	RNA helicase
CG4152	l(2)35Df	R	RNA helicase activity
CG6375	pitchoune	R	RNA helicase activity
CG4901	CG4901	R	RNA helicase; spliceosome
CG7246	CG7246	R	RNA processing
CG4033	RpI135	R	RNAPi subunit; transcription
CG4038	Pen101	R	rRNA processing
CG9799	CG9799	R	rRNA processing
CG5258	NHP2	R	rRNA processing; rRNA pseudouridine synthesis
CG1210	dPDK1	R	serine/threonine kinase
CG7838	BubR1	R	serine/threonine kinase activity
CG33162	SrpRβ	R	signal recognition particle binding
CG1883	RpS7	R	structural ribosomal component; translation
CG4759	RpL27	R	structural ribosomal component; mitotic spindle organization
CG3018	DmUbc9	R	SUMO ligase activity; post-translational modifications
CG10122	RpI1	R	transcription
CG11121	sine oculis	R	transcription factor
CG5575	Ken	R	transcription factor
CG9305	Bdp1	R	transcription factor
CG5380	CG5380	R	transcription from RNA polymerase III promoter
CG9677	Int6	R	translational initiation; phagocytosis, engulfment
CG11606	Rpp30	R	tRNA processing; ribonuclease P complex
CG10341	CG10341	R	unknown
CG11417	EG:8D8.4	R	unknown
CG12050	CG12050	R	unknown
CG12325	CG12325	R	unknown
CG12499	CG12499	R	unknown
CG14210	CG14210	R	unknown
CG30349	CG30349	R	unknown
CG5018	CG5018	R	unknown
CG6686	SART1	R	unknown
CG7516	l(2)34Fd	R	unknown
CG7686	CG7686	R	unknown
CG7845	WDR74	R	unknown
CG8326	CG8326	R	unknown
CG6817	fear of intimacy	R	Zn transporter activity

Supplementary Table 1. (*continued*).

Gene	Synonym	Neuroblast phenotype	GO annotation
CG4062	Aats-val	NC	amino acid-tRNA ligase
CG5353	Aats-thr	NC	amino acid-tRNA ligase
CG5414	CG5414	NC	amino acid-tRNA ligase
CG6335	Aats-his	NC	amino acid-tRNA ligase
CG5462	scribbled	NC	asymmetric protein localization
CG32104	anon-69Ag	NC	ATPase activity
CG6815	belphegor	NC	ATPase activity
CG4908	CG4908	NC	ATPase; may be mitochondrial
CG6512	DmCG6512	NC	ATP-dependent proteolysis
CG1234	CG1234	NC	binding
CG1845	Br140	NC	binds phosphopentatheine, Zn, protein
CG4589	Letm1	NC	Ca2+ ion binding
CG3938	Cyclin E	NC	cell cycle; G-S phase transition; inhibition of apoptosis.
CG9187	Psf1	NC	DNA helicase; DNA replication
CG8598	deco	NC	DNA repair; mitotic spindle; sister chromatid cohesion
CG7578	sec71	NC	ER to Golgi vesicle-mediated transport
CG14788	nucleostemin 3	NC	GTP binding
CG3983	ns1	NC	GTP binding
CG4567	iconoclast	NC	GTPase activity; translation elongation
CG3307	pr-set7	NC	H4/K20 histone methylation
CG8531	CG8531	NC	heat shock protein binding
CG10691	l(2)37Cc	NC	instar larval or pupal development
CG5786	peter pan	NC	larval & imaginal disc development
CG4143	mbf1	NC	methyl-CpG binding; transcriptional coactivation
CG7015	Unr	NC	mRNA 3'UTR binding; regulation of translation
CG12924	Lsm11	NC	mRNA alternative splicing
CG10418	CG10418	NC	mRNA alternative splicing; spliceosome
CG1691	Imp	NC	mRNA binding; neurogenesis
CG4043	Rrp46	NC	mRNA processing; exoribonuclease activity
CG3619	Delta	NC	Notch binding; signal transduction
CG4579	Nup154	NC	nuclear transport; nuclear pore
CG11267	Hsp10	NC	protein folding; mitochondrial
CG6155	Roe1	NC	protein folding; protein targeting to mitochondrion
CG12101	Hsp60	NC	protein folding; stress response
CG7338	CG7338	NC	ribosome biogenesis
CG4510	Surfeit 6	NC	ribosome biogenesis; heme transporter activity
CG5033	EG:52C10.1	NC	ribosome biogenesis; rRNA processing
CG3333	Nop60B	NC	ribosome biosynthesis; rRNA processing
CG7006	CG7006	NC	RNA binding; protein binding. Ribosome assembly
CG5589	DmRH17	NC	RNA helicase
CG32344	DmRH20	NC	RNA helicase activity
CG2173	Rs1	NC	RNA helicase; ribosome biogenesis
CG11130	Rtc1	NC	RNA-3'-phosphate cyclase activity
CG8545	CG8545	NC	rRNA processing; methyltransferase activity
CG11177	BthD	NC	selenium binding; cell redox homeostasis

Supplementary Table 1. (*continued*).

Gene	Synonym	Neuroblast phenotype	GO annotation
CG12373	mRpL18	NC	structural ribosomal component
CG13922	mRpL46	NC	structural ribosomal component
CG6754	nbs	NC	telomere capping
CG10798	dMyc	NC	transcription factor
CG17117	Homothorax	NC	transcription factor
CG3114	erect wing	NC	transcription factor
CG7614	Mat1	NC	transcription factor
CG13628	Rpb10	NC	transcription; regulation of txn.; RNAPII core complex
CG2969	Atet	NC	transmembrane transport
CG9772	Skp2	NC	ubiquitin ligase process
CG2013	Dhr6	NC	ubiquitin ligase process; mitotic spindle organization
CG11030	CG11030	NC	unknown
CG11125	CG11125	NC	unknown
CG12975	CG12975	NC	unknown
CG14174	CG14174	NC	unknown
CG1430	bystin	NC	unknown
CG14921	CG14921	NC	unknown
CG15081	l(2)03709	NC	unknown
CG2875	CG2875	NC	unknown
CG2972	CG2972	NC	unknown
CG3735	CG3735	NC	unknown
CG3817	CG3817	NC	unknown
CG5190	CG5190	NC	unknown
CG7637	CG7637	NC	unknown
CG7639	CG7639	NC	unknown
CG7993	CG7993	NC	unknown
CG2092	scraps	NA	actin binding; MT binding; cytokinesis
CG9735	Aats-trp	NA	amino acid-tRNA ligase
CG12265	Deterin	NA	anti-apoptosis
CG5940	Cyclin A	NA	asymm. neuroblast divisions; G2/M transition
CG16928	mre11	NA	DNA repair/maintenance; nuclease activity
CG9633	RpA-70	NA	DNA replication
CG3041	Orc2	NA	DNA replication; chromatin condensation
CG17265	CG17265	NA	involved in RNAi
CG10302	bsf	NA	mRNA 3'-UTR binding
CG6015	prp17	NA	mRNA alternative splicing; spliceosome
CG1258	pavarotti	NA	MT motor; cytokinesis
CG13345	tumbleweed	NA	signal transduction
CG10583	Separase	NA	sister chromatid separation; peptidase
CG9353	mRpL54	NA	structural ribosomal component
CG5904	mRpS31	NA	structural ribosomal component; translation
CG10648	Rbm13	NA	structural ribosomal component; mitotic spindle elongation
CG5149	CG5149	NA	structural; tight junction
CG8365	E(spl)	NA	transcription repressor
CG1683	Ant2	NA	transmembrane transport

Supplementary Table 1. (*continued*).

Gene	Synonym	Neuroblast phenotype	GO annotation
CG14057	CG14057	NA	tRNA processing; ribonuclease P activity
CG3298	JhI-1	NA	tRNA splicing
CG15445	CG15445	NA	unknown

APPENDIX B

SUPPLEMENTARY MATERIALS FOR CHAPTER III

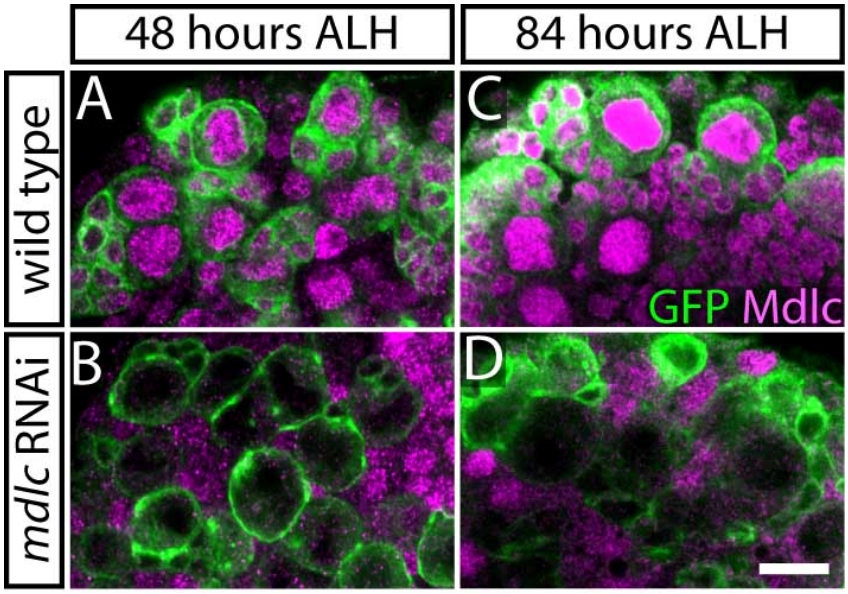

Supplementary Figure 1. *mdlc* RNAi reduces Mdlc protein levels.
All panels depict fields of central brain neuroblasts stained for Mdlc; neuroblasts are marked by mCD8:GFP driven by *wor-Gal4*. (A & C) Mdlc is expressed robustly in wild type neuroblast lineages. (B & D) *mdlc* RNAi causes a strong reduction in Mdlc protein at both 48 hours ALH (B) and 84 hours ALH (D). Scale bar: 10 μm.

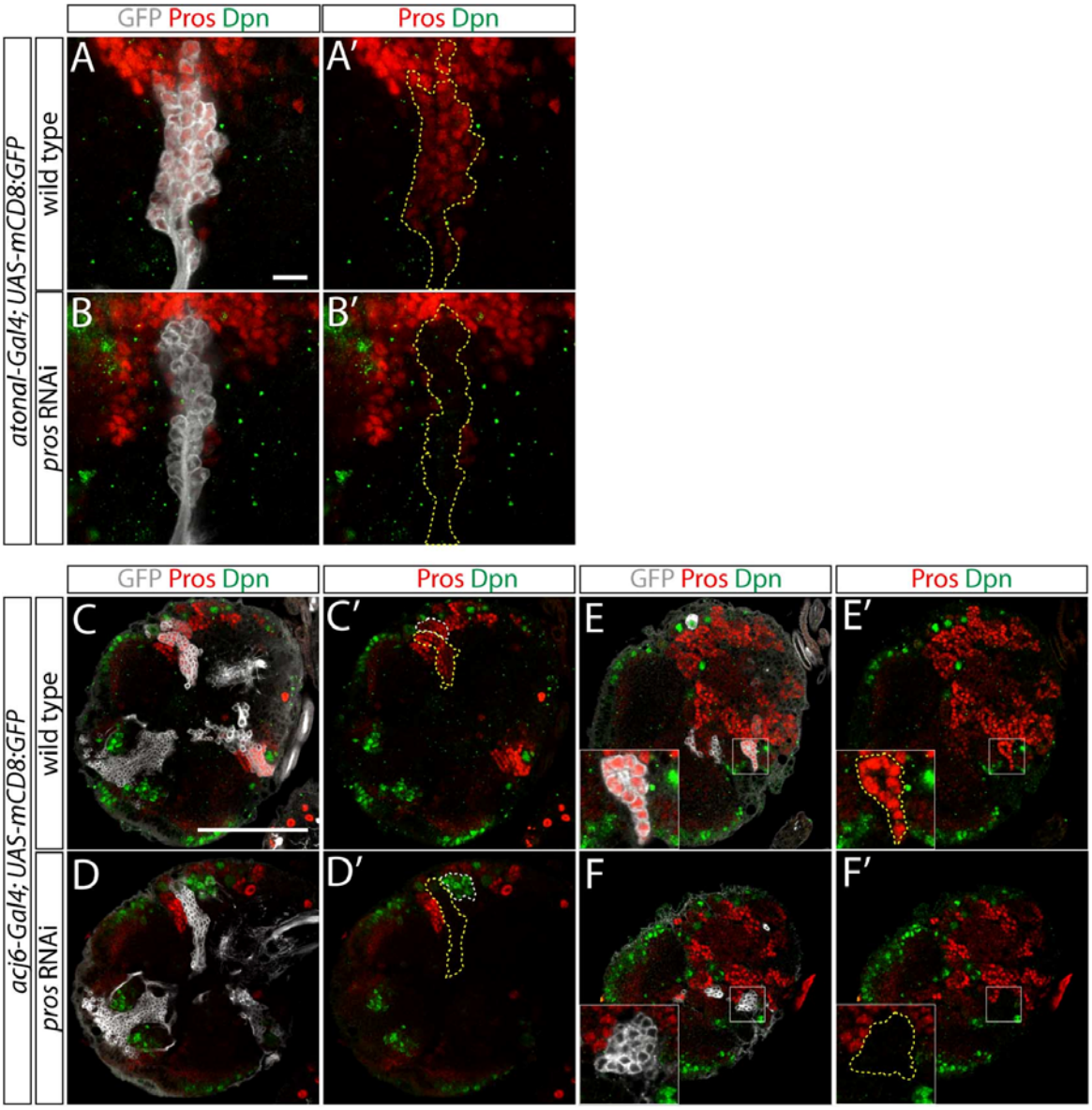

Supplementary Figure 2. Loss of Pros in postmitotic neurons does not cause derepression of neuroblast genes.

Gal4-expressing cells were identified by expression of *UAS-mCD8:GFP* and outlined with yellow or white dotted lines. (A-B) *atonal-Gal4* drives expression in a cluster of neurons which is $Pros^{+}$ Dpn^{-} in wild type (A, A′); Pros staining is strongly reduced in *pros* RNAi with no derepression of Dpn (B, B′). (C-F) *acj6-Gal4* expression is depicted in multiple lineages: deep in the central brain (C & D) and superficial, near the dorsoposterior surface (E & F). Pros is expressed in these lineages in wild type (C, C′ & E, E′) while *pros* RNAi ablates this expression (D, D′ & F, F′). *acj6-Gal4* does not express in the neuroblasts of the lineages outlined in yellow, but it expresses strongly in the neuroblast of the lineage outlined in white. *pros* RNAi in this lineage causes a neuroblast overproliferation phenotype (note cluster of Dpn^{+} cells in D′), further illustrating the efficacy of *pros* knockdown. Insets in E & F are high magnification views of the regions marked with white boxes. In each lineage, *pros* RNAi causes a robust loss of Pros staining without a concomitant derepression of Dpn. Scale bars: 10 μm in A; 100 μm in C-F.

REFERENCES CITED

Chapter I

Atwood, S. X., Prehoda, K. E., 2009. aPKC phosphorylates Miranda to polarize fate determinants during neuroblast asymmetric cell division. Curr Biol. 19**,** 723-9.

Bello, B., et al., 2006. The brain tumor gene negatively regulates neural progenitor cell proliferation in the larval central brain of *Drosophila*. Development. 133**,** 2639-48.

Bello, B. C., et al., 2008. Amplification of neural stem cell proliferation by intermediate progenitor cells in *Drosophila* brain development. Neural Dev. 3**,** 5.

Betschinger, J., et al., 2006. Asymmetric segregation of the tumor suppressor brat regulates self-renewal in *Drosophila* neural stem cells. Cell. 124**,** 1241-53.

Boone, J. Q., Doe, C. Q., 2008. Identification of *Drosophila* type II neuroblast lineages containing transit amplifying ganglion mother cells. Dev Neurobiol. 68**,** 1185-95.

Bowman, S. K., et al., 2006. The *Drosophila* NuMA Homolog Mud regulates spindle orientation in asymmetric cell division. Dev Cell. 10**,** 731-42.

Bowman, S. K., et al., 2008. The tumor suppressors Brat and Numb regulate transit-amplifying neuroblast lineages in *Drosophila*. Dev Cell. 14**,** 535-46.

Boyan, G. S., Reichert, H., 2011. Mechanisms for complexity in the brain: generating the insect central complex. Trends Neurosci. 34**,** 247-57.

Broadus, J., et al., 1998. Staufen-dependent localization of prospero mRNA contributes to neuroblast daughter-cell fate. Nature. 391**,** 792-5.

Cabernard, C., Doe, C. Q., 2009. Apical/basal spindle orientation is required for neuroblast homeostasis and neuronal differentiation in *Drosophila*. Dev Cell. 17**,** 134-41.

Choksi, S. P., et al., 2006. Prospero acts as a binary switch between self-renewal and differentiation in *Drosophila* neural stem cells. Developmental cell. 11**,** 775-89.

Doe, C. Q., 2008. Neural stem cells: balancing self-renewal with differentiation. Development. 135**,** 1575-87.

Egger, B., et al., Regulating the balance between symmetric and asymmetric stem cell division in the developing brain. Fly (Austin). 5**,** 237-41.

Gillies, T. E., Cabernard, C., Cell division orientation in animals. Curr Biol. 21**,** R599-609.

Hirata, J., et al., 1995. Asymmetric segregation of the homeodomain protein Prospero during *Drosophila* development. Nature. 377**,** 627-30.

Homem, C. C., Knoblich, J. A., *Drosophila* neuroblasts: a model for stem cell biology. Development. 139**,** 4297-310.

Ikeshima-Kataoka, H., et al., 1997. Miranda directs Prospero to a daughter cell during *Drosophila* asymmetric divisions. Nature. 390**,** 625-9.

Izergina, N., et al., 2009. Postembryonic development of transit amplifying neuroblast lineages in the *Drosophila* brain. Neural Dev. 4**,** 44.

Izumi, Y., et al., 2006. *Drosophila* Pins-binding protein Mud regulates spindle-polarity coupling and centrosome organization. Nat Cell Biol. 8**,** 586-93.

Johnston, C. A., et al., 2009. Identification of an Aurora-A/PinsLINKER/Dlg spindle orientation pathway using induced cell polarity in S2 cells. Cell. 138**,** 1150-63.

Kelsom, C., Lu, W., 2012. Uncovering the link between malfunctions in *Drosophila* neuroblast asymmetric cell division and tumorigenesis. Cell Biosci. 2**,** 38.

Knoblich, J. A., 2008. Mechanisms of asymmetric stem cell division. Cell. 132**,** 583-97.

Knoblich, J. A., 2010. Asymmetric cell division: recent developments and their implications for tumour biology. Nature reviews. Molecular cell biology. 11**,** 849-60.

Knoblich, J. A., et al., 1995. Asymmetric segregation of Numb and Prospero during cell division. Nature. 377**,** 624-7.

Lee, C. Y., et al., 2006a. Lgl, Pins and aPKC regulate neuroblast self-renewal versus differentiation. Nature. 439**,** 594-8.

Lee, C. Y., et al., 2006b. Brat is a Miranda cargo protein that promotes neuronal differentiation and inhibits neuroblast self-renewal. Dev Cell. 10**,** 441-9.

Li, L., Vaessin, H., 2000. Pan-neural Prospero terminates cell proliferation during *Drosophila* neurogenesis. Genes & development. 14**,** 147-51.

Lu, B., et al., 1998. Partner of Numb colocalizes with Numb during mitosis and directs Numb asymmetric localization in *Drosophila* neural and muscle progenitors. Cell. 95**,** 225-35.

Lu, M. S., Johnston, C. A., Molecular pathways regulating mitotic spindle orientation in animal cells. Development. 140**,** 1843-56.

Nicolay, B. N., et al., 2010. Combined inactivation of pRB and hippo pathways induces dedifferentiation in the *Drosophila* retina. PLoS Genet. 6**,** e1000918.

Ohshiro, T., et al., 2000. Role of cortical tumour-suppressor proteins in asymmetric division of *Drosophila* neuroblast. Nature. 408**,** 593-6.

Prehoda, K. E., 2009. Polarization of *Drosophila* neuroblasts during asymmetric division. Cold Spring Harb Perspect Biol. 1**,** a001388.

Reichert, H., 2011. *Drosophila* neural stem cells: cell cycle control of self-renewal, differentiation, and termination in brain development. Results Probl Cell Differ. 53**,** 529-46.

Rolls, M. M., et al., 2003. *Drosophila* aPKC regulates cell polarity and cell proliferation in neuroblasts and epithelia. J Cell Biol. 163**,** 1089-98.

Schnabel, R., Priess, J. R., 1997. Specification of Cell Fates in the Early Embryo.

Shen, C. P., et al., 1997. Miranda is required for the asymmetric localization of Prospero during mitosis in *Drosophila*. Cell. 90**,** 449-58.

Siegrist, S. E., Doe, C. Q., 2005. Microtubule-induced Pins/Galphai cortical polarity in *Drosophila* neuroblasts. Cell. 123**,** 1323-35.

Siller, K. H., Doe, C. Q., 2008. Lis1/dynactin regulates metaphase spindle orientation in *Drosophila* neuroblasts. Dev Biol. 319**,** 1-9.

Siller, K. H., Doe, C. Q., 2009. Spindle orientation during asymmetric cell division. Nat Cell Biol. 11**,** 365-74.

Smith, C. A., et al., 2007. aPKC-mediated phosphorylation regulates asymmetric membrane localization of the cell fate determinant Numb. EMBO J. 26**,** 468-80.

Spana, E. P., Doe, C. Q., 1995. The prospero transcription factor is asymmetrically localized to the cell cortex during neuroblast mitosis in *Drosophila*. Development. 121**,** 3187-95.

Viktorin, G., et al., 2011. Multipotent neural stem cells generate glial cells of the central complex through transit amplifying intermediate progenitors in *Drosophila* brain development. Dev Biol.

Wirtz-Peitz, F., et al., 2008. Linking cell cycle to asymmetric division: Aurora-A phosphorylates the Par complex to regulate Numb localization. Cell. 135**,** 161-73.

Xiong, W., et al., 2012. The Abelson tyrosine kinase regulates Notch endocytosis and signaling to maintain neuronal cell fate in *Drosophila* photoreceptors. Development. 140**,** 176-84.

CHAPTER II

Albertson, R., Chabu, C., Sheehan, A., Doe, C.Q., 2004. Scribble protein domain mapping reveals a multistep localization mechanism and domains necessary for establishing cortical polarity. J Cell Sci 117, 6061-6070.

Almeida, M.S., Bray, S.J., 2005. Regulation of post-embryonic neuroblasts by *Drosophila* Grainyhead. Mech Dev 122, 1282-1293.

Ashraf, S.I., Ganguly, A., Roote, J., Ip, Y.T., 2004. Worniu, a Snail family zinc-finger protein, is required for brain development in *Drosophila*. Dev Dyn 231, 379-386.

Atwood, S.X., Prehoda, K.E., 2009. aPKC phosphorylates Miranda to polarize fate determinants during neuroblast asymmetric cell division. Curr Biol 19, 723-729.

Bayraktar, O.A., Boone, J.Q., Drummond, M.L., Doe, C.Q., 2010. *Drosophila* type II neuroblast lineages keep Prospero levels low to generate large clones that contribute to the adult brain central complex. Neural Dev 5, 26.

Bello, B.C., Izergina, N., Caussinus, E., Reichert, H., 2008. Amplification of neural stem cell proliferation by intermediate progenitor cells in *Drosophila* brain development. Neural Dev 3, 5.

Betschinger, J., Mechtler, K., Knoblich, J.A., 2006. Asymmetric segregation of the tumor suppressor brat regulates self-renewal in *Drosophila* neural stem cells. Cell 124, 1241-1253.

Bier, E., Vaessin, H., Younger-Shepherd, S., Jan, L.Y., Jan, Y.N., 1992. deadpan, an essential pan-neural gene in *Drosophila*, encodes a helix-loop-helix protein similar to the hairy gene product. Genes Dev 6, 2137-2151.

Boone, J.Q., Doe, C.Q., 2008. Identification of *Drosophila* type II neuroblast lineages containing transit amplifying ganglion mother cells. Dev Neurobiol 68, 1185-1195.

Bowman, S.K., Rolland, V., Betschinger, J., Kinsey, K.A., Emery, G., Knoblich, J.A., 2008. The tumor suppressors Brat and Numb regulate transit-amplifying neuroblast lineages in *Drosophila*. Dev Cell 14, 535-546.

Brand, M., Jarman, A.P., Jan, L.Y., Jan, Y.N., 1993. asense is a *Drosophila* neural precursor gene and is capable of initiating sense organ formation. Development 119, 1-17.

Broadus, J., Fuerstenberg, S., Doe, C.Q., 1998. Staufen-dependent localization of prospero mRNA contributes to neuroblast daughter-cell fate. Nature 391, 792-795.

Caldwell, M.C., Datta, S., 1998. Expression of cyclin E or DP/E2F rescues the G1 arrest of trol mutant neuroblasts in the *Drosophila* larval central nervous system. Mech Dev 79, 121-130.

Chabu, C., Doe, C.Q., 2008. Dap160/intersectin binds and activates aPKC to regulate cell polarity and cell cycle progression. Development 135, 2739-2746.

Chia, W., Somers, W.G., Wang, H., 2008. *Drosophila* neuroblast asymmetric divisions: cell cycle regulators, asymmetric protein localization, and tumorigenesis. J Cell Biol 180, 267-272.

Choksi, S.P., Southall, T.D., Bossing, T., Edoff, K., de Wit, E., Fischer, B.E., van Steensel, B., Micklem, G., Brand, A.H., 2006. Prospero acts as a binary switch between self-renewal and differentiation in *Drosophila* neural stem cells. Dev Cell 11, 775-789.

Davis, R.J., Tavsanli, B.C., Dittrich, C., Walldorf, U., Mardon, G., 2003. *Drosophila* retinal homeobox (drx) is not required for establishment of the visual system, but is required for brain and clypeus development. Dev Biol 259, 272-287.

Dietzl, G., Chen, D., Schnorrer, F., Su, K.C., Barinova, Y., Fellner, M., Gasser, B., Kinsey, K., Oppel, S., Scheiblauer, S., Couto, A., Marra, V., Keleman, K., Dickson, B.J., 2007. A genome-wide transgenic RNAi library for conditional gene inactivation in *Drosophila*. Nature 448, 151-156.

Doe, C.Q., 2008. Neural stem cells: balancing self-renewal with differentiation. Development 135, 1575-1587.

Dominguez, M., Campuzano, S., 1993. asense, a member of the *Drosophila* achaete-scute complex, is a proneural and neural differentiation gene. EMBO J 12, 2049-2060.

Eggert, T., Hauck, B., Hildebrandt, N., Gehring, W.J., Walldorf, U., 1998. Isolation of a *Drosophila* homolog of the vertebrate homeobox gene Rx and its possible role in brain and eye development. Proc Natl Acad Sci U S A 95, 2343-2348.

Ge, H., Liu, Z., Church, G.M., Vidal, M., 2001. Correlation between transcriptome and interactome mapping data from Saccharomyces cerevisiae. Nat Genet 29, 482-486.

Hirata, J., Nakagoshi, H., Nabeshima, Y., Matsuzaki, F., 1995. Asymmetric segregation of the homeodomain protein Prospero during *Drosophila* development. Nature 377, 627-630.

Hosoya, T., Takizawa, K., Nitta, K., Hotta, Y., 1995. glial cells missing: a binary switch between neuronal and glial determination in *Drosophila*. Cell 82, 1025-1036.

Izergina, N., Balmer, J., Bello, B., Reichert, H., 2009. Postembryonic development of transit amplifying neuroblast lineages in the *Drosophila* brain. Neural Dev 4, 44.

Jaekel, R., Klein, T., 2006. The *Drosophila* Notch inhibitor and tumor suppressor gene lethal (2) giant discs encodes a conserved regulator of endosomal trafficking. Dev Cell 11, 655-669.

Jansen, R., Greenbaum, D., Gerstein, M., 2002. Relating whole-genome expression data with protein-protein interactions. Genome Res 12, 37-46.

Kenyon, K.L., Li, D.J., Clouser, C., Tran, S., Pignoni, F., 2005. Fly SIX-type homeodomain proteins Sine oculis and Optix partner with different cofactors during eye development. Dev Dyn 234, 497-504.

Knoblich, J.A., 2008. Mechanisms of asymmetric stem cell division. Cell 132, 583-597.

Knoblich, J.A., Jan, L.Y., Jan, Y.N., 1995. Asymmetric segregation of Numb and Prospero during cell division. Nature 377, 624-627.

Lee, C.Y., Andersen, R.O., Cabernard, C., Manning, L., Tran, K.D., Lanskey, M.J., Bashirullah, A., Doe, C.Q., 2006a. *Drosophila* Aurora-A kinase inhibits neuroblast self-renewal by regulating aPKC/Numb cortical polarity and spindle orientation. Genes Dev 20, 3464-3474.

Lee, C.Y., Robinson, K.J., Doe, C.Q., 2006b. Lgl, Pins and aPKC regulate neuroblast self-renewal versus differentiation. Nature 439, 594-598.

Lee, C.Y., Wilkinson, B.D., Siegrist, S.E., Wharton, R.P., Doe, C.Q., 2006c. Brat is a Miranda cargo protein that promotes neuronal differentiation and inhibits neuroblast self-renewal. Dev Cell 10, 441-449.

Li, L., Vaessin, H., 2000. Pan-neural Prospero terminates cell proliferation during *Drosophila* neurogenesis. Genes Dev 14, 147-151.

Merkle, F.T., Alvarez-Buylla, A., 2006. Neural stem cells in mammalian development. Curr Opin Cell Biol 18, 704-709.

Miller, M.R., Robinson, K.J., Cleary, M.D., Doe, C.Q., 2009. TU-tagging: cell type-specific RNA isolation from intact complex tissues. Nat Methods 6, 439-441.

Morrison, S.J., Kimble, J., 2006. Asymmetric and symmetric stem-cell divisions in development and cancer. Nature 441, 1068-1074.

Ohshiro, T., Yagami, T., Zhang, C., Matsuzaki, F., 2000. Role of cortical tumour-suppressor proteins in asymmetric division of *Drosophila* neuroblast. Nature 408, 593-596.

Ouyang, Y., Petritsch, C., Wen, H., Jan, L., Jan, Y.N., Lu, B., 2011. Dronc caspase exerts a non-apoptotic function to restrain phospho-Numb-induced ectopic neuroblast formation in *Drosophila*. Development 138, 2185-2196.

Parmentier, M.L., Woods, D., Greig, S., Phan, P.G., Radovic, A., Bryant, P., O'Kane, C.J., 2000. Rapsynoid/partner of inscuteable controls asymmetric division of larval neuroblasts in *Drosophila*. J Neurosci 20, RC84.

Peng, C.Y., Manning, L., Albertson, R., Doe, C.Q., 2000. The tumour-suppressor genes lgl and dlg regulate basal protein targeting in *Drosophila* neuroblasts. Nature 408, 596-600.

Robinow, S., White, K., 1988. The locus elav of *Drosophila* melanogaster is expressed in neurons at all developmental stages. Dev Biol 126, 294-303.

Rolls, M.M., Albertson, R., Shih, H.P., Lee, C.Y., Doe, C.Q., 2003. *Drosophila* aPKC regulates cell polarity and cell proliferation in neuroblasts and epithelia. J Cell Biol 163, 1089-1098.

Sabherwal, N., Tsutsui, A., Hodge, S., Wei, J., Chalmers, A.D., Papalopulu, N., 2009. The apicobasal polarity kinase aPKC functions as a nuclear determinant and regulates cell proliferation and fate during Xenopus primary neurogenesis. Development 136, 2767-2777.

Seimiya, M., Gehring, W.J., 2000. The *Drosophila* homeobox gene optix is capable of inducing ectopic eyes by an eyeless-independent mechanism. Development 127, 1879-1886.

Southall, T.D., Brand, A.H., 2009. Neural stem cell transcriptional networks highlight genes essential for nervous system development. EMBO J 28, 3799-3807.

Spana, E.P., Doe, C.Q., 1995. The prospero transcription factor is asymmetrically localized to the cell cortex during neuroblast mitosis in *Drosophila*. Development 121, 3187-3195.

Toy, J., Yang, J.M., Leppert, G.S., Sundin, O.H., 1998. The optx2 homeobox gene is expressed in early precursors of the eye and activates retina-specific genes. Proc Natl Acad Sci U S A 95, 10643-10648.

Uv, A.E., Harrison, E.J., Bray, S.J., 1997. Tissue-specific splicing and functions of the *Drosophila* transcription factor Grainyhead. Mol Cell Biol 17, 6727-6735.

van Noort, V., Snel, B., Huynen, M.A., 2003. Predicting gene function by conserved co-expression. Trends Genet 19, 238-242.

Viktorin, G., Riebli, N., Popkova, A., Giangrande, A., Reichert, H., 2011. Multipotent neural stem cells generate glial cells of the central complex through transit amplifying intermediate progenitors in *Drosophila* brain development. Dev Biol 356, 553-565.

Wallace, K., Liu, T.H., Vaessin, H., 2000. The pan-neural bHLH proteins DEADPAN and ASENSE regulate mitotic activity and cdk inhibitor dacapo expression in the *Drosophila* larval optic lobes. Genesis 26, 77-85.

Wang, H., Somers, G.W., Bashirullah, A., Heberlein, U., Yu, F., Chia, W., 2006. Aurora-A acts as a tumor suppressor and regulates self-renewal of *Drosophila* neuroblasts. Genes Dev 20, 3453-3463.

Weng, M., Golden, K.L., Lee, C.Y., 2010. dFezf/Earmuff maintains the restricted developmental potential of intermediate neural progenitors in *Drosophila*. Dev Cell 18, 126-135.

Xiong, W.C., Okano, H., Patel, N.H., Blendy, J.A., Montell, C., 1994. repo encodes a glial-specific homeo domain protein required in the *Drosophila* nervous system. Genes Dev 8, 981-994.

CHAPTER III

Albertson, R., et al., 2004. Scribble protein domain mapping reveals a multistep localization mechanism and domains necessary for establishing cortical polarity. J Cell Sci. 117**,** 6061-70.

Anders, S., Huber, W., 2010. Differential expression analysis for sequence count data. Genome biology. 11**,** R106.

Ashraf, S. I., et al., 2004. Worniu, a Snail family zinc-finger protein, is required for brain development in *Drosophila*. Dev Dyn. 231**,** 379-86.

Bayraktar, O. A., et al., 2010. *Drosophila* type II neuroblast lineages keep Prospero levels low to generate large clones that contribute to the adult brain central complex. Neural Dev. 5**,** 26.

Bello, B. C., et al., 2008. Amplification of neural stem cell proliferation by intermediate progenitor cells in *Drosophila* brain development. Neural Dev. 3**,** 5.

Bessonov, S., et al., 2008. Isolation of an active step I spliceosome and composition of its RNP core. Nature. 452**,** 846-50.

Bier, E., et al., 1992. deadpan, an essential pan-neural gene in *Drosophila*, encodes a helix-loop-helix protein similar to the hairy gene product. Genes Dev. 6**,** 2137-51.

Bischof, J., et al., 2007. An optimized transgenesis system for *Drosophila* using germ-line-specific phiC31 integrases. Proceedings of the National Academy of Sciences of the United States of America. 104**,** 3312-7.

Boone, J. Q., Doe, C. Q., 2008. Identification of *Drosophila* type II neuroblast lineages containing transit amplifying ganglion mother cells. Dev Neurobiol. 68**,** 1185-95.

Bowman, S. K., et al., 2008. The tumor suppressors Brat and Numb regulate transit-amplifying neuroblast lineages in *Drosophila*. Dev Cell. 14**,** 535-46.

Brand, M., et al., 1993. asense is a *Drosophila* neural precursor gene and is capable of initiating sense organ formation. Development. 119**,** 1-17.

Broadus, J., et al., 1998. Staufen-dependent localization of prospero mRNA contributes to neuroblast daughter-cell fate. Nature. 391**,** 792-5.

Cabernard, C., Doe, C. Q., 2009. Apical/basal spindle orientation is required for neuroblast homeostasis and neuronal differentiation in *Drosophila*. Dev Cell. 17**,** 134-41.

Carney, T. D., et al., 2012. Functional genomics identifies neural stem cell sub-type expression profiles and genes regulating neuroblast homeostasis. Developmental biology. 361**,** 137-46.

Chabu, C., Doe, C. Q., 2008. Dap160/intersectin binds and activates aPKC to regulate cell polarity and cell cycle progression. Development. 135**,** 2739-46.

Chan, S. P., et al., 2003. The Prp19p-associated complex in spliceosome activation. Science. 302**,** 279-82.

Choksi, S. P., et al., 2006. Prospero acts as a binary switch between self-renewal and differentiation in *Drosophila* neural stem cells. Developmental cell. 11**,** 775-89.

Chu-Lagraff, Q., et al., 1991. The prospero gene encodes a divergent homeodomain protein that controls neuronal identity in *Drosophila*. Development. Suppl 2**,** 79-85.

Coltri, P. P., Oliveira, C. C., 2012. Cwc24p Is a General Saccharomyces cerevisiae Splicing Factor Required for the Stable U2 snRNP Binding to Primary Transcripts. PloS one. 7**,** e45678.

Deshaies, R. J., Joazeiro, C. A., 2009. RING domain E3 ubiquitin ligases. Annual review of biochemistry. 78**,** 399-434.

Dietzl, G., et al., 2007. A genome-wide transgenic RNAi library for conditional gene inactivation in *Drosophila*. Nature. 448**,** 151-6.

Doe, C. Q., 2008. Neural stem cells: balancing self-renewal with differentiation. Development. 135**,** 1575-87.

Goldfeder, M. B., Oliveira, C. C., 2008. Cwc24p, a novel Saccharomyces cerevisiae nuclear ring finger protein, affects pre-snoRNA U3 splicing. The Journal of biological chemistry. 283**,** 2644-53.

Hosoya, T., et al., 1995. glial cells missing: a binary switch between neuronal and glial determination in *Drosophila*. Cell. 82**,** 1025-36.

Ikeshima-Kataoka, H., et al., 1997. Miranda directs Prospero to a daughter cell during *Drosophila* asymmetric divisions. Nature. 390**,** 625-9.

Izergina, N., et al., 2009. Postembryonic development of transit amplifying neuroblast lineages in the *Drosophila* brain. Neural Dev. 4**,** 44.

Jaekel, R., Klein, T., 2006. The *Drosophila* Notch inhibitor and tumor suppressor gene lethal (2) giant discs encodes a conserved regulator of endosomal trafficking. Dev Cell. 11**,** 655-69.

Katz, Y., et al., 2010. Analysis and design of RNA sequencing experiments for identifying isoform regulation. Nature methods. 7**,** 1009-15.

Kenyon, K. L., et al., 2005. Fly SIX-type homeodomain proteins Sine oculis and Optix partner with different cofactors during eye development. Dev Dyn. 234**,** 497-504.

Knoblich, J. A., 2010. Asymmetric cell division: recent developments and their implications for tumour biology. Nature reviews. Molecular cell biology. 11**,** 849-60.

Knoblich, J. A., et al., 1995. Asymmetric segregation of Numb and Prospero during cell division. Nature. 377**,** 624-7.

Lai, S. L., et al., 2012. The snail family member worniu is continuously required in neuroblasts to prevent elav-induced premature differentiation. Developmental cell. 23**,** 849-57.

Lee, C. Y., et al., 2006a. Lgl, Pins and aPKC regulate neuroblast self-renewal versus differentiation. Nature. 439**,** 594-8.

Lee, C. Y., et al., 2006b. Brat is a Miranda cargo protein that promotes neuronal differentiation and inhibits neuroblast self-renewal. Dev Cell. 10**,** 441-9.

Lee, T., Luo, L., 2001. Mosaic analysis with a repressible cell marker (MARCM) for *Drosophila* neural development. Trends Neurosci. 24**,** 251-4.

Li, L., Vaessin, H., 2000. Pan-neural Prospero terminates cell proliferation during *Drosophila* neurogenesis. Genes & development. 14**,** 147-51.

Li, W., et al., 2008. Genome-wide and functional annotation of human E3 ubiquitin ligases identifies MULAN, a mitochondrial E3 that regulates the organelle's dynamics and signaling. PloS one. 3**,** e1487.

Lipscombe, D., 2005. Neuronal proteins custom designed by alternative splicing. Current opinion in neurobiology. 15**,** 358-63.

Matsuzaki, F., et al., 1998. miranda localizes staufen and prospero asymmetrically in mitotic neuroblasts and epithelial cells in early *Drosophila* embryogenesis. Development. 125**,** 4089-98.

Miller, M. R., et al., 2009. TU-tagging: cell type-specific RNA isolation from intact complex tissues. Nat Methods. 6**,** 439-41.

Mulder, K. W., et al., 2007. Modulation of Ubc4p/Ubc5p-mediated stress responses by the RING-finger-dependent ubiquitin-protein ligase Not4p in Saccharomyces cerevisiae. Genetics. 176**,** 181-92.

Nelles, D. A., Yeo, G. W., 2010. Alternative splicing in stem cell self-renewal and differentiation. Advances in experimental medicine and biology. 695**,** 92-104.

Neumuller, R. A., et al., 2011. Genome-wide analysis of self-renewal in *Drosophila* neural stem cells by transgenic RNAi. Cell stem cell. 8**,** 580-93.

Ohi, M. D., et al., 2002. Proteomics analysis reveals stable multiprotein complexes in both fission and budding yeasts containing Myb-related Cdc5p/Cef1p, novel pre-mRNA splicing factors, and snRNAs. Molecular and cellular biology. 22**,** 2011-24.

Peng, C. Y., et al., 2000. The tumour-suppressor genes lgl and dlg regulate basal protein targeting in *Drosophila* neuroblasts. Nature. 408**,** 596-600.

Robinow, S., White, K., 1988. The locus elav of *Drosophila* melanogaster is expressed in neurons at all developmental stages. Dev Biol. 126**,** 294-303.

Rolls, M. M., et al., 2003. *Drosophila* aPKC regulates cell polarity and cell proliferation in neuroblasts and epithelia. J Cell Biol. 163**,** 1089-98.

Sabherwal, N., et al., 2009. The apicobasal polarity kinase aPKC functions as a nuclear determinant and regulates cell proliferation and fate during Xenopus primary neurogenesis. Development. 136**,** 2767-77.

Scamborova, P., et al., 2004. An intronic enhancer regulates splicing of the twintron of *Drosophila* melanogaster prospero pre-mRNA by two different spliceosomes. Molecular and cellular biology. 24**,** 1855-69.

Seimiya, M., Gehring, W. J., 2000. The *Drosophila* homeobox gene optix is capable of inducing ectopic eyes by an eyeless-independent mechanism. Development. 127**,** 1879-86.

Shen, C. P., et al., 1997. Miranda is required for the asymmetric localization of Prospero during mitosis in *Drosophila*. Cell. 90**,** 449-58.

Shen, C. P., et al., 1998. Miranda as a multidomain adapter linking apically localized Inscuteable and basally localized Staufen and Prospero during asymmetric cell division in *Drosophila*. Genes & development. 12**,** 1837-46.

Southall, T. D., Brand, A. H., 2009. Neural stem cell transcriptional networks highlight genes essential for nervous system development. The EMBO journal. 28**,** 3799-807.

Spana, E. P., Doe, C. Q., 1995. The prospero transcription factor is asymmetrically localized to the cell cortex during neuroblast mitosis in *Drosophila*. Development. 121**,** 3187-95.

Srinivasan, S., et al., 1998. Biochemical analysis of ++Prospero protein during asymmetric cell division: cortical Prospero is highly phosphorylated relative to nuclear Prospero. Dev Biol. 204**,** 478-87.

Thibault, S. T., et al., 2004. A complementary transposon tool kit for *Drosophila* melanogaster using P and piggyBac. Nature genetics. 36**,** 283-7.

Toy, J., et al., 1998. The optx2 homeobox gene is expressed in early precursors of the eye and activates retina-specific genes. Proc Natl Acad Sci U S A. 95**,** 10643-8.

Uv, A. E., et al., 1997. Tissue-specific splicing and functions of the *Drosophila* transcription factor Grainyhead. Mol Cell Biol. 17**,** 6727-35.

van Noort, V., et al., 2003. Predicting gene function by conserved co-expression. Trends Genet. 19**,** 238-42.

van Wijk, S. J., et al., 2009. A comprehensive framework of E2-RING E3 interactions of the human ubiquitin-proteasome system. Molecular systems biology. 5**,** 295.

Weng, M., et al., 2010. dFezf/Earmuff maintains the restricted developmental potential of intermediate neural progenitors in *Drosophila*. Developmental cell. 18**,** 126-35.

Wu, T. D., Nacu, S., 2010. Fast and SNP-tolerant detection of complex variants and splicing in short reads. Bioinformatics. 26**,** 873-81.

Xiong, W. C., et al., 1994. repo encodes a glial-specific homeo domain protein required in the *Drosophila* nervous system. Genes Dev. 8**,** 981-94.

CHAPTER IV

Schneiderman, J. I., et al., 2010. Perturbation analysis of heterochromatin-mediated gene silencing and somatic inheritance. PLoS Genet. 6.